Gas Explosion Characterization, Wave Propagation: (Half-Scale Experiments)

Larsen, Gunner Chr.; Roed, Jørn; Andersen, S.I.

Publication date:
1987

Document Version
Publisher's PDF, also known as Version of record

Risø-R-499

RISØ

Risø-R-499

Gas Explosion Characterization, Wave Propagation

G. C. Larsen, J. Roed, S. I. Andersen

Risø National Laboratory, DK-4000 Roskilde, Denmark
October 1985

RISØ-R-499

GAS EXPLOSION CHARACTERIZATION, WAVE PROPAGATION
(Half-Scale Experiments)

G.C. Larsen, J. Roed, S.I. Andersen

Abstract. A number of experiments have been performed with blast waves arising from the ignition of homogeneous and well defined mixtures of methane, oxygen and nitrogen, contained within spherical balloons with controlled initial dimensions.

The maximum flame speed has been of the order of 100 m/s, resulting in positive peak pressures of $50\text{-}100 \cdot 10^2$Pa in 5-10 m distance from the source. The explosion process was found to be reasonable symmetric.

The attenuation of the blast wave due to vegetation and the influence of obstacles as banks, walls and houses on the pressure field have been investigated. The presence of the bank and the house was felt in a zone with a length corresponding to a typical dimension of the obstacles, whereas the overall pressure field is shown to be unaffected by the the type of obstacles and vegetation investigated.

For the wall and house, reflection factors have been established, and some variation over the surface has been measured.

(continued on next page)

October 1985
Risø National Laboratory, DK-4000 Roskilde, Denmark

The scatter of the pressure measurements is estimated for stable, neutral and unstable atmospheric conditions, and an attempt to determine the ground reflection factor has been performed.

Finally the accelerations of a house exposed to the blast wave have been examined.

ISBN 87-550-1121-7
ISSN 0106-2840

Grafisk Service, Risø 1986

CONTENTS PAGE

1. PREFACE..... 5

2. INTRODUCTION..... 6

3. EXPERIMENTS..... 7
3.1. Description of equipment..... 7
3.2. Results describing the characteristics of the source..... 15
3.3. Estimation of the scatter on the pressure measurements..... 22
3.4. Estimate of the ground reflection factor..... 31
3.5. Summary of explosions performed..... 40
3.6. Free-field tests..... 42
3.7. Pressure propagation in a wood..... 55
3.8. Pressure propagation around a bank of earth..... 62
3.9. Pressure propagation in the presence of a wall... 69
3.10. Regression analysis..... 101
3.11. Pressure and acceleration measurements around a group of houses..... 104

4. SUMMARY..... 143

5. REFERENCES..... 145

6. LIST OF SYMBOLS..... 147

APPENDIX 1: Print of high-speed film no. 3..... 150

1. PREFACE

Within the framework of EEC's indirect action programme on Reactor Safety, an investigation on "Gas Explosion Characterization, wave propagation" has been carried out by Risø National Laboratory under EEC contract no: 025 - SR - DK. Prof. L. Bjørnø, of the Technical University of Denmark, has been scientific advicer on the project.

The present final report describes primarily the medium-scale experiments, in which the blast waves were generated by burning 5 - 10 m^3 of methane/oxygen/nitrogen contained within spherical latex balloons. The small-scale experiments, conducted in the introductory phase of the programme, are presented separately [11].

The medium-scale experiments were all carried out at Farum-Kaserne - a military training ground north-west of Copenhagen - and could not have been conducted to a successful end without the kind assistance and patience of Sjællandske Ingeniørregimer (The Zealand Regiment of Engineers). Our presence in their training area continued considerably longer than originally anticipated due to difficulties with the measuring equipment and unsuitable weather conditions. We want to thank the regiment and especially Captain V. Matzen for their helpfulness and patience.

Several persons and organizations have supported the experiments through their loan of measuring equipment. In particular, we want to thank Brüel and Kjær A/S, Nærum, Forskningsgruppen for Industriel Akustik[1], DTH, Lydteknisk Laboratorium[2], Lyngby, E.A.Andersen M.Sc., Forsvarets Forskningstjeneste[3] and Uffe

---

[1] The Industrial Research Group.

[2] Acoustical Laboratory.

[3] Danish Defence Research Establishment.

Lind M.Sc., Skibsteknisk Laboratorium[4]. Finally, we also thank Major E.K. Lauritzen, Søværnet[5] for advice as well as loan of measuring equipment.

2. INTRODUCTION

The plan was to study pressure wave propagation under different conditions (meteorology, topography) by means of small and medium scale experiments as well as the interaction between pressure wave and natural or man-made obstacles.

In the present report, main emphasis has been put on the presentation of the measured results and on the conditions under which these results are obtained.

A thorough description of the experimental setup is given, and an attempt is made to assess the accuracy of the measurements.

The evaluation and comparison of the individual experiments are mainly based on normalised peak-pressure/distance curves, reflection coefficients where applicable and accelerations related to peak pressure, derived from time records.

In some experiments, high-speed photography was performed, and attempts were also made to measure particle velocities by hot-wire anemometry. However, the velocities proved to be low, less than 1 $^{m}/s$, and as it was not possible to calibrate the hot-wire in the field with the equipment available and no reliable formulas for transforming calibration under different temperature and pressure conditions exist for that low velocities, the measured results were discarded.

---

[4]Danish Ship Research Laboratory.

[5]The Danish Royal Navy.

The original contract has been extended to include supplementary measurements on a group of buildings, including acceleration measurements at selected positions, and these measurements are included.

3. EXPERIMENTS

3.1. DESCRIPTION OF EQUIPMENT

3.1.1. SOURCE OF EXPLOSION

The explosion was established in a balloon filled with an inflammable gas mixture. Four different types of spherical balloons have been used in the experiments: 100 g and 1250 g natural rubber Beritex Meteorological Balloons from Phillips Rubber LTD, Manchester, England and 600 g and 1100 g natural rubber balloons from Delasson-Dossunet S.A., Montreuil Paris, France.

	NECK LENGTH (mm)	NECK DIAMETER (mm)	APP. UNSTRETCHED DIAMETETER (m)
Phillips 100 g	60	10	0.40
Phillips 1250 g	100	30	1.67
Delasson 600 g	110	40	0.97
Delasson 1100 g	110	40	1.34

Table 3.1.1.1. Balloon data.

The balloon was filled with gas from high-pressure gas containers. The quantities were measured by weighing with a strain gauge load cell and supplied to the balloon by 100 m long pvc tubings, and controlled by magnetic valves situated close to

the balloon. The gasfilling process is illustrated in Fig. 3.1.1.1. below.

Fig. 3.1.1.1. Gasfilling from a high pressure gas container in the strain gauge balance.

The balloon was carried by a horizontal beam mounted on a 9 m high lattice mast. The center of the balloon was 4 m above the ground. A hoisting apparatus was mounted in the mast to operate the beam.

In order to keep the balloon in its correct position, it was fixed by a net consisting of 8 vertical nylon strings, kept together by horizontal strings at the equatorial position. The vertical cords were released by a detonator immediately before the gas explosion; thus the balloon will hang freely when it is fired. The detonator was covered by a pail in order to protect the balloon from being destroyed by flying debris from the detonation.

The explosion was initiated by a small charge of gunpowder heated by an electric filament. The charge was mounted to the rubber tube through which the gas was fed, and positioned in the center of the balloon.

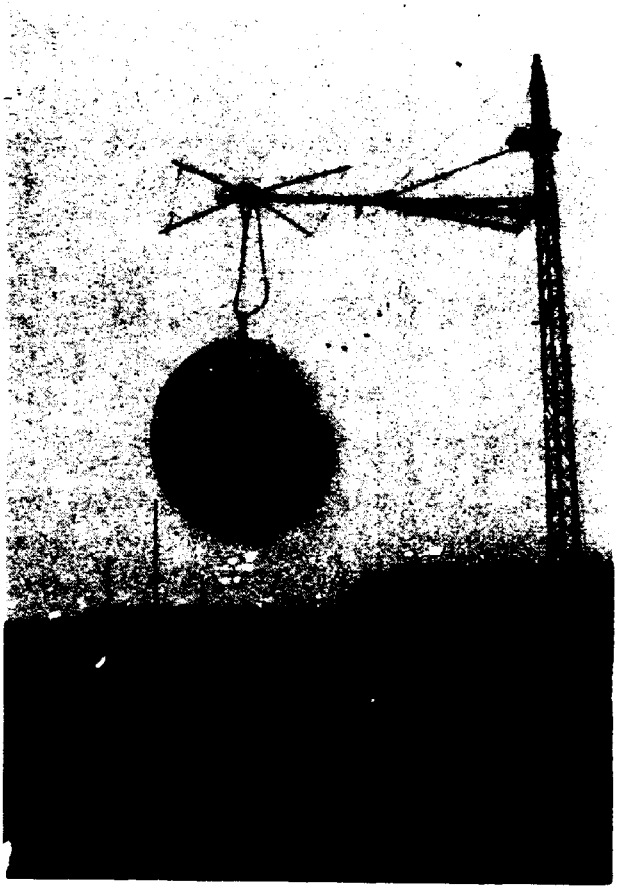

Fig. 3.1.1.2. Lattice mast with the beam and balloon during the gasfilling process.

Fig. 3.1.1.3. Electric filament with gunpowder used for ignition of the gas.

3.1.2. PRESSURE AND ACCELERATION MEASURING EQUIPMENT

The measuring equipment used for recording the pressures and accelerations given in this report have been manufactured by Brüel and Kjær, Nærum, Denmark.

The pressure transducers were hydrophones type 8100 and 8103. In the construction of these transducers arrangements have been made in order to provide vibration insulation of the sensing element.

The signals from the hydrophones had to be routed through a signal-conditioning amplifier. For this purpose charge amplifiers type 2635 and 2651 were used. The hydrophone measuring chain is illustrated in Fig. 3.1.2.1 below.

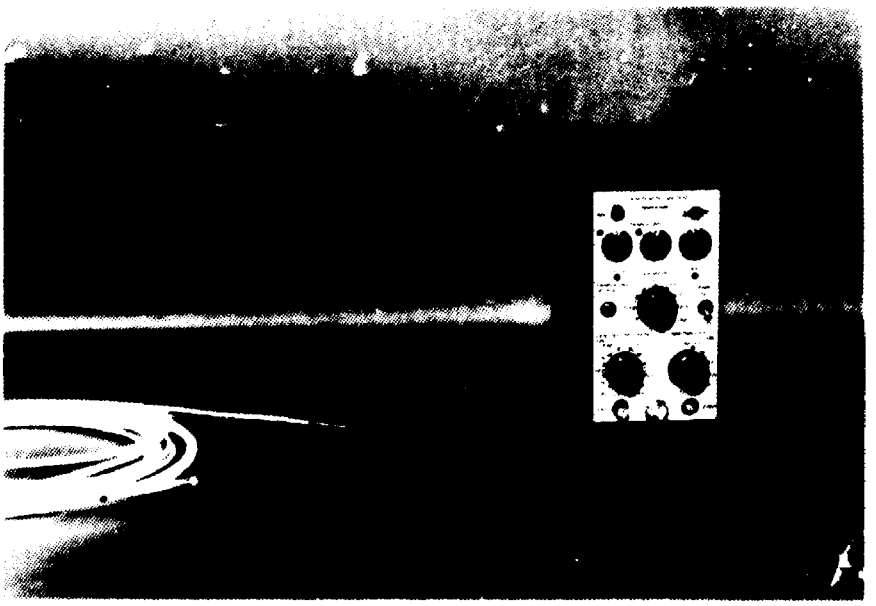

Fig. 3.1.2.1. Brüel and Kjær Hydrophones 8103, 8100 and amplifier 2635.

For weak pressures (<80mbar) at long distances (60 - 100 m) or behind obstacles, the hydrophones were supplemented by 1/4" condenser microphones type 4136. These microphones were used together with amplifier type 2619 and power supply type 2804.

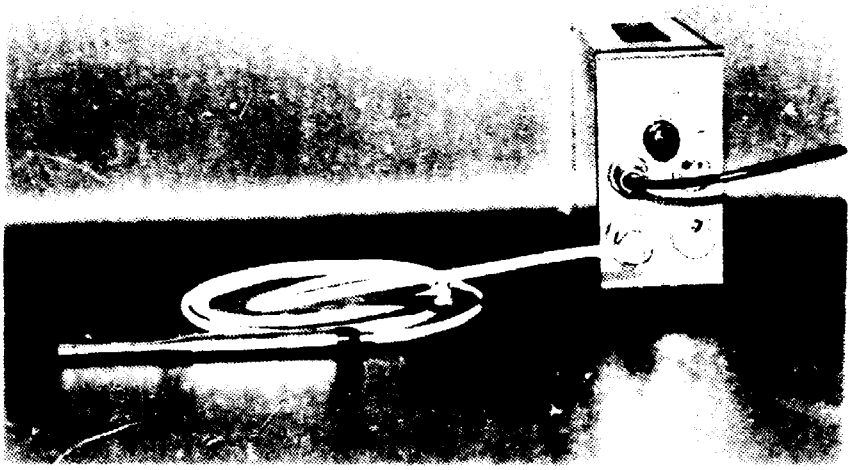

Fig. 3.1.2.2. Brüel and Kjær Microphone 4136, amplifier 2619 and power supply 2804.

In the measuring positions the transducers were placed on 3/8" tubes mounted by a laboratory clamp as illustrated in Fig. 3.1.2.3.

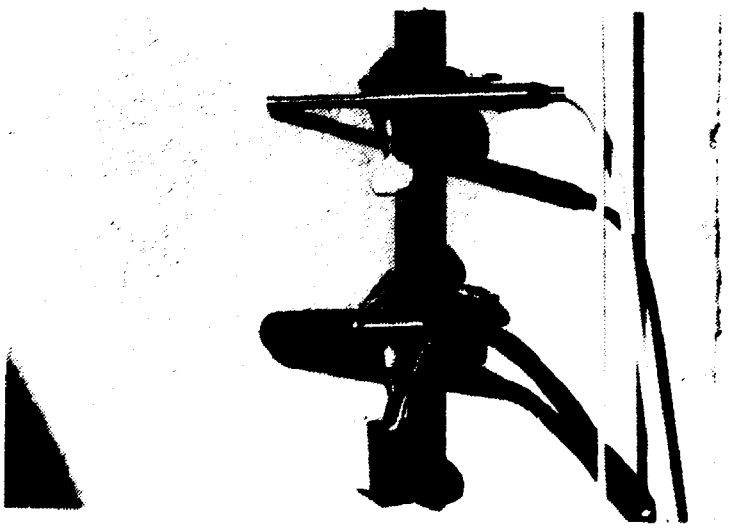

Fig. 3.1.2.3. Microphone and hydrophone mounted by laboratory clamps.

At an earlier stage in the experiments a pressure transducer and a preamplifier were developed and produced in 20 spe-

cimens. As these transducers were suspected of being amplitude sensitive at pressures above 5 mbar, the results from the first scarcely 10 half-scale explosions were discarded.

The vibration measurements were performed with accelerometers type 4368, 4370, 4371 and 4381, together with charge amplifiers type 2635 and 2651.

The signals were led from the amplifiers in BNC-cables to the FM record amplifiers of a 21-channel Teac instrumentation tape recorder type SR-70.

The further data handling consisted in an analog-to-digital conversion in a two-channel transient recorder type Datalab DL902. The digital signals were stored on floppy discs on a microcomputer Commodore type 8032.

The record amplifiers on the tape recorder were equipped with attenuators to adjust the level of the input signals. The final adjustment was performed in the transient recorder.

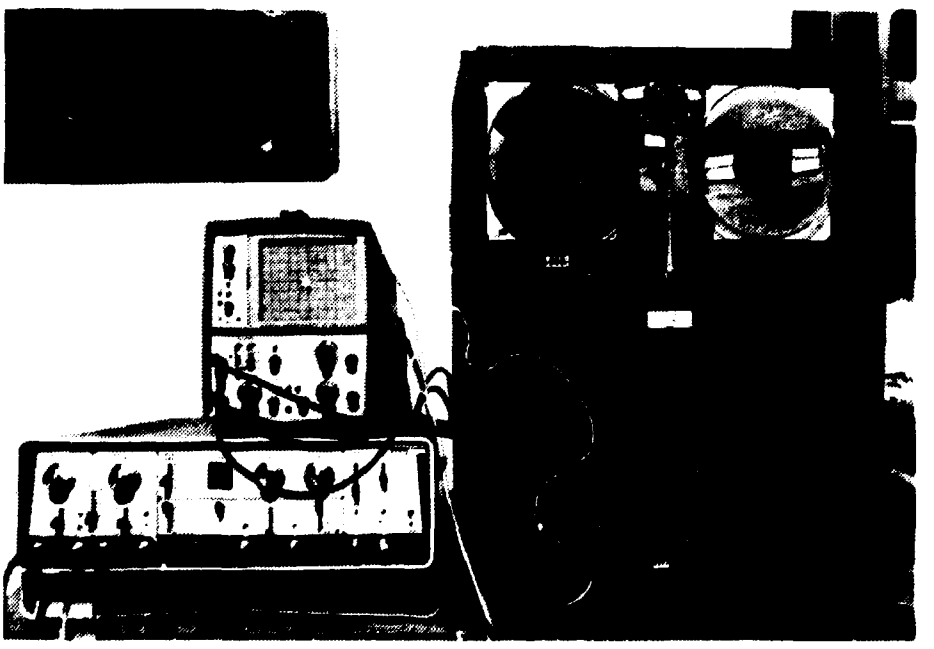

Fig. 3.1.2.4. Tape recorder, transient recorder and oscilloscope.

The data storing equipment was housed in a caravan, situated about 100 m from the explosion and close to the weighing station for the gas-filling equipment.

The power supply for the equipment and the caravan was a 1.8 kW Honda generator.

3.1.3. DATA ANALYSIS EQUIPMENT

The data stored on floppy discs were transmitted to Risø's central computer (Burroughs type B 7800), and stored there for further processing.

A program (GSA/DKV) was used to read the characteristics of a specific channel in a specific experiment into the actual file giving the modified datafile, that is a translation from binary to ordinary numbers.

The modified datafile acted as input to another program (GSA/IMP) which as output had one or more of the following possibilities:

Plot of time series, pressure/time.
Plot of power spectrum, power/frequency.
Plot of amplitude spectrum, pressure/frequency.
Plot of phase spectrum, radian/frequency.

3.1.4. EQUIPMENT FOR METEOROLOGICAL OBSERVATIONS

Two meteorology stations had been erected on the test site. One in an existing observation tower which acted as a main meteorology station, and one in a 9 m high lattice mast, placed approximately 30 m from the balloon mast and as a local meteorology station moved to the different test sites.

The main station measured the wind direction in 20.5 m above ground level, and wind speed with cup anemometers 5, 15, 17.5 and 20.5 m above. Thermometers were placed in 5 and 20.5 m and difference thermometers 5, 15, and 20.5 m above the ground. This station was placed between 500 and 1000 m from the explosion.

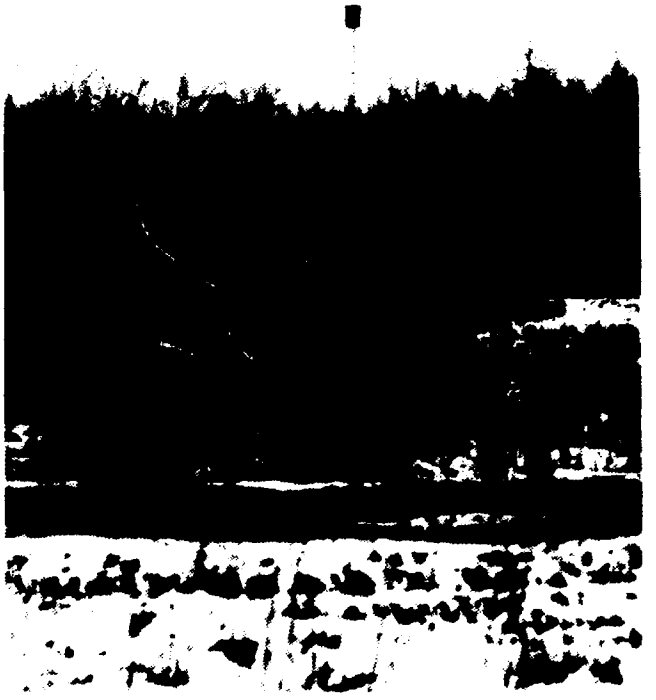

Fig. 3.1.4.1. Main meteorology station (observation tower).

The local station measured wind direction 8.5 m above ground level, wind speed with cup anemometers in 2, 4.3 and 8.5 m height and temperature with thermometers and difference thermometers 2 and 8.5 m above the ground.

Both stations had a datalogger (tape recorder) with clock, in which the mean value of the observations during a 10-minute period, was stored.

The barometric reading was given by the Meteorological Service at the neighbouring Værløse air base.

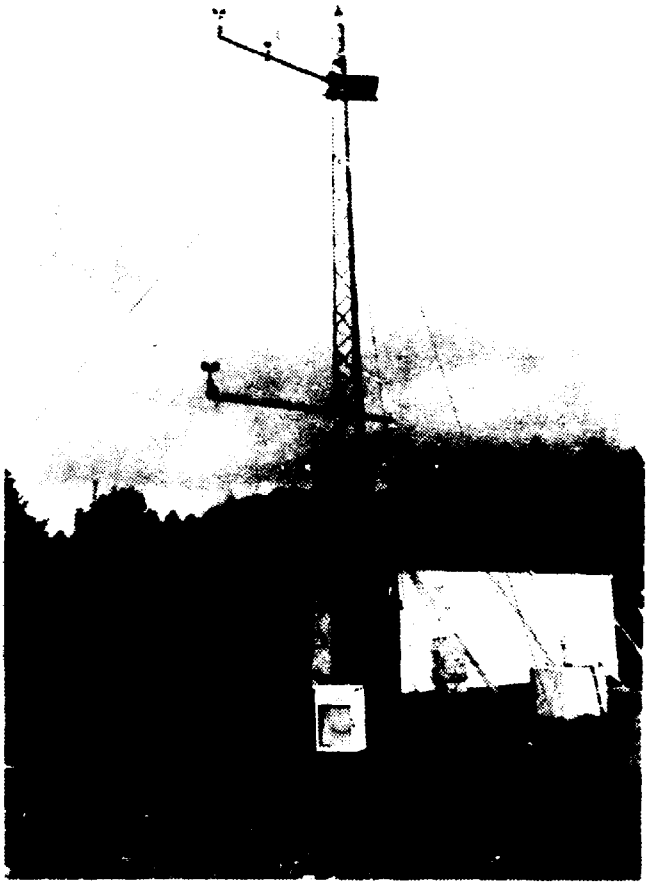

Fig. 3.1.4.2. Local meteorology station.

3.2. RESULTS DESCRIBING THE CHARACTERISTICS OF THE SOURCE

In order to check the symmetry of the source, and in addition to get input data for theoretical models predicting the pressure build-up originating from deflagrations, a number of explosions have been recorded by a high-speed camera. The high-speed camera was of the type FASTAX - WF - 14/WEBI - SP/ WEBI - PRO.

The specific data for each experiment appears from Table 3.2.1 below

EXPERIMENT NO.	FILM NO.	INITIAL RADIUS (m)	VOLUME (m^3)	MIXTURE CH_4 (vol%)	O_2 (vol%)	N_2 (vol%)	PICTURES/ sec.
168	1	1.08	5	25	50	25	1980
169	2	1.08	5	25	50	25	1980
176	3	1.36	10	25	50	25	3240
177	4	1.08	5	25	50	25	3240
178	5	0.63	1	25	50	25	3240
179	6	0.84	2.7	25	50	25	3240

Table 3.2.1. Data for the explosions recorded by a high-speed camera.

A sequence from one of the films (film no. 3) is shown in Appendix 1. As is seen, the source behaves reasonably symmetrically (at least in the film plane) in all stages of the explosion process. This is also the case for the rest of the above-described experiments.

On the basis of these high-speed films, the "horizontal radius" of the exploding gas cloud has been plotted as a function of time. The results are given in Figures 3.2.1-6

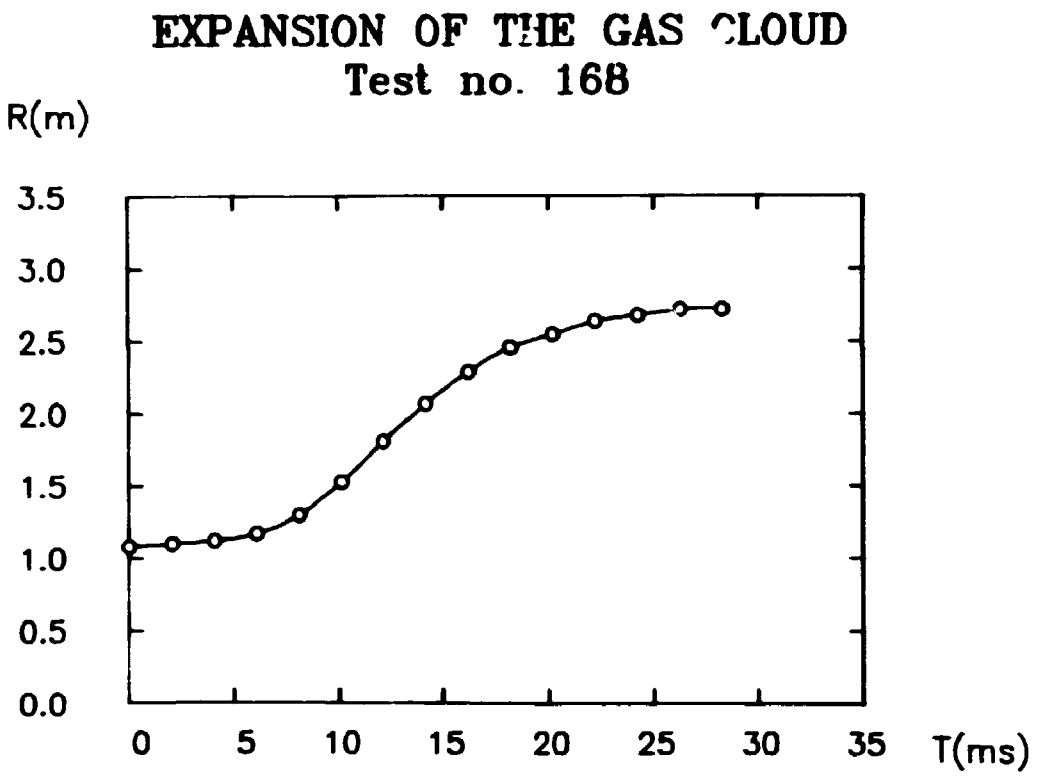

Fig. 3.2.1. The radius as a function of time for test no. 168.

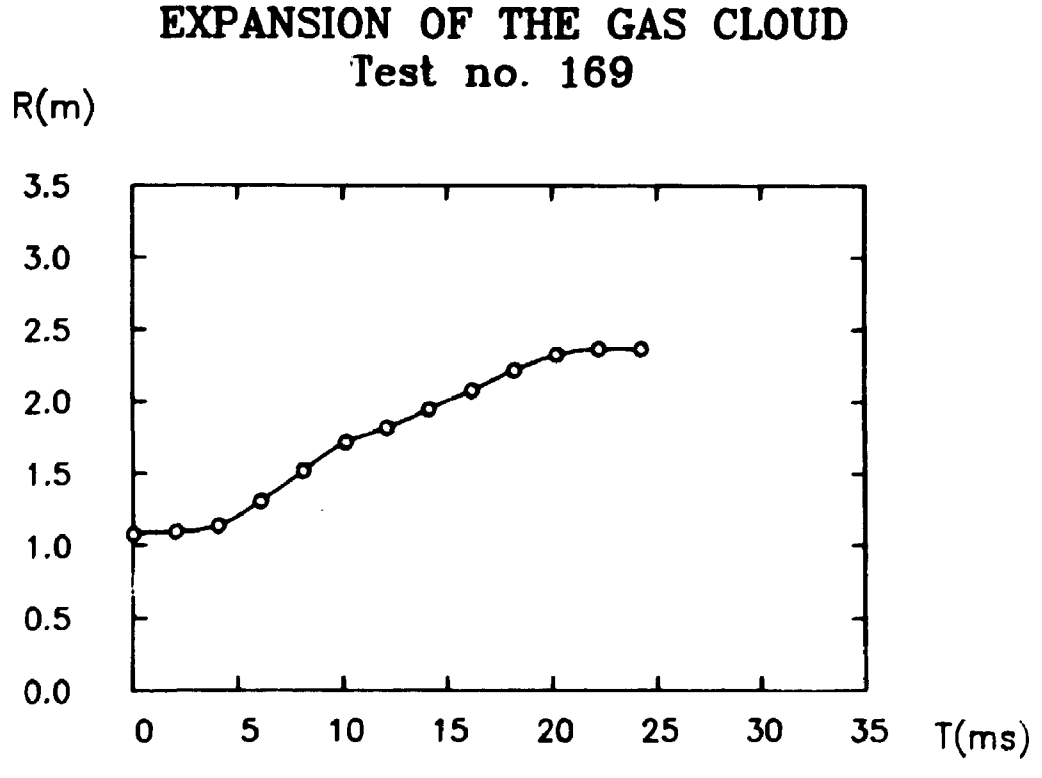

Fig. 3.2.2. The radius as a function of time for test no. 169.

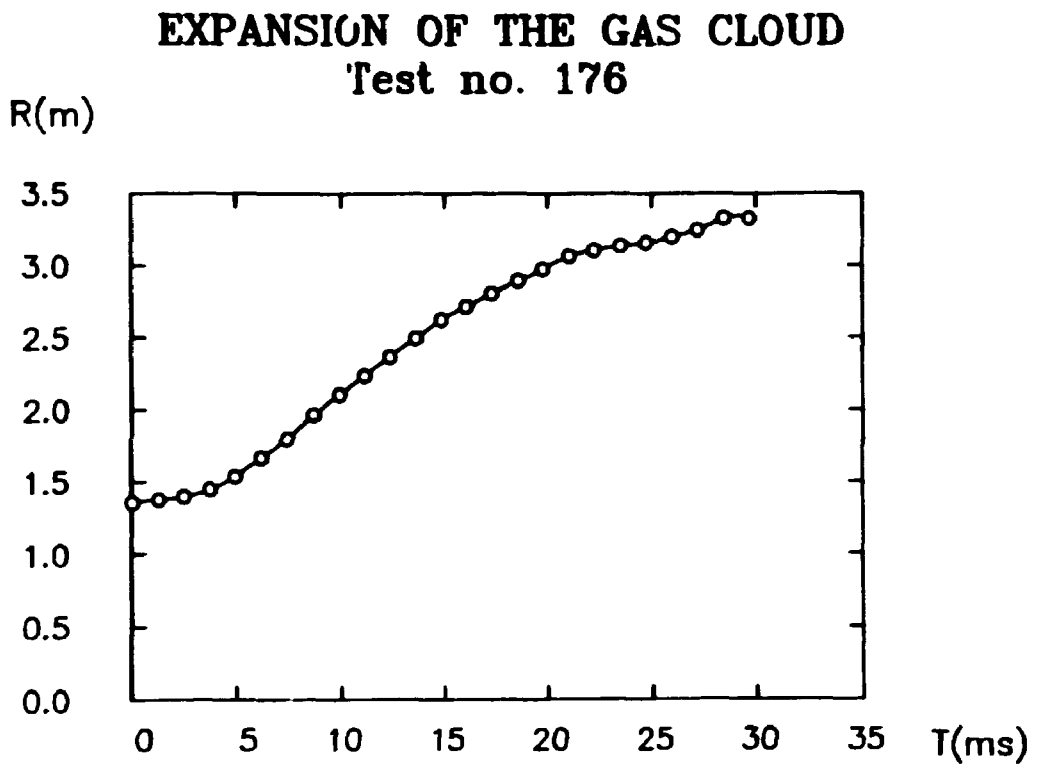

Fig. 3.2.3. The radius as a function of time for test no. 176.

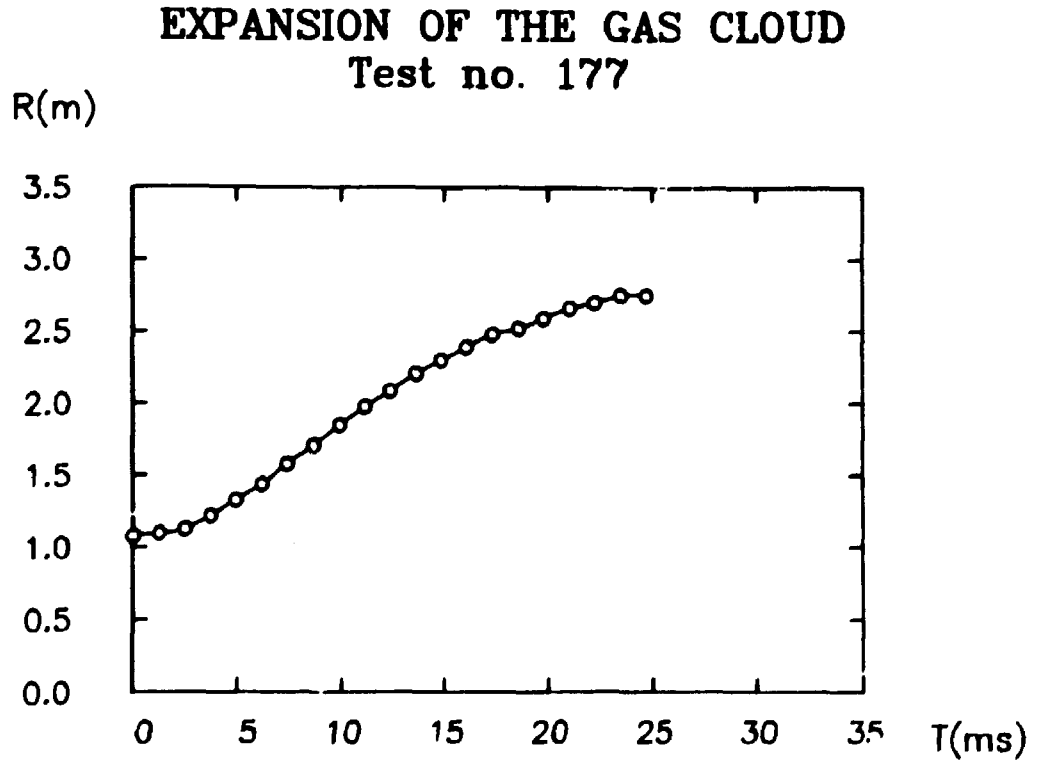

Fig. 3.2.4. The radius as a function of time for test no. 177.

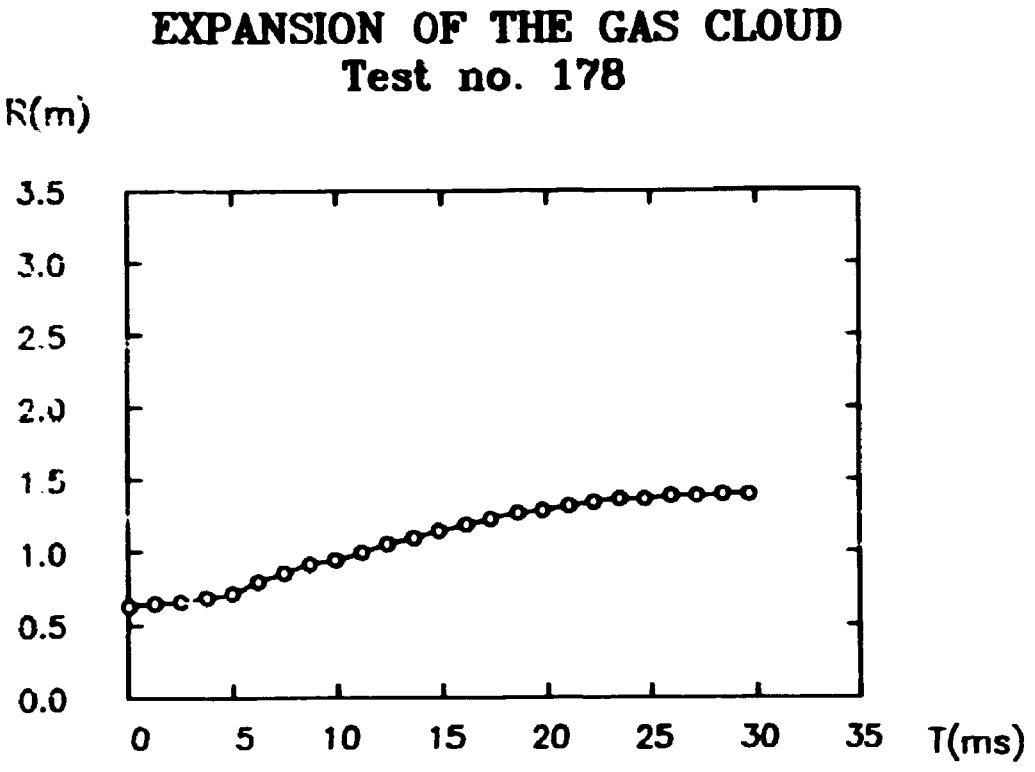

Fig. 3.2.5. The radius as a function of time for test no. 178.

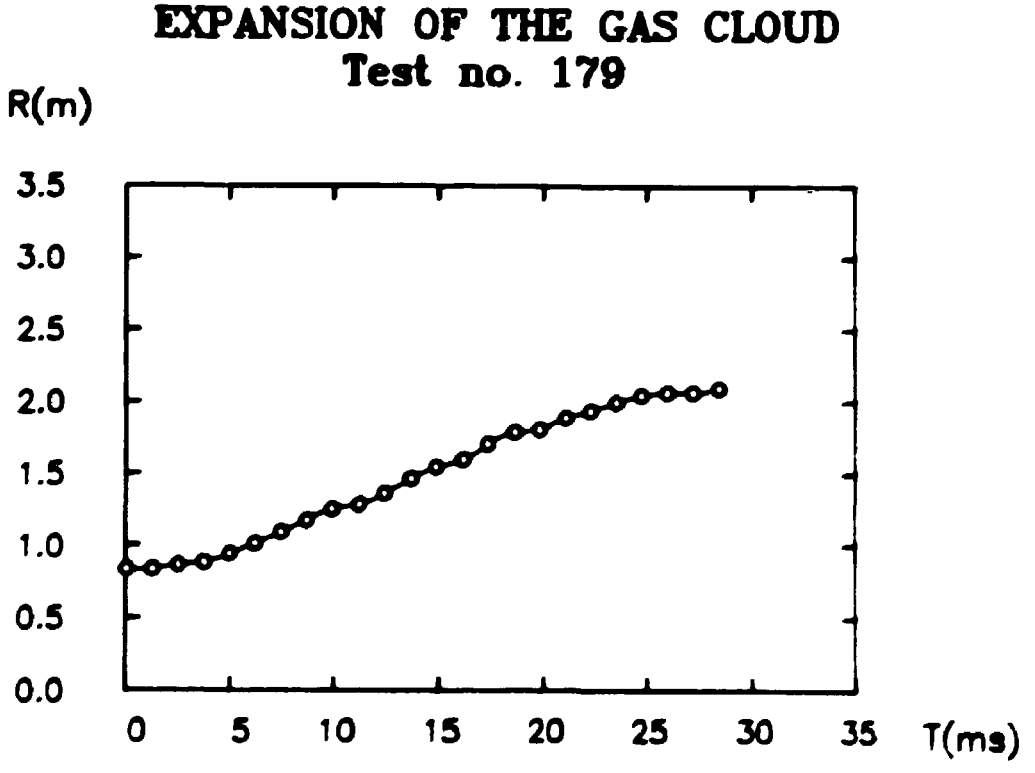

Fig. 3.2.6. The radius as a function of time for test no. 179.

Inspection of these curves shows that they are qualitatively equal and furthermore in agreement with the results obtained from small-scale experiments [11]. Moreover, it appears that the effect of a change in the initial radius is a change in the deformation scale, whereas the time scale seems unaffected. This is a remarkable result.

The curves corresponding to films no. 1, 2 and 4 were supposed to agree quantitatively as they correspond to gas clouds with the same initial radius. However this is not the case, and the reason may be that the ignitions did not occur exactly in the center of the mixtures, in spite of the observed symmetry of the flame path. This will cause a reduced pressure level [1], and can explain the poor reproduceability of the pressure levels in the experiments. An other explanation could be the not reproduceable character of the turbulence coupled to the combustion.

If the deformation-time curves, corresponding to experiments number 168, 169 and 177, are compared, it is seen that the most pronounced flame acceleration occurs in test no. 168 and that the weakest occurs in no. 169. In accordance with [7] it is then expected that

$$P_1\ (168) > P_1\ (177) > P_1\ (169)$$

where

P_1 (X) denotes the pressure level in test no. X.

The measured pressure levels, chosen as the peak pressures measured in 5 m distance from the source $P_{M,5m}$, are given in Table 3.2.2 below, and these measurements are seen to exhibit the expected trend.

TEST NO.	$P_{M,5m}$ (mbar)
168	129
169	75
177	110

Table 3.2.2. Measured pressure levels.

Finally, the measured expansion factor is compared with the theoretical expansion factor for the actual mixture.

Assuming that the burned gas is in a homogeneous state, the measured expansion factor is given as the cubed ratio between the final radius and the initial radius of the gas cloud.

The actual values are given in Table 3.2.3 below, together with the mean value and the standard deviation in percentage of the mean value.

TEST NO.	168	169	176	177	178	179
α	16.00	10.65	14.71	16.39	11.09	15.63

$$\langle\alpha\rangle = 14.1$$
$$\sigma_{\%} = 18.1\%$$

Table 3.2.3. Measured expansion factors.

The theoretical expansion factor has been calculated by means of the "Two-Gamma" heat-addition model given in [4]

$$\alpha = \frac{(\gamma_2 - 1)}{(\gamma_1 - 1)} \frac{\gamma_1}{\gamma_2} + \frac{\tilde{q}}{\gamma_2} \qquad (3.2.1)$$

where

γ_1 denotes the heat-capacity ratio of the unburned mixture

γ_2 denotes the heat-capacity ratio of the burned mixture

$\tilde{q}$ denotes the dimensionless heat added by the flame.

The values for γ_1, γ_2 and $\tilde{q}$ are modified compared to the values given in [4], in accordance with the actual mixture and the actual temperature conditions. The modified values are calculated in accordance with the model described in [11], and physical constants given in [10]. The values given in Table 3.2.4 below have been obtained.

γ_1	γ_2	$\tilde{q}$
1.4	1.045	9.65

Table 3.2.4. Values for γ_1, γ_2 and $\tilde{q}$.

The expansion factor is then calculated using the formula (3.2.1) and the values given in Table 3.2.4. The following value is then obtained

$$\alpha = 9.4$$

It appears that the theoretical expansion factor deviates considerably from the measured value of this quantity. The explanation might be that the measured values are calculated on the basis of the "horizontal radius", which is greater than the "vertical radius" at the end of the explosion process due to the presence of the ground.

3.3. ESTIMATION OF THE SCATTER ON THE PRESSURE MEASUREMENTS

A central factor in the evaluation of the results is the scatter on the actual measurements. This factor shall be dealt with in the present section.

Basically, two factors contribute to the total scatter on the pressure measurements. One is the uncertainty in the

measuring chain (transducers, amplifiers, recording equipment etc.). As the same type of equipment has been used in all the measuring channels, this uncertainty will be independent of the actual channel. The second factor is the natural variations in the atmosphere. The meteorological data (temperature, windspeed and wind direction) are given as mean values over a 10-min period. This mean value will characterize the meteorological conditions in the measuring period (~ 0.3 s). However, whithin these 10 min the pressure propagation, and with it the measured pressure, will be affected by changes in the meteorological conditions in space as well as in time due to the turbulence. Intuitively one should expect that the uncertainty of a measurement made far from the source must be greater than the uncertainty of a measurement made close to the source, as the effect of the variations in the atmosphere should be somewhat "proportional" to the time they act on the pressure-wave. The scatter due to the natural variations in the atmosphere is thus expected to depend on the actual channel.

A proper way of estimating the total scatter on the pressure measurements would be to measure the signals from 10 gas explosions, instead of 1, within the 10-min sampling period, and then evalute the standard deviation in percent of the mean value for every channel. This would then be our estimate for the scatter on the measurements.

However, this has not been possible for practical reasons, and instead the procedure outlined above has been carried out with pressure waves originating from maroons. This has been done for a stable, neutral and unstable atmosphere. Assuming that

- the scatter due to the natural variations in the atmosphere is independent of the frequency of the pressure wave (at least independent of a change in the frequency within a factor of 10),

- all stable atmospheres will give rise to the same scatter in the pressure measurements,

- all neutral atmospheres will give rise to the same scatter in the pressure measurements,
- and all unstable atmospheres will give rise to the same scatter in the pressure measurements,

these test series will form a basis for evaluating the scatter on a given measurement channel in a given experiment, on the background of the 10 min mean values of the meterological parameters.

3.3.1. EXPERIMENTAL SETUP

The experimental setup for the maroon tests is outlined in Fig. 3.3.i.1 below.

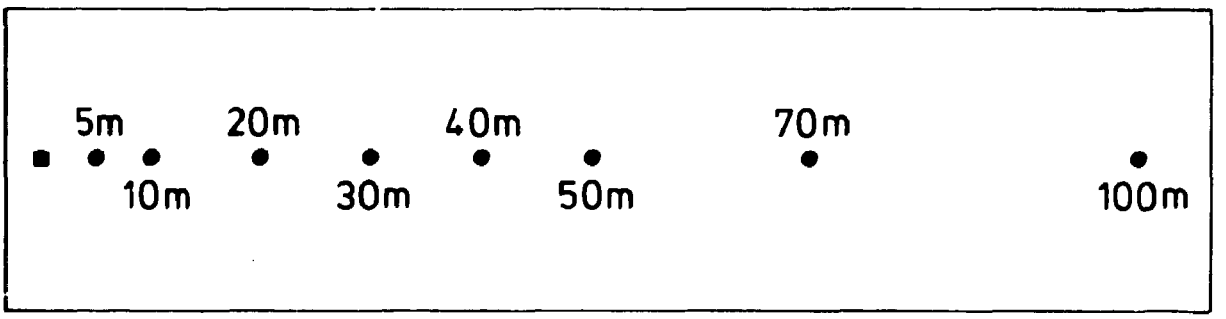

Fig. 3.3.1.1. The experimental setup.

The "■" symbolize the maroon source, and the "●" symbolize the pressure measuring points placed at different distances from source.

3.3.2. RESULTS

The tests corresponding to the unstable atmosphere are numbered 130, 131, ..., 139.

The tests corresponding to the neutral atmosphere are numbered 140, 141, ..., 149.

The tests corresponding to the stable atmosphere are numbered 150, 151, ..., 159.

The meterological data corresponding to each of these 3 test-series are given in Table 3.3.2.1 below

EXPERIMENT NO.	ATMOSPHERE TYPE	WIND SPEED {m/sec} 2.0 m	4.3 m	8.5 m	WIND DIRECTION {°from N}
130 - 139	UNSTABLE	2.16	2.48	3.00	225
140 - 149	NEUTRAL	2.16	2.55	3.07	273
150 - 159	STABLE	1.26	1.61	2.23	234

EXPERIMENT NO.	TEMPERATURE {°C} 2.0 m	8.5 m	MEASURED TEMP. DIFF. {°C} 8.5 m/2.0 m
130 - 139	15.0	14.7	-0.39
140 - 149	13.6	13.7	0.00
150 - 159	11.5	11.7	0.15

Table 3.3.2.1. Local meteorological data.

In Fig. 3.3.2.1 an example of a pressure-time curve corresponding to one of these experiments has been presented.

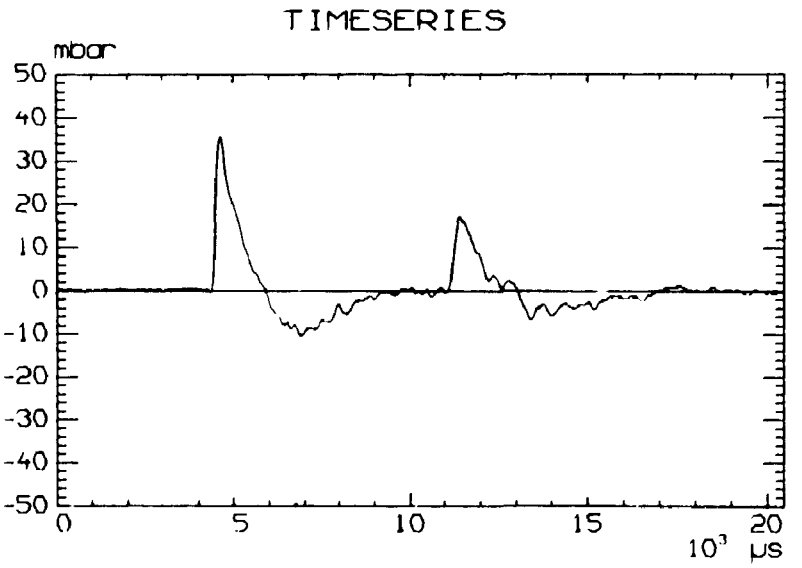

Fig. 3.3.2.1. Pressure-time curve corresponding to experiment no. 130.

For each test the peak pressure (denoted by P_M in the figures) as well as the peak-to-peak pressure (denoted by P_{p-p} in the figures) have been normalized with respect to the peak pressure measured at a 5 m distance from the explosion source, in order to compensate for variations in the strength of the explosions.

An example of these normalized pressure distribution curves is presented in Fig. 3.3.2.2.

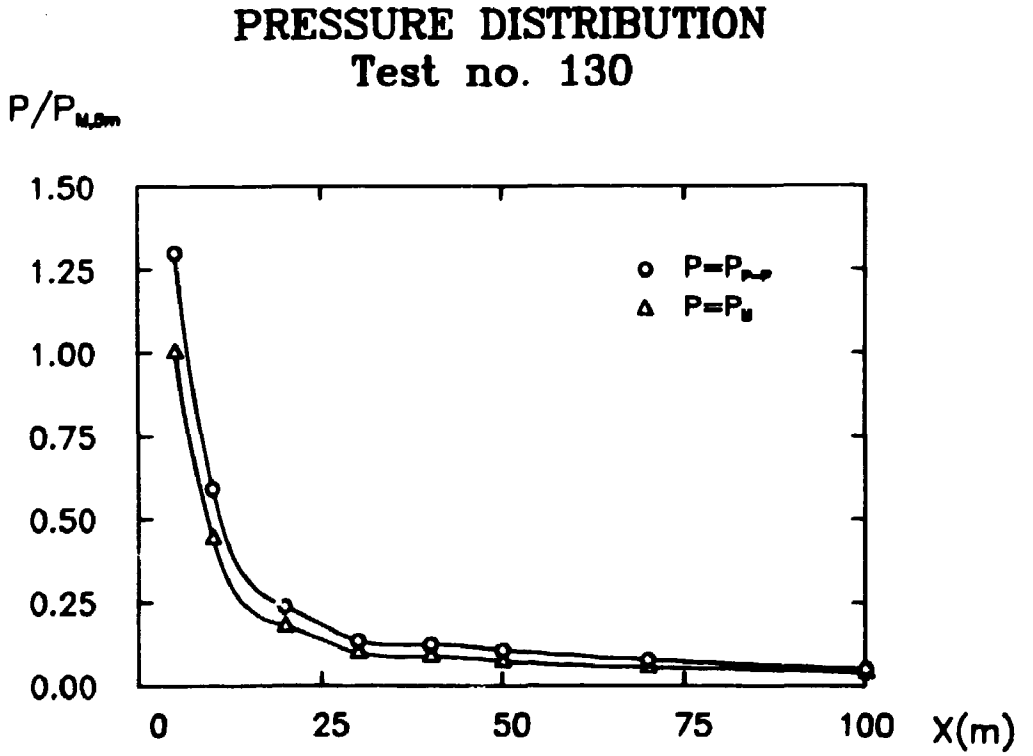

Fig. 3.3.2.2. Normalized pressure.

The time variation of the normalized pressure signals for each test series appears from Fig. 3.3.2.3 below.

PRESSURE DISTRIBUTION
Stable atmosphere

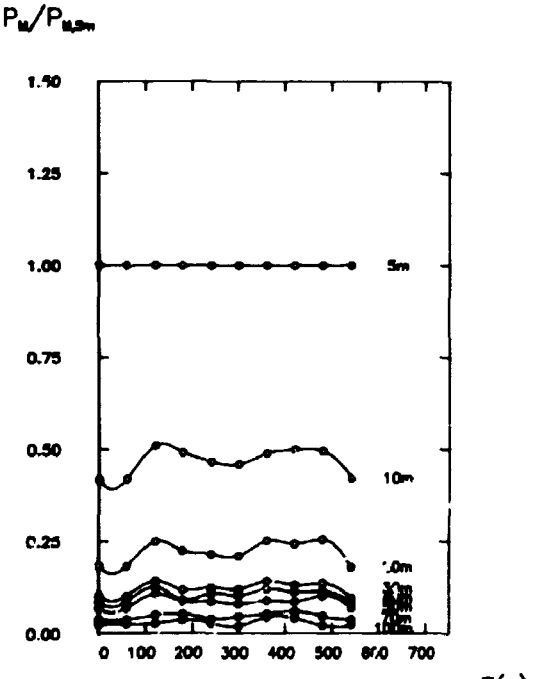

PRESSURE DISTRIBUTION
Stable atmosphere

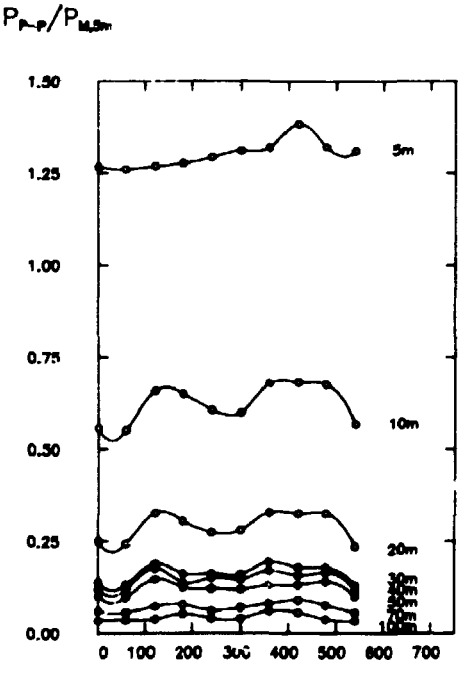

PRESSURE DISTRIBUTION
Neutral atmosphere

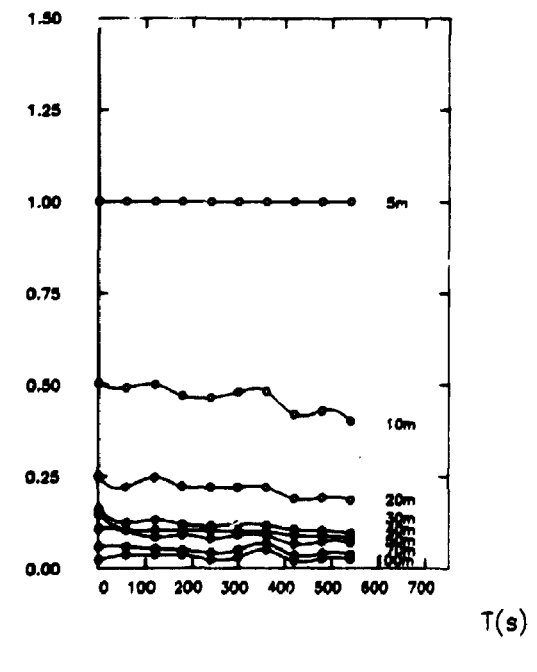

PRESSURE DISTRIBUTION
Neutral atmosphere

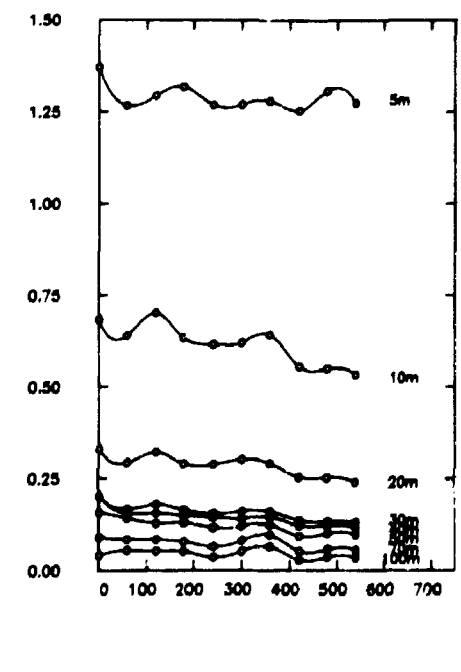

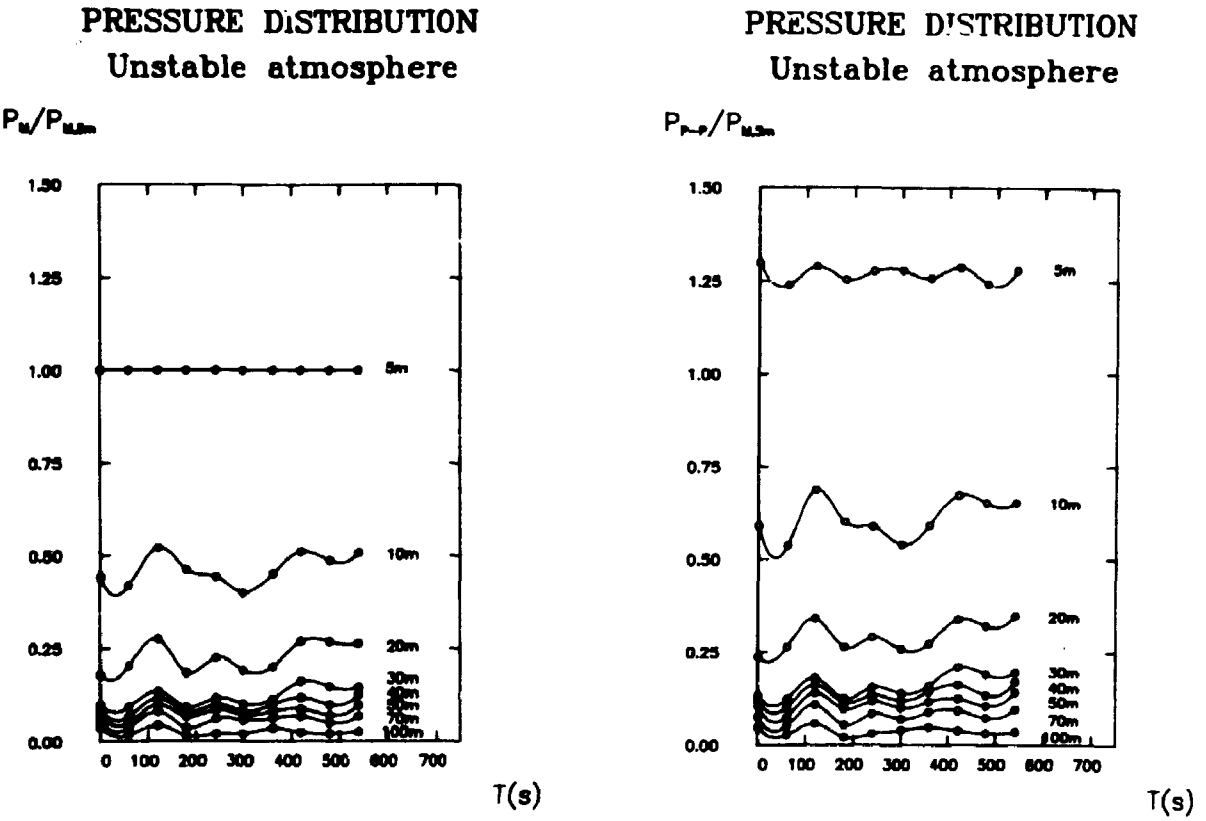

Fig. 3.3.2.3. Time variation of the normalized pressure signals.

In Fig. 3.3.2.4. below the mean of the normalized presssure distributions is given for each test series.

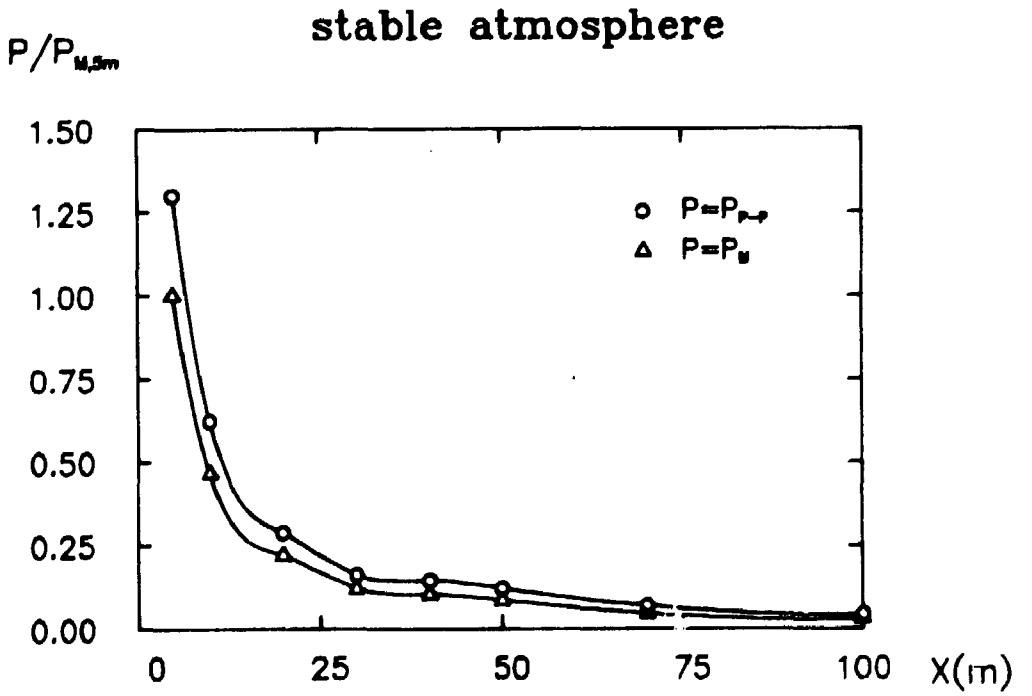

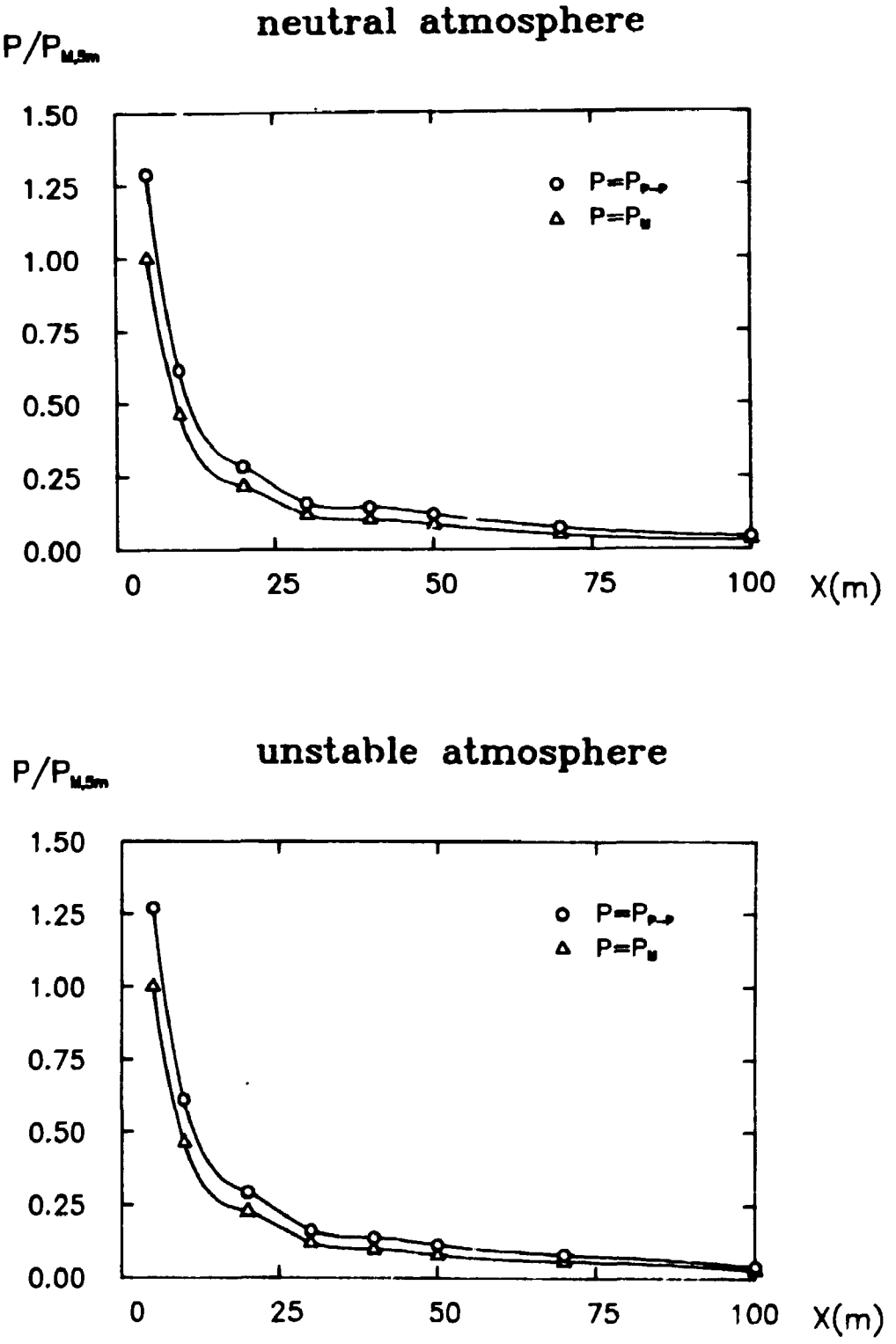

Fig. 3.3.2.4. Mean of the normalized pressure distributions.

Finally, the scatter corresponding to each of these three types of atmospheres is illustrated in Fig. 3.3.2.5, where the standard deviation in percentage of the mean value ($\sigma_{\%}$) has been given as a function of the distance between the transducer and source (X).

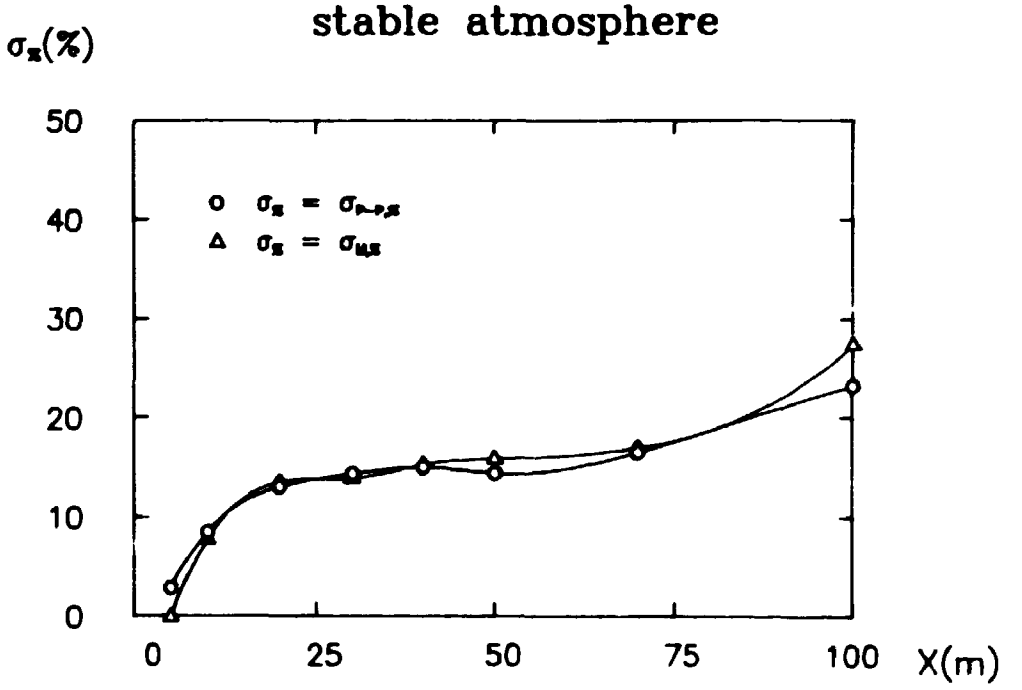

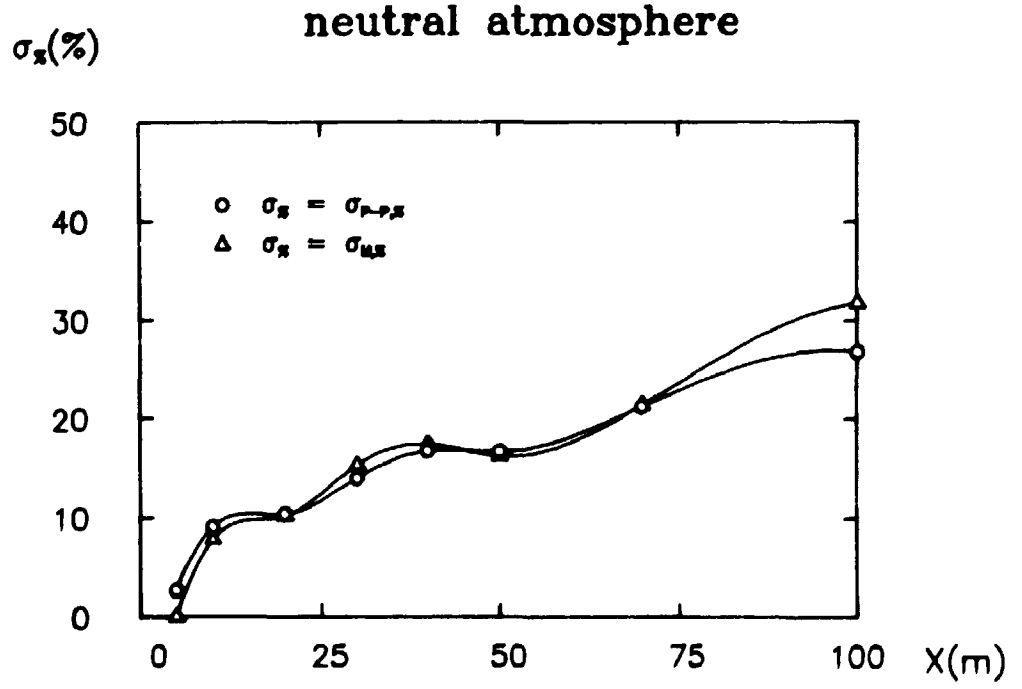

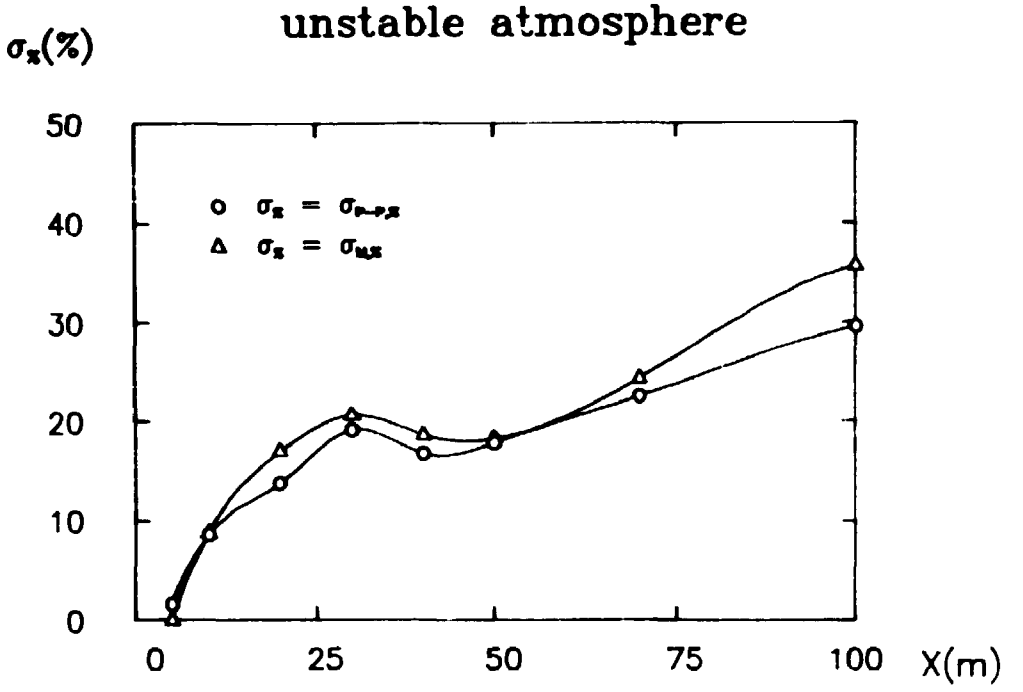

Fig. 3.3.2.5. The scatter in different distances from the source.

3.3.3. EVALUATION OF THE RESULTS

It is seen that the scatter, as expected, becomes greater with increasing distance from the explosion source. Furthermore, it seems as if the scatter corresponding to the unstable atmosphere is greater than that corresponding to the neutral atmosphere, which again is greater than the scatter corresponding to the stable atmosphere. This is a reasonable result, as the atmospheric variations due to turbulence are most pronounced in an unstable atmosphere and least pronounced in a stable one.

3.4. ESTIMATE OF THE GROUND REFLECTION FACTOR

Inspection of the pressure-time curves from the tests 130 - 159 showed that the leading pulse was followed by a smaller and retarded one. This retarded pulse was expected to be the reflection from the ground. To probe this hypothesis the time distance between the two pulses is evaluated at different

distances from the source and compared with the measured values. The actual situation (test no. 130) appears from Fig. 3.4.1 below,

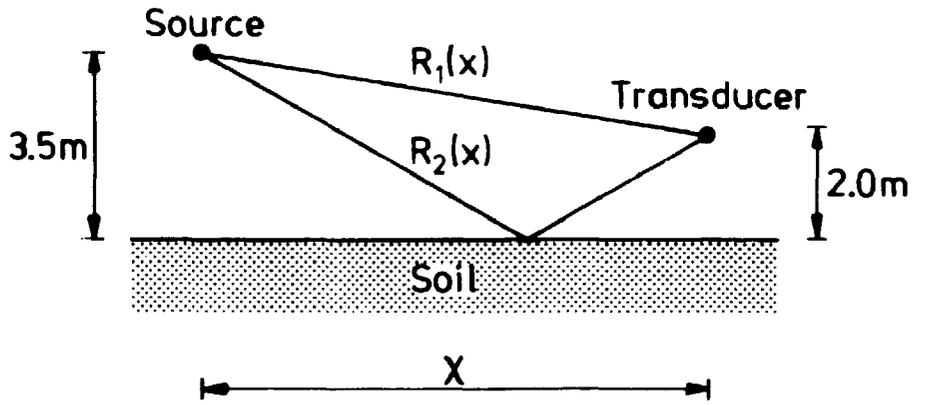

Fig. 3.4.1. Sketch of the situation in test no. 130.

where

$R_1(X)$ denotes the distance traveled by the "direct" signal

$R_2(X)$ denotes the distance traveled by the "reflected" signal

X denotes the horizontal distance between the source and transducer.

Provided that the speed of sound, c_0, is constant over the distance considered (and equals 340 m/s), and that the source can be regarded as a point source (which is a reasonable approximation as the characteristic dimension of the source is much less than the distance between the source and transducer), the following result can be obtained

$$\Delta R = R_2 - R_1$$

$$= \left(\frac{49}{121} X^2 + \frac{49}{4}\right)^{\frac{1}{2}} + \left(\frac{16}{121} X^2 + 4\right)^{\frac{1}{2}} - \left(X^2 + \frac{9}{4}\right)^{\frac{1}{2}} \qquad (3.4.1)$$

$$\Delta t_c = \frac{\Delta R}{c_0} \qquad (3.4.2)$$

$c_0 = 340$ m/s ,

where Δt_c denote the computed time interval between the arrival of the two pressure pulses. In Fig. 3.4.2 Δt_c is given as a function of horizontal distance X.

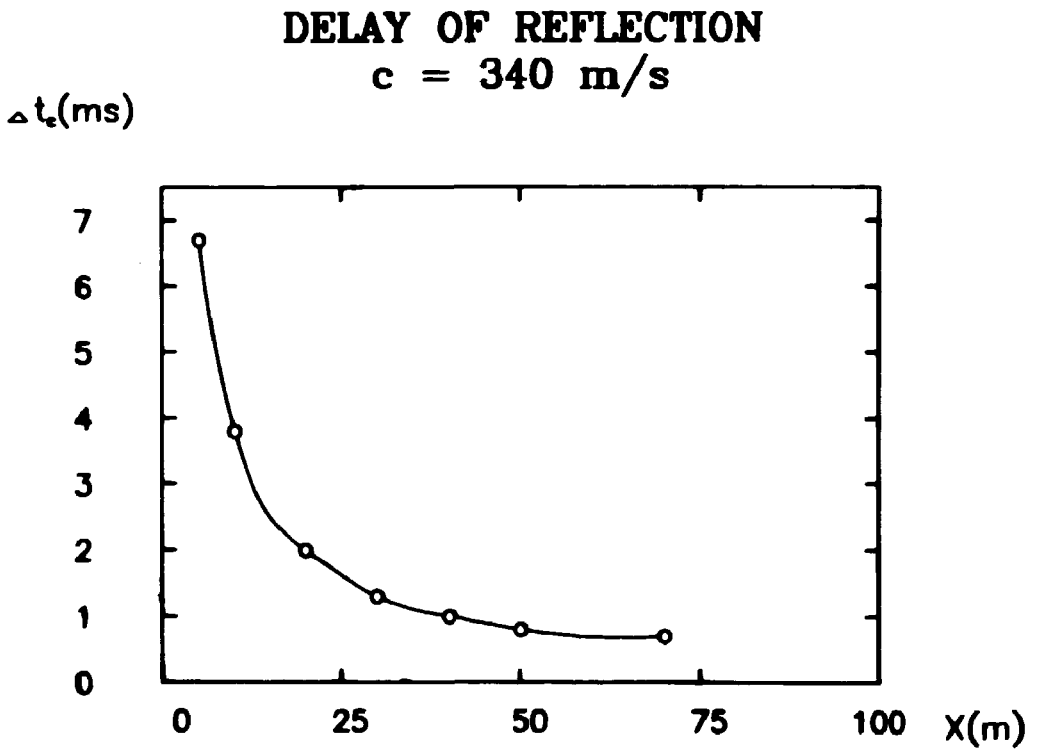

Fig. 3.4.2. Calculated time delay as a function of the horizontal distance between the source and the transducer.

The measured time delay values, Δt_m (from test no. 130), together with the corresponding Δt_c values, are given in Table 3.4.1 below

x[m]	5	10	20	30	40	50	70	100
Δt_c[ms]	6.5	3.8	2.0	1.4	1.0	0.8	0.6	0.4
Δt_m[ms]	6.7	3.8	2.0	1.3	1.0	0.8	0.7	

Table 3.4.1. Comparison of the calculated and measured time delay.

It appears that the agreement is very good, and it is then noted that the observed retarded pulse is the reflection of the pressure pulse. This information has been used in the following in an attempt to calculate the reflection factor of the actual soil for signals with the same frequency content as the maroon signals.

It is assumed, that

- the acoustic theory is valid, and consequently that the pressure attenuates as 1/R,
- the coefficient of reflection is independent of the signal level,
- the specific admittance is uniform over the surface,
- and the surface is one of local reaction.

The model used for the calculations make use of the image source technique and is illustrated in Fig. 3.4.3 below,

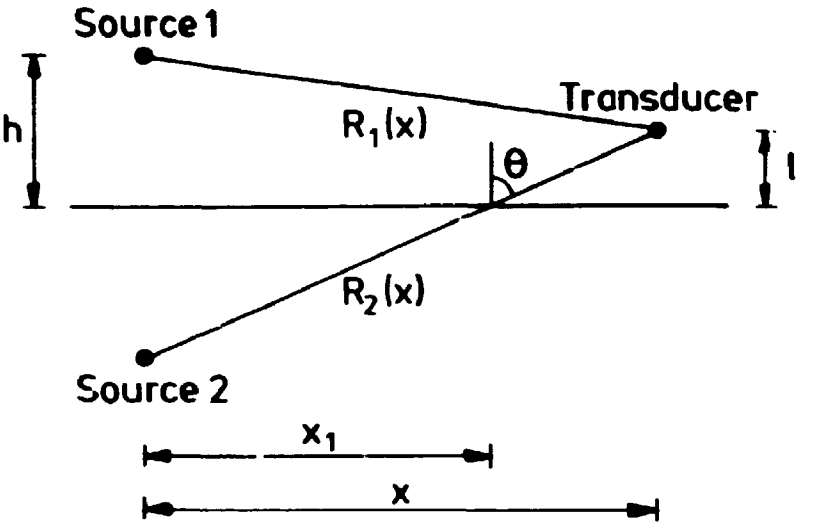

Fig. 3.4.3. Model for calculation of the reflection factor.

where

l	denotes the transducer level
h	denotes the source level
$R_1(X)$	denotes the distance travelled by the "direct" signal
$R_2(X)$	denotes the distance travelled by the "reflected" signal
X	denotes the horizontal distance between the source and transducer
X_1	denotes the horizontal distance between the source and point of reflection
θ	denotes the angle between the reflected beam and normal to the surface.

In the following, indices 1 and 2 refer to the "direct" and "reflected" signals, respectively. The expressions for the amplitudes can be presented in the following form:

$$A_1(X) = \frac{P_f}{R_1(X)} = P_f \left((h-1)^2 + X^2\right)^{-\frac{1}{2}}$$

$$A_2(X) = \frac{P_f \, f(\theta)}{R_2(X)} = P_f \, f(\theta) \left((h+1)^2 + X^2\right)^{-\frac{1}{2}}$$

The expression for $f(\theta)$ can then be given as

$$f(\theta) = \frac{A_2(X)}{A_1(X)} \frac{\left((h+1)^2 + X^2\right)^{\frac{1}{2}}}{\left((h-1)^2 + X^2\right)^{\frac{1}{2}}} \qquad (3.4.3)$$

where P_f is the "strength" of the source and $f(\theta)$ the reflection factor depending on the angle θ.

When the measurement point is not closer to the boundary surface than a half wavelength (which obviously is the case here), [3] gives the following approximate expression for $f(\theta)$:

$$f(\theta) = \frac{\cos\theta + \beta}{\cos\theta - \beta}$$

where β denote the specific admittance of the actual surface.

β can then be expressed as

$$\beta = \frac{h}{\left(h^2 + X_1^2\right)^{\frac{1}{2}}} \frac{(1 - f(\theta))}{(1 + f(\theta))} \qquad (3.4.4)$$

Now A_1 and A_2 can be found in the pressure-time curves corresponding to the maroon experiments, and with the aid of the formulas (3.4.3) and (3.4.4) $f(\theta)$ and β can be calculated.

In order to minimize the influence from inhomogenities in the atmosphere, the experiments with the neutral atmosphere (the experiments 140-149) are used for the calculations. In these experiments $h = 3.0$ m and $l = 2.0$ m. The results concerning the $f(\theta)$-values are presented in Table 3.4.2 below

REFLECTION FACTOR f(ϑ)

x[m]	x_1[m]	140	141	142	143	144	145	146	147	148	149	<f(ϑ)>	σ%
5	3	0.87	0.84	0.79	0.74	0.85	0.75	0.98	0.69	0.62	0.63	0.78	15%
10	6	0.49	0.41	0.42	0.58	0.42	0.56	0.60	0.72	0.58	0.60	0.54	19%
20	12	0.44	0.45	0.45	0.39	0.38	0.36	0.50	0.37	0.31	0.30	0.40	16%
30	18	0.62	0.63	0.64	0.55	0.65	0.58	0.68	0.47	0.38	0.52	0.57	16%
40	24	0.58	0.63	0.77	0.57	0.60	0.55	0.68	0.46	0.45	0.53	0.58	17%
50	30	0.59	0.56	0.62	0.54	0.64	0.45	0.64	0.52	0.43	0.55	0.55	13%
70	42		0.72	0.85	0.74	0.89	0.64	0.63	0.81	0.69	0.69	0.74	12%
100	60	0.96	0.55	0.67	0.50	0.81	0.52	0.50	0.79	0.64	0.55	0.65	24%

Table. 3.4.2 Computed f(ϑ) values, mean of f(ϑ) values and scatter on the results.

where the symbol <> denotes the mean value and the symbol $\sigma_{\%}$ the standard deviation in percent of the mean value.

It is seen that although the scatter is of the same order of magnitude as that on the pressure measurements, there is no systematic trend in these $\sigma_{\%}$-values. This indicates that inhomogenities in the atmosphere are of lesser importance, and that inhomogenities in the soil (β is not constant) as well as deviations in the h-values (resulting in deviations in X_1 and θ) are more reasonable explanations.

The corresponding results concerning the β-values are presented in the following Table 3.4.3:

SPECIFIC ADMITTANCE β

X[m]	X_1[m]	140	141	142	143	144	145	146	147	148	149	<β>	$\sigma_{\%}$
5	3	0.0492	0.0615	0.0830	0.1057	0.0573	0.1010	0.0071	0.1297	0.1659	0.1605	0.0921	55%
10	6	0.1510	0.1846	0.1802	0.1173	0.1803	0.1244	0.1103	0.0718	0.1173	0.1103	0.1347	28%
20	12	0.0943	0.0920	0.0920	0.1064	0.1089	0.1141	0.0808	0.1115	0.1277	0.1306	0.1058	15%
30	18	0.0432	0.0418	0.0405	0.0535	0.0391	0.0490	0.0351	0.0664	0.0828	0.0582	0.0510	29%
40	24	0.0330	0.0218	0.0161	0.0340	0.0310	0.0360	0.0236	0.0459	0.0470	0.0381	0.0327	31%
50	30	0.0257	0.0281	0.0233	0.0297	0.0218	0.0377	0.0218	0.0314	0.0397	0.0289	0.0288	21%
70	42		0.0116	0.0058	0.0106	0.0041	0.0156	0.0162	0.0075	0.0131	0.0131	0.0108	39%
100	60	0.0100	0.0145	0.0099	0.0166	0.0052	0.0158	0.0166	0.0059	0.0110	0.0145	0.0111	49%
	<β>	0.0568	0.0570	0.0564	0.0592	0.0560	0.0617	0.0389	0.0588	0.0756	0.0693		
	$\sigma_{\%}$	89%	102%	106%	74%	108%	72%	94%	77%	76%	82%		

Table 3.4.3 Computed β values, mean of β values and scatter on the results.

where the terminology is the same as the the one used for the presentation of the f(θ) values.

It is seen that the scatter on the β-values is increased compared to the f(θ)-values. The reasons for the considerable scatter in the results is believed to be the same as the explanations given for the scatter in the f(θ)-values. The assumption that β varies with X_1 is supported by the following: The σ_β-values that correspond to β-values calculated from measurements made at different distances from the source are about twice as large as those that correspond to β-values from measurements made at the same source distance.

In conclusion, the assumption that β is uniform over the surface seems to be invalid. The present model is therefore unsatisfactory.

3.5. SUMMARY OF EXPLOSIONS PERFORMED

In this section a brief overview of the experiments carried out with exploding gas clouds is given.

The single experiment is identified by an experiment number, the date and time for the performance, and a keyword indicating the purpose of the present experiment.

The data from the meteorology measurements (where executed), and the peak pressures measured in 5 and 10 m distance from the source are also presented.

No.	Date	Time	Atmosphere	Windspeed (m/sec)			Direction (°from N)	Temperature (°C)		Atm. pressure (mbar)	Max pressure (mbar)	
				2m	4,3m	8,5m		2m	8,5m		5m	10m
125 wall	29.9	11.46	unstable	0.84	0.98	1.15	98	10.7	10.5	1022.3	41.0	28.2
126 wall	29.9	14.55	unstable	0.39	0.42	0.60	83	10.5	10.4	1020.6	145.8	97.6
127 wall	30.9	11.08	unstable	1.26	1.36	1.64	308	10.4	10.0	1022.5	86.0	67.0
128 wall	4.10	9.45	neutral	2.06	2.37	2.69	209	13.4	13.4	1012.7	138.4	107.5
129 wall	4.10	12.30	unstable	2.30	2.84	3.42	197	15.5	15.4	1011.6	117.2	79..
164 wall	7.11	12.41	neutral	1.47	1.78	1.99	180	9.3	9.3	1022.0	69.1	60.9
165 wall	9.11	9.41	unstable	1.09	1.36	1.47	197	6.4	6.3	1021.5	68.3	58.2
166 wall	9.11	11.00	unstable	0.77	0.95	1.02	169	7.2	6.9	1021.6	30.0	20.0
167 wall	9.11	13.17	unstable	1.22	1.47	1.61	205	9.0	8.5	1021.5	78.1	55.5
168 wall	10.11	12.00	unstable	2.09	2.44	2.72	310	8.0	7.9	1021.0	129.0	82.0
169 wall	10.11	14.06	unstable	2.16	2.58	2.79	295	8.5	8.4	1019.7	75.0	59.0
170 house	14.11	14.10	unstable	2.89	3.42	3.73	273	4.9	4.8	1022.4		
171 house	14.11	16.00	neutral	2.96	3.56	3.94	278	4.9	4.9	1020.1	30.0	22.0
172 house	17.11	11.55	unstable	1.22	1.43	1.57	5	1.4	1.3	1015.5	87.9	60.3
173 house	17.11	13.47	unstable	0.88	1.05	1.02	308	1.9	1.7	1016.0	141.8	100.0
174 house	18.11	12.16	neutral	3.66	4.22	4.63	297	6.5	6.5	1008.7	52.3	32.4
175 house	18.11	14.21	neutral	3.03	3.56	4.39	348	6.4	6.4	1009.7	36.7	23.0
176 house	23.11	13.15	unstable	1.15	1.40	1.47	306	2.1	1.8	1018.4	125.0	89.1
177 house	23.11	14.07	unstable	1.19	1.43	1.64	236	1.9	1.8	1018.6	110.0	63.0
178 house	29.11	12.35	neutral	0.95	1.26		147	-1.1	-1.1	1005.9	8.9	
179 house	29.11	13.15	unstable	1.09	1.36		189	-0.9	-1.0	1005.5	68.9	
180 house	29.11	14.10	unstable	0.42	0.60		111	-1.3	-1.4	1005.4	48.8	
181 house	29.11	14.45	unstable	0.70	0.91		146	-1.2	-1.3	1005.4	53.9	
182 house	6.12	11.40								1010.1	61.5	
183 house	6.12	12.55								1010.3	4.4	
184 house	6.12	13.15								1009.3	3.1	
185 bank	20.12	13.07	neutral	2.23	2.62		211	4.0	4.0	994.2	122.0	103.0
186 bank	20.12	14.35	stable	1.96	2.30		209	4.1	4.1	994.6	95.0	75.0
187 wood	21.12	12.19	neutral	3.07	3.38		136	3.5	3.5	994.2	48.0	39.0
188 wood	21.12	13.57	neutral	3.24	3.63		135	3.5	3.5	993.8	100.0	87.0
189 free	29.12	12.17	unstable	3.49	4.08		274	5.2	5.1	1025.3	40.0	35.0
190 free	5.1	11.25	neutral	3.14	3.66		288	2.5	2.5	1008.1	119.0	124.0
191 free	5.1	12.50	unstable	3.38	3.94		260	2.8	2.7	1008.4	55.0	43.0

Fig. 3.5.1 Review of gas exposions performed.

3.6. FREE FIELD TESTS

The scope for the free-field tests is threefold,

- to obtain reference measurements for the following tests,
- to test the symmetry of the blast wave,
- and to probe the geometric 1/R attenuation.

These tests were carried out on a plane area covered with low grass.

3.6.1. EXPERIMENTAL SETUP

In order to check for the symmetry of the explosions, the measurements have been performed in 3 different directions from the source. In the following these are denoted by string 1 (west), string 2 (south) and string 3 (east). In string 2 the measurements were performed at distances 5, 10, 20, 30, 40, 50, 60, 70, 80, 90 and 100 m from the center of the explosion. In strings 1 and 3 the measurements were performed 20 m from the center of the explosion. The transducers were all placed 1.8 m above the ground.

Fig. 3.6.1.1. Hydrophone in the free field.

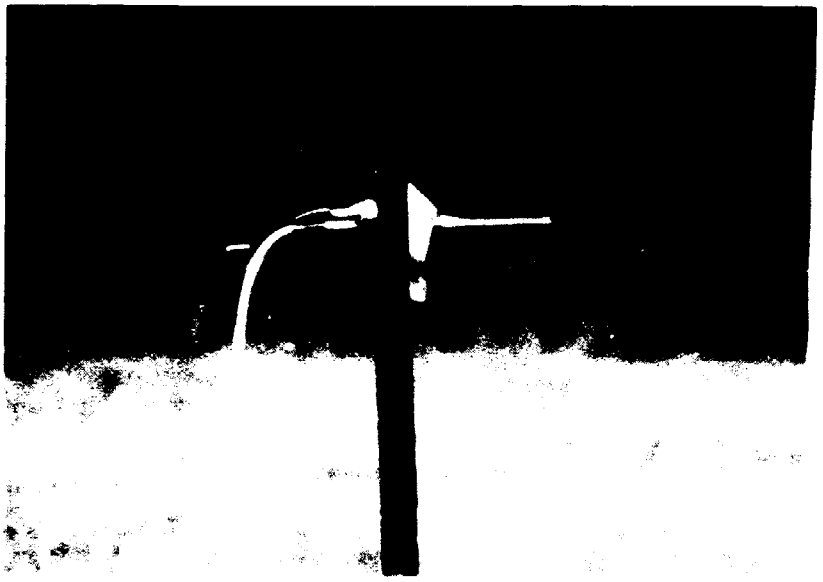

Fig. 3.6.1.2. Microphone in the free field.

3.6.2. RESULTS

The experimental data and the data concerning the meteorological measurements are given in the following tables referring to experiment numbers 189 to 191.

For each channel the pressure has been recorded as a function of the time. Typical examples of the pressure-time history recorded at 5 m and at 20 m's distance from the center of the source are presented in Figs. 3.6.2.1-2 below.

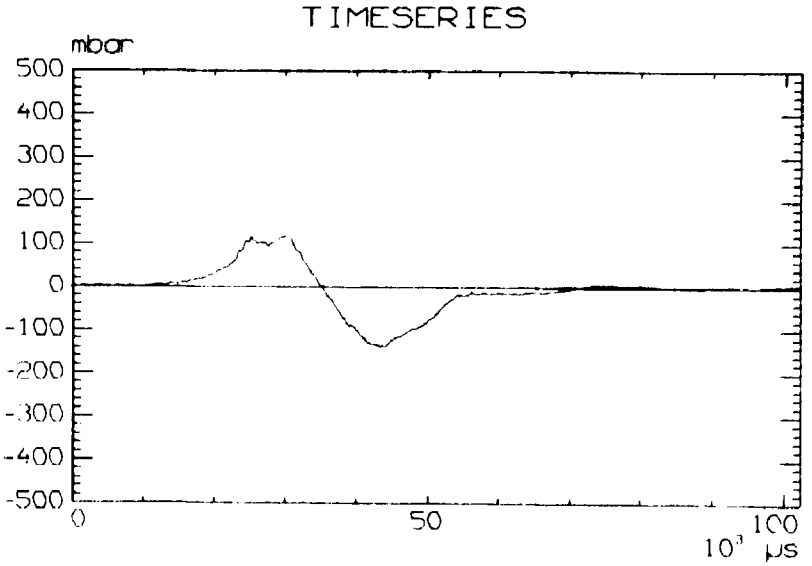

Fig. 3.6.2.1. Typical pressure history measured at 5 m's distance from the source.

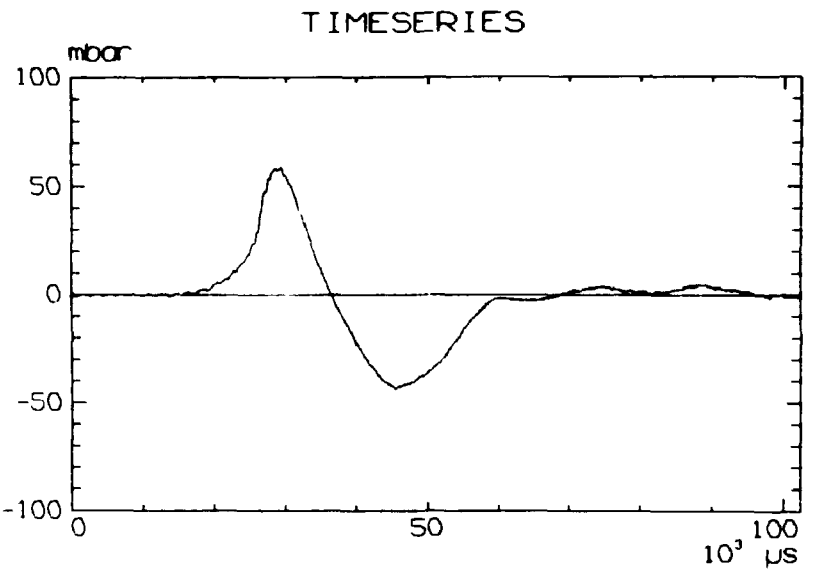

Fig. 3.6.2.2. Typical pressure history measured at 20 m's distance from the source.

From this type of curves the peak and peak-to-peak pressures normalized with respect to the peak pressure at 5 m are evaluated and in Figures 3.6.2.3-9 given as a function of the distance from the center of the gas cloud.

For experiment number 190 the maximum pressure at a distance of 5 m from the center of the balloon is smaller than that at a distance of 10 m, but the content of energy is larger at 5 m. Therefore, the minimum pressures P_{MI}, have been drawn too, since they do not show the same anomaly.

No. 189

Date: 29/12-83

Time: 12.17

Purpose: To investigate the pressure wave propagation over a free field.

Atmosphere: unstable

Windspeed {m/sec} 2.0 m : 3.49
4.3 m : 4.08
8.5 m :

Wind direction {°from N}: 274

Temperature {°C} 2.0 m : 5.2
8.5 m : 5.1

Direct measured temperature difference {°C}: -0.14

Atmospheric pressure {mbar}: 1025.3

Balloon: 1100 g Delasson

Gas mixture {vol. %}: CH_4= 25, O_2= 50, N_2= 25

Volume {m^3}: 10

Explosion max. pressure {mbar} 5.0 m : 46
pp. pressure {mbar} 5.0 m : 133

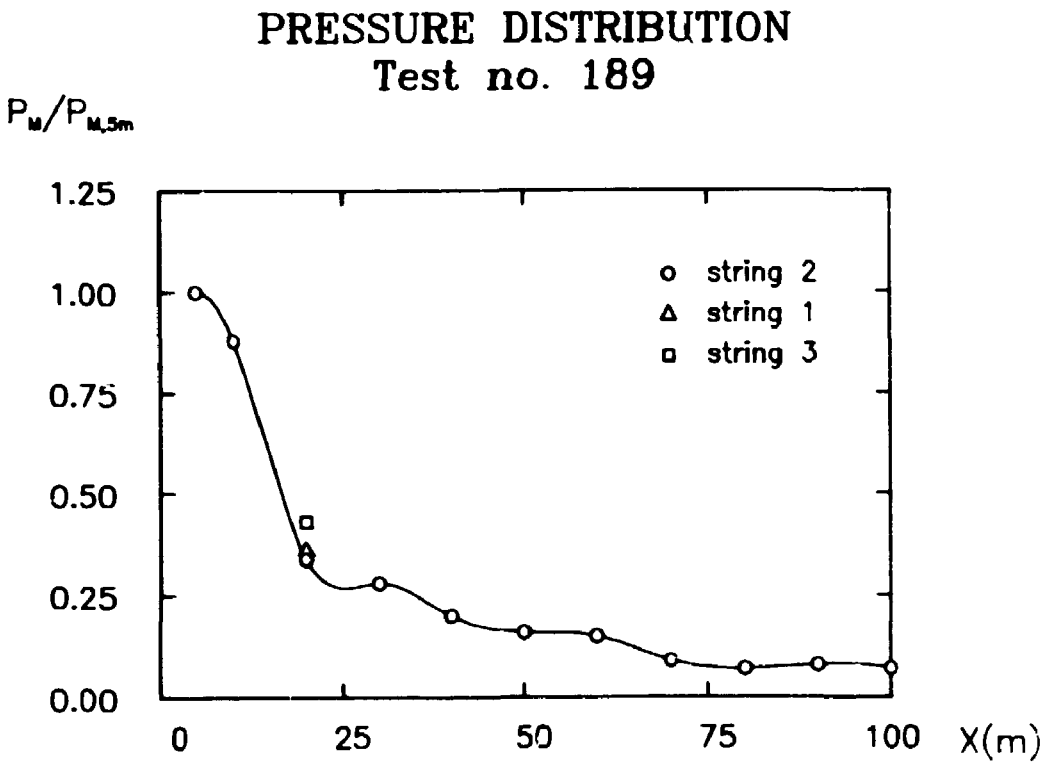

Fig. 3.6.2.3. Normalized peak pressure.

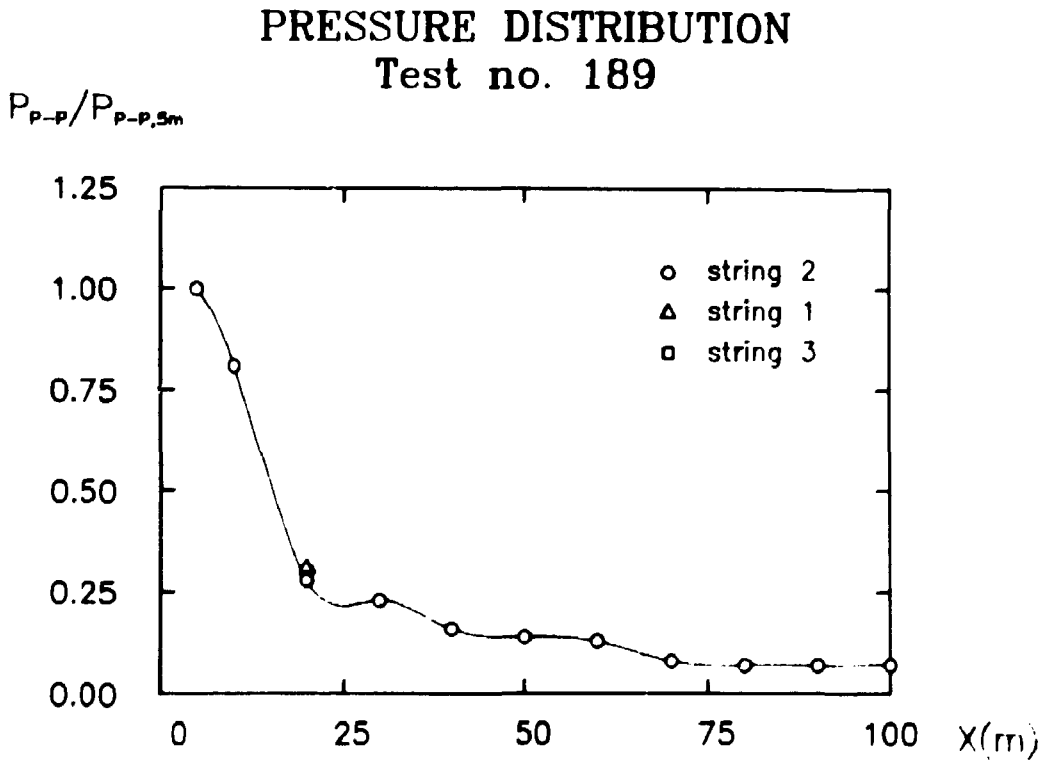

Fig. 3.6.2.4. Normalized peak-to-peak pressure.

No. 190

Date: 5/1-84

Time: 11.25

Purpose: To investigate the pressure wave propagation over a free field.

Atmosphere: neutral

Windspeed {m/sec} 2.0 m : 3.14
4.3 m : 3.66
8.5 m :

Wind direction {°from N}: 288

Temperature {°C} 2.0 m : 2.5
8.5 m : 2.5

Direct measured temperature difference {°C}: -0.04

Atmospheric pressure {mbar}: 1008.1

Balloon: 1100 g Delasson

Gas mixture {vol. %}: CH_4= 25, O_2= 50, N_2= 25

Volume {m^3}: 10

Explosion max. pressure {mbar} 5.0 m : 119
pp. pressure {mbar} 5.0 m : 258

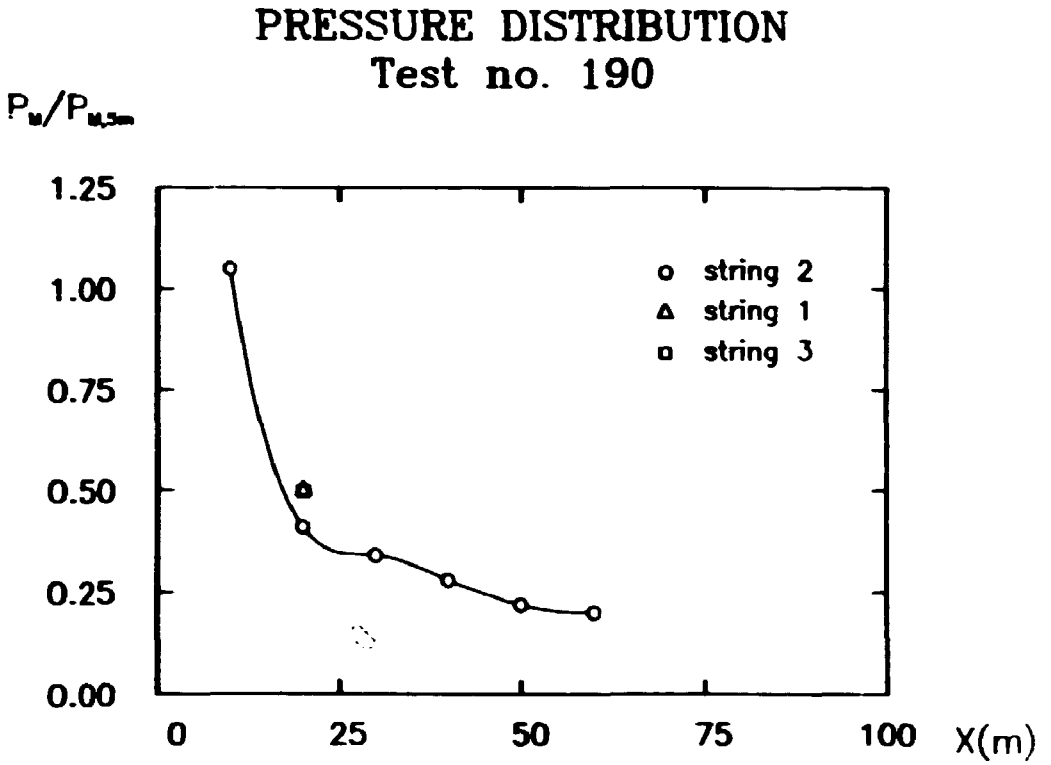

Fig. 3.6.2.5. Normalized peak pressure.

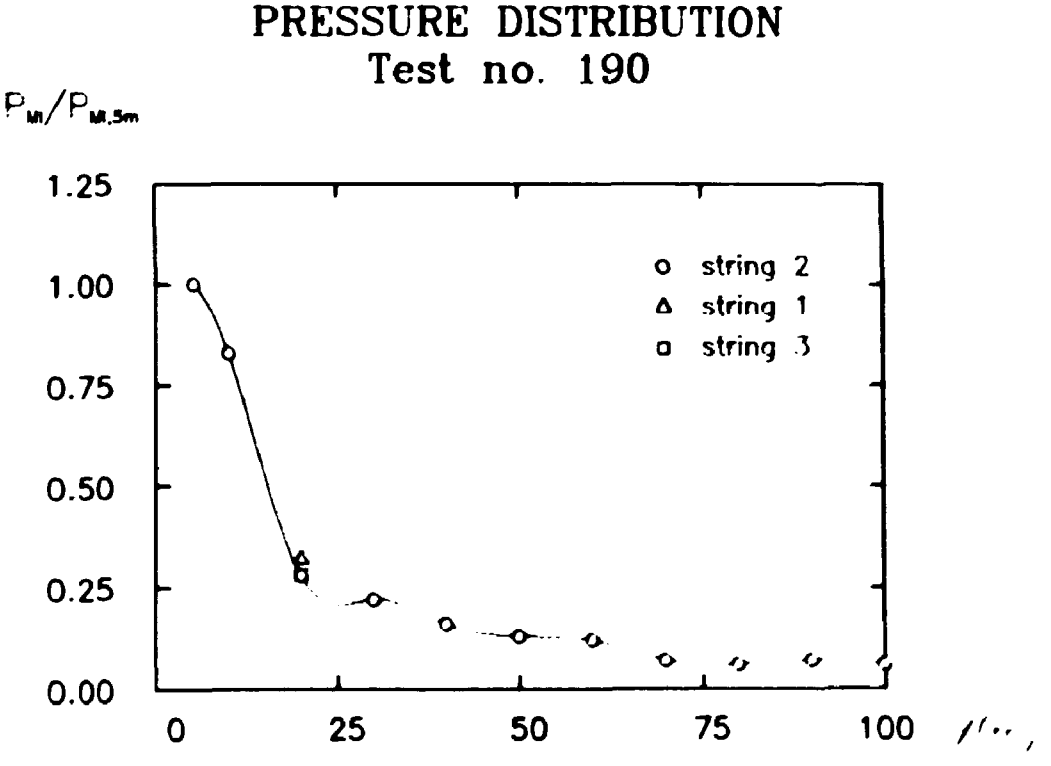

Fig. 3.6.2.6. Normalized min. peak pressure.

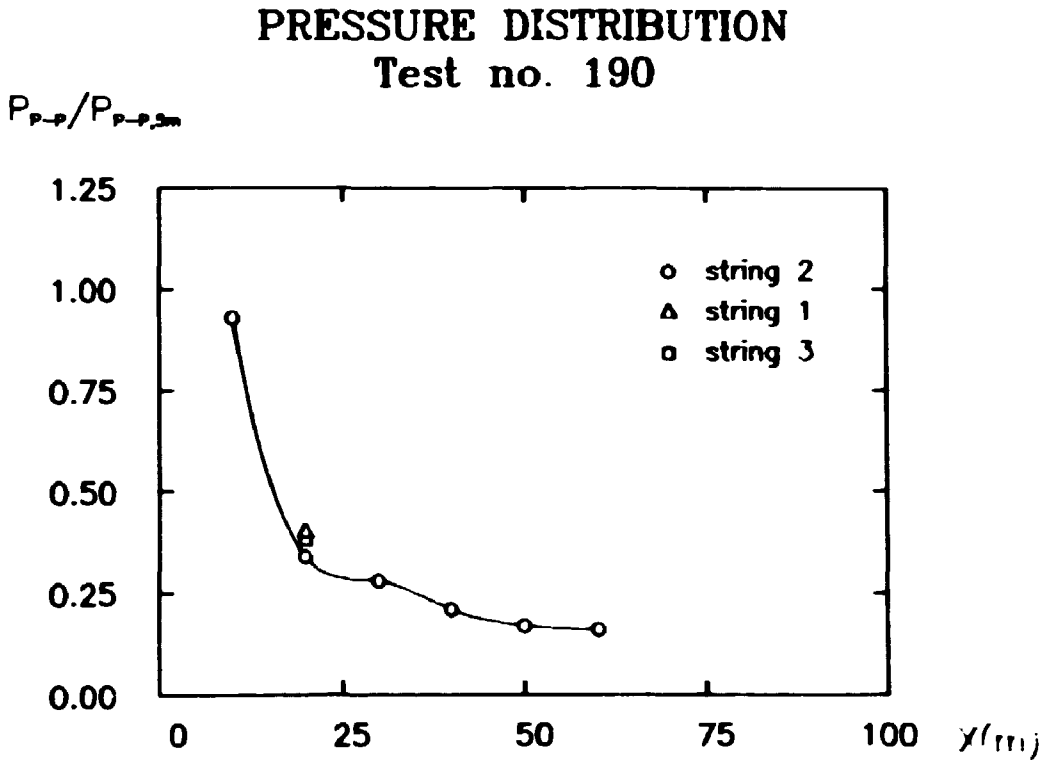

Fig. 3.6.2.7. Normalized peak-to-peak pressure.

No. 191

Date: 5/1-84

Time: 12.50

Purpose: To investigate the pressure wave propagation over a free field.

Atmosphere: unstable

Windspeed {m/sec} 2.0 m : 3.38
4.3 m : 3.94
8.5 m :

Wind direction {°from N}: 260

Temperature {°C} 2.0 m : 2.8
8.5 m : 2.7

Direct measured temperature difference {°C}: -0.09

Atmospheric pressure {mbar}: 1008.4

Balloon: 1100 α Delasson

Gas mixture {vol. %}: CH_4= 25, O_2= 50, N_2= 25

Volume {m^3}: 5

Explosion max. pressure {mbar} 5.0 m : 55
pp. pressure {mbar} 5.0 m : 131

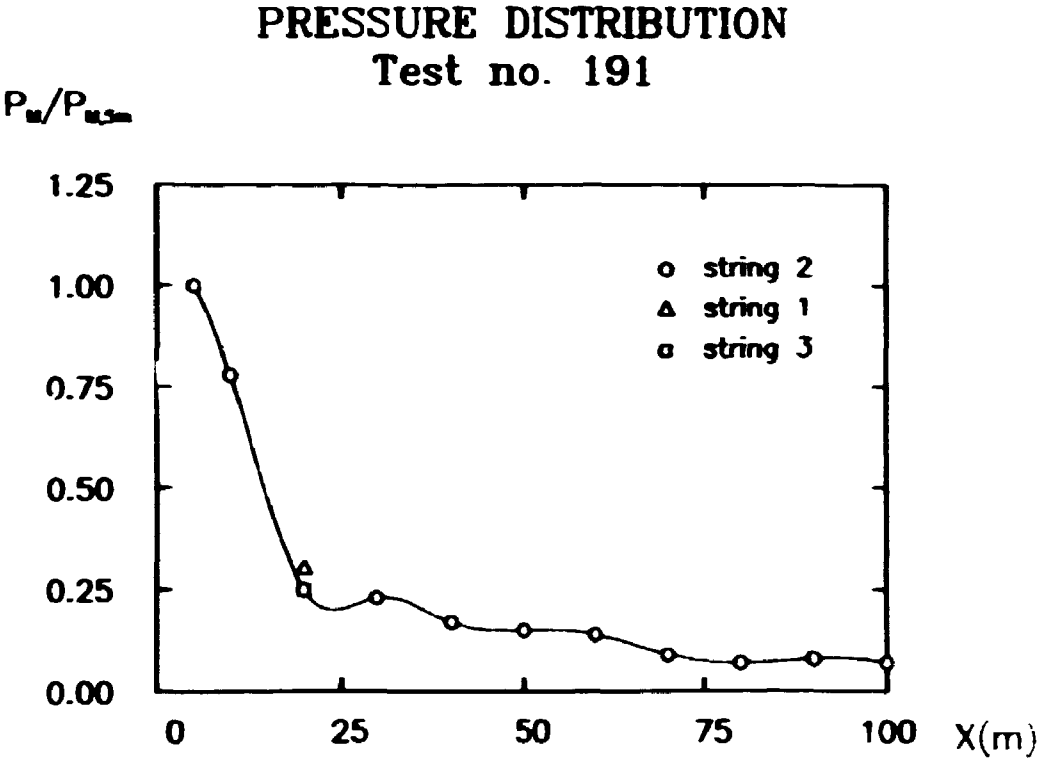

Fig. 3.6.2.8. Normalized peak pressure.

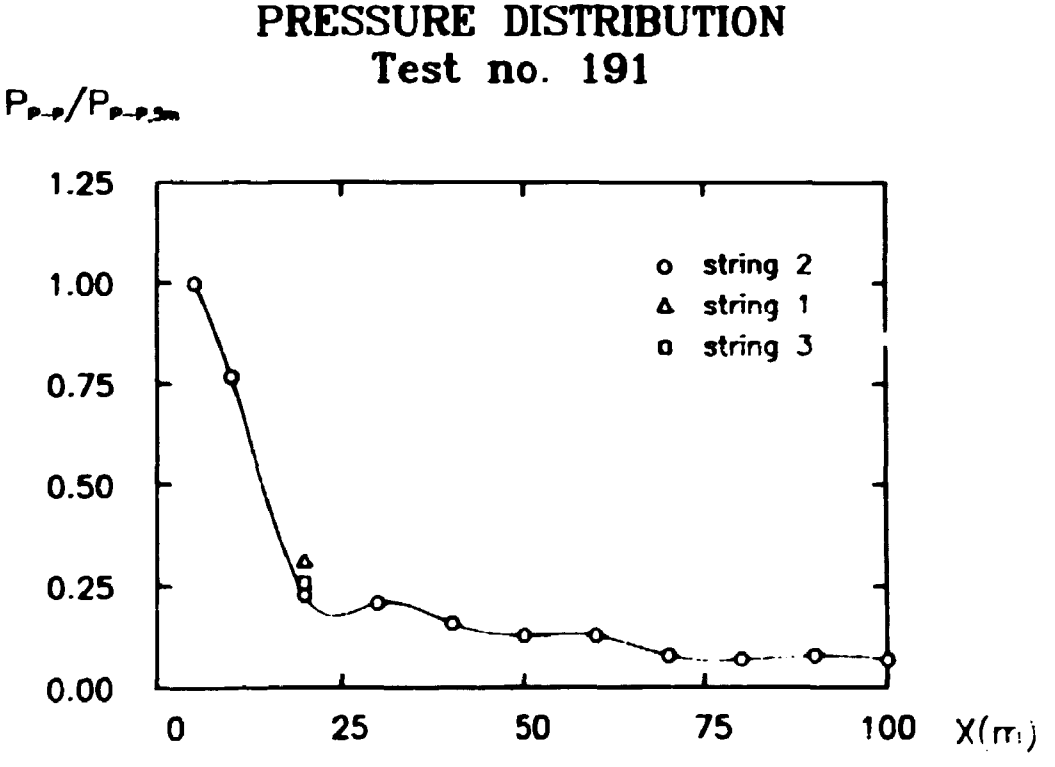

Fig. 3.6.2.9. Normalized peak-to-peak pressure.

3.6.3. EVALUATION OF THE RESULTS

The measurements along a line in a free area (tests number 189, 190 and 191) show good agreement with the 1/R attenuation (section 3.10).

The results from the measurements of the symmetry are presented in Table 3.6.3.1 below.

EXP. NO.	STRING 1 {mbar}	STRING 2 {mbar}	STRING 3 {mbar}	WIND DIRECTION {°from N}	WIND SPEED {m/s}
189	15	14	17	274°	4.0
190	59	48	59	288°	3.7
191	17	14	14	260°	4.0

Table 3.6.3.1. Measurements of the symmetry 20 m from the center of the explosion.

The mean value of the above pressure measurements performed in different directions together with the standard deviation in percentage of the mean value are, for each particular experiment, given in Table 3.6.3.2 below.

EXP. NO.	MEAN {mbar}	$\sigma_{\%}$ {%}
189	15.3	10
190	55.3	12
191	15.0	12

Table 3.6.3.2. Mean and coefficient of variation corresponding to the symmetry measurements.

It is seen, that the $\sigma_{\%}$ - values are within the estimated scatter (section 3.3.2) at the actual measuring distance, and it is therefore concluded, that the explosions possess full rotational symmetry.

3.6.4. SHOCK-UP PHENOMENON

In a few tests, the shock-up phenomenon as mentioned by Essers [9] has been observed (for example test number 190).

For large overpressures the propagation of the explosion wave will be nonlinear. As a result the local speed of sound directly in front of the propagating wave will become greater, and therefore the front will be still steeper. In experiment number 190 the initial pressure was high enough to generate this phenomenon. This is illustrated in Fig. 3.6.4.1.

The time taken from the wave starts the pressure built up until it has reached the maximum pressure in a given position is $\tau \approx 0.013$s, and the maximum overpressure is $P_M \approx 119$ mbar measured at the 5 m mast.

The analytic expressions for time and distance for building up a shock are [9]

$$\theta = \frac{1}{2} \frac{U_f + c_f + c_0}{U_f + c_f - c_0} \tau$$

$$\lambda = \frac{1}{4} \frac{(U_f + c_f + c_0)^2}{U_f + c_f - c_0} \tau$$

where θ is the time required for the shock formation, and $\gamma = 1.4$ is the ratio of specific heats. c_f is the speed of sound and U_f the particle velocity corresponding to the flow at the end of the compression phase. λ is the distance required for complete shock formation, and c_0 is the speed of sound in the undisturbed atmosphere.

The isentropic expressions for U_f and c_f are [9]

$$U_f = c_0 \left(\frac{1}{\gamma} \frac{P_M}{P_0} \left[1 - \left[1 + \frac{P_M}{P_0} \right]^{-\frac{1}{\gamma}} \right] \right)^{\frac{1}{2}}$$

$$c_f = c_0 + \Delta c = c_0 + c_0 \left[1 + \frac{P_M}{P_0} \right]^{\frac{\gamma-1}{2\gamma}} - c_0 = c_0 \left[1 + \frac{P_M}{P_0} \right]^{\frac{\gamma-1}{2\gamma}}$$

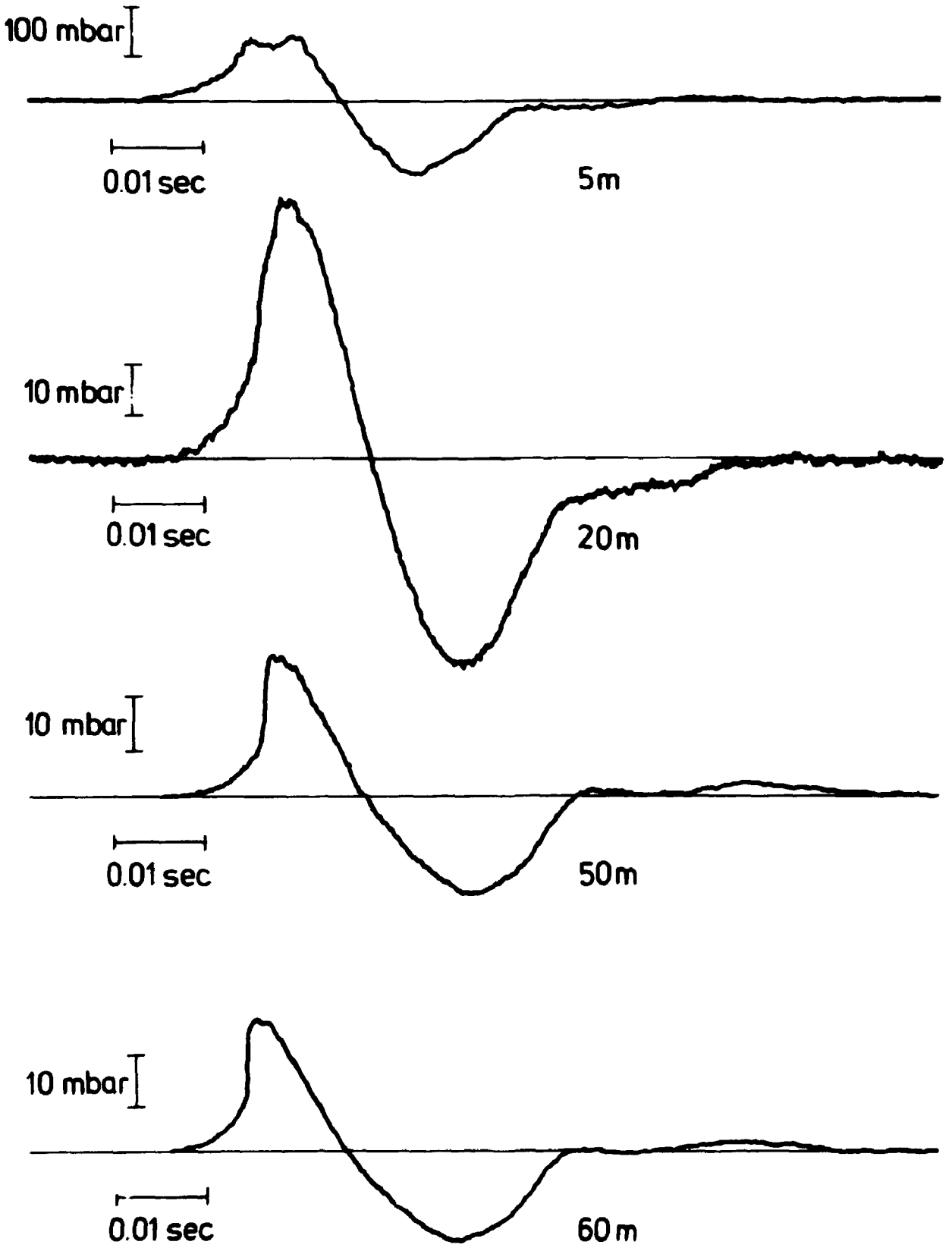

Fig. 3.6.4.1. Shock-up phenomena observed in the experiment no. 190.

Since P_M is the overpressure at the end of the compression phase, it is obtained using the pressure at the 5 m mast and not taking the drop of pressure into account. Setting the speed of sound $c_0 = 330$ m/sec you get $\lambda \approx 54$ m.

The model is given for waves without geometrical damping. Therefore this value is only a rough approximation and a new calculation with this as starting point gives $\lambda \approx 91$ m. Further interpolations will not be worth while, taking the accuracy of the measurements into account. The corresponding value is $\theta = 0.26$ sec.

3.7. PRESSURE PROPAGATION IN A WOOD

In order to investigate the blast wave attenuation due to vegetation, a series of experiments, concerning the pressure wave propagation in a wood, has been carried out. The forest consists mainly of larch trees, and since the measurements were done at the end of December the trees were without needles. The forest is situated on a comparatively plane area, which means that disturbing effects due to depressions and banks in the terrain, are avoided. As a measure of the planting density, the distance between the trees ranged between 1.5 and 2.0 m. Figures 3.7.1 and 3.7.2 give an impression of the forest.

Fig. 3.7.1. The edge of the forest.

Fig. 3.7.2. A view inside the forest.

3.7.1. EXPERIMENTAL SETUP

The experimental setup for the wood-tests is outlined in Fig. 3.7.1.1 below

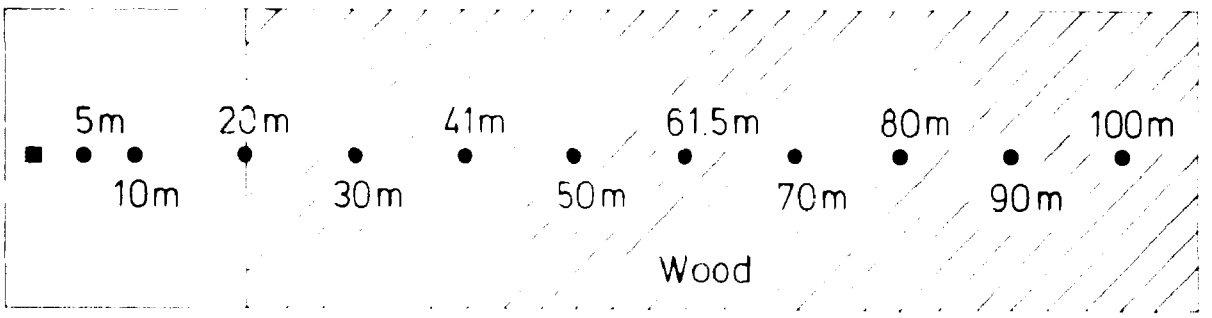

Fig. 3.7.1.1. The experimental setup.

The " ■ " symbolize the source, and the "●" symbolize the pressure measuring poles placed at different distances from the source, all at a height of 1.8 m from the ground. The hatching symbolize the forest, and it is seen, that the center of the source is located 1.2 m outside the edge of the wood.

As mentioned in [2], there should be no measurable differences between the attenuation rates over the row of trees and diago-

nally across them. This means that the angle between the direction of measurements and the direction of "planting" can be neglected in the present experiments.

3.7.2. RESULTS

The experimental data and the data from the meteorological measurements are given in the following tables referring to experiment numbers 187 and 188.

The pressure-time history recorded in different distances from the source are qualitatively similar to the ones obtained in the free field tests.

On the basis of such pressure-time curves, the normalized peak and the normalized peak-to-peak pressures are evaluated. The distance attenuation is shown in the Figures 3.7.2.1-4, where the normalized pressure values have been given as a function of the distance from the center of the gas cloud.

No. 187

Date: 21/12-83

Time: 12.19

Purpose: To investigate the pressure wave propagation in a wood.

Atmosphere: neutral

Windspeed {m/sec} 2.0 m : 3.24
4.3 m : 3.63
8.5 m :

Wind direction {°from N}: 135

Temperature {°C} 2.0 m : 3.5
8.5 m : 3.5

Direct measured temperature difference {°C}: - 0.04

Atmospheric pressure {mbar}: 994.2

Balloon: 1100 g Delasson

Gas mixture {vol. %}: CH_4= 25, O_2= 50, N_2= 25

Volume {m^3}: 10

Explosion max. pressure {mbar} 5.0 m : 49
pp. pressure {mbar} 5.0 m : 134

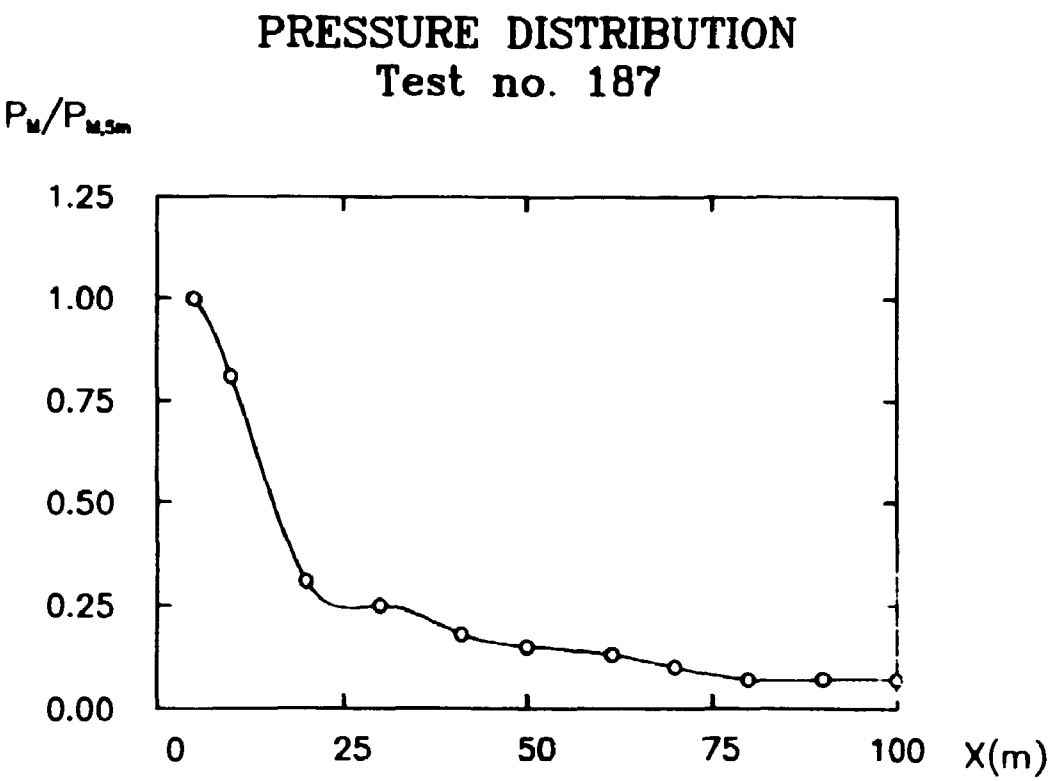

Fig. 3.7.2.1. Normalized peak pressure.

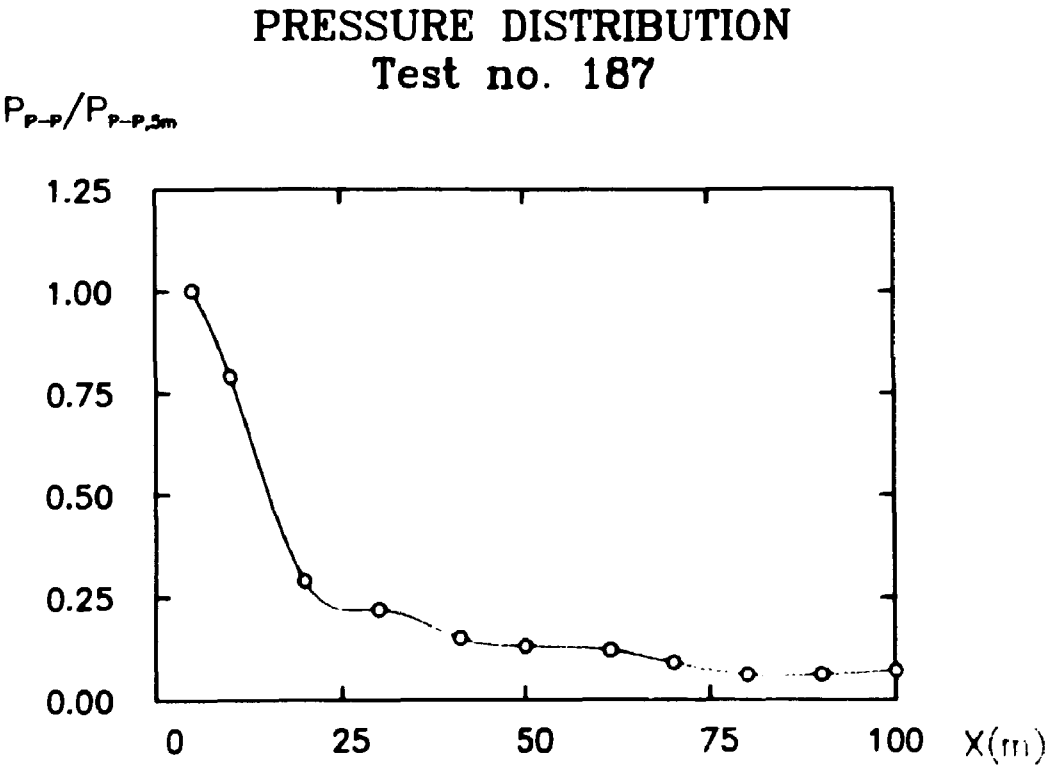

Fig. 3.7.2.2. Normalized peak-to-peak pressure.

No. 188

Date: 21/12-85

Time: 13.57

Purpose: To investigate the pressure wave propagation in a wood.

Atmosphere: neutral

Windspeed {m/sec} 2.0 m : 3.24
4.3 m : 3.63
8.5 m :

Wind direction {°from N}: 135

Temperature {°C} 2.0 m : 3.5
8.5 m : 3.5

Direct measured temperature difference {°C}: 0.00

Atmospheric pressure {mbar}: 993.8

Balloon: 1100 g Delasson

Gas mixture {vol. %}: CH_4= 25, O_2= 50, N_2= 25

Volume {m^3}: 10

Explosion max. pressure {mbar} 5.0 m : 100
pp. pressure {mbar} 5.0 m : 200

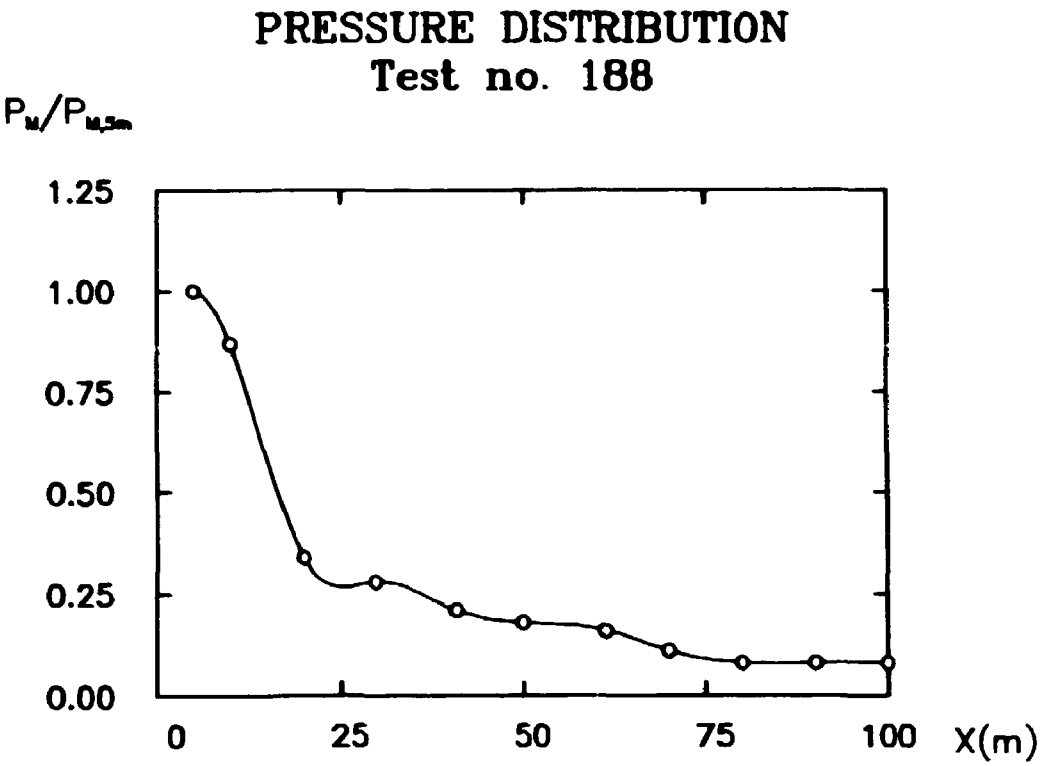

Fig. 3.7.2.3. Normalized peak pressure.

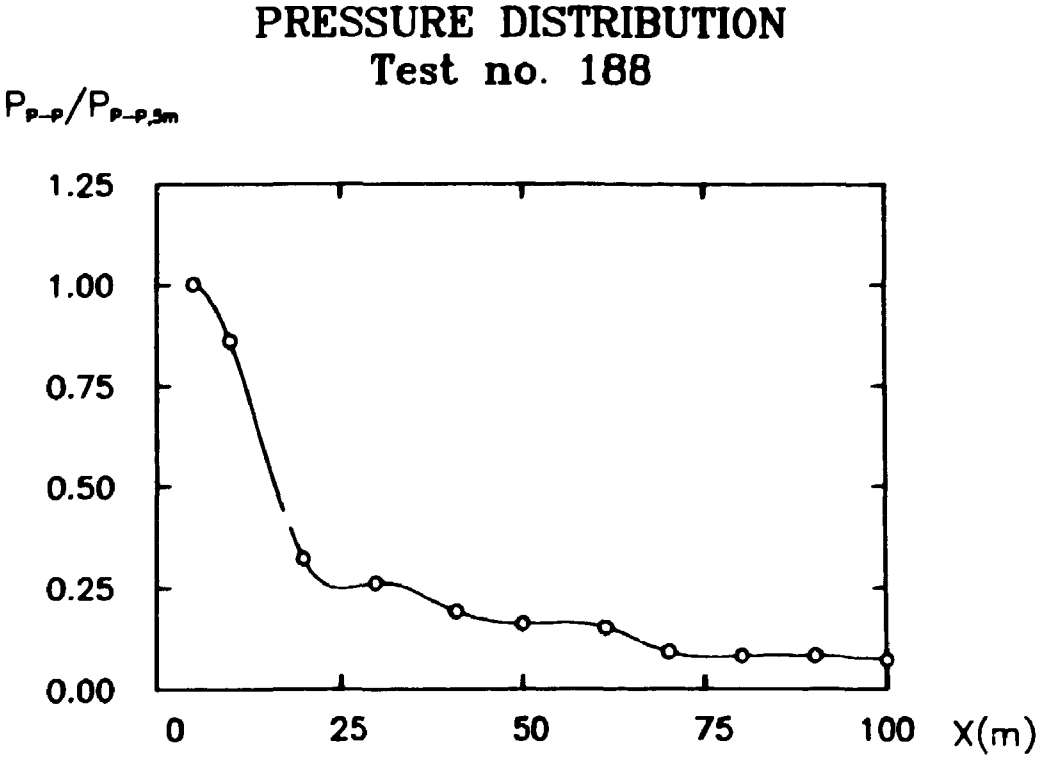

Fig. 3.7.2.4. Normalized peak-to-peak pressure.

3.7.3. EVALUATION OF THE RESULTS

It is seen that the results corresponding to test numbers 187 and 188 are in mutual agreement, taking the estimated uncertainties of the measurements into account. Furthermore, the curves presented in Figures 3.7.2.1-4 are qualitatively in agreement with the corresponding results obtained from the free-field measurements. Finally, the regression analysis performed in the succeeding section 3.10 shows that these corresponding results, in this specific sense, are also quantitatively in agreement.

This means that no significant pressure wave attenuation due to this specific vegetation is observed. Moreover, as the pressure wave cannot feel the vegetation, there will be no "edge" effects in the transition zone between the free field and the forest (stagnation pressure etc.).

These results are in agreement with the results obtained in [6] for harmonic signals, where it is concluded that vegetation will have an effect on sound propagation only at high frequencies (> 1kHz). The dominant frequency of the present blast waves is 15 Hz.

3.8. PRESSURE PROPAGATION AROUND A BANK OF EARTH

The objective of the present section is to study the influence from the topography on the pressure wave propagation. For this purpose a bank of earth has been erected on the test-site formerly used for the free field measurements. This test-site is plane and without vegetation. A sketch of this simple and geometrically well-defined obstacle is given in Fig. 3.8.1.

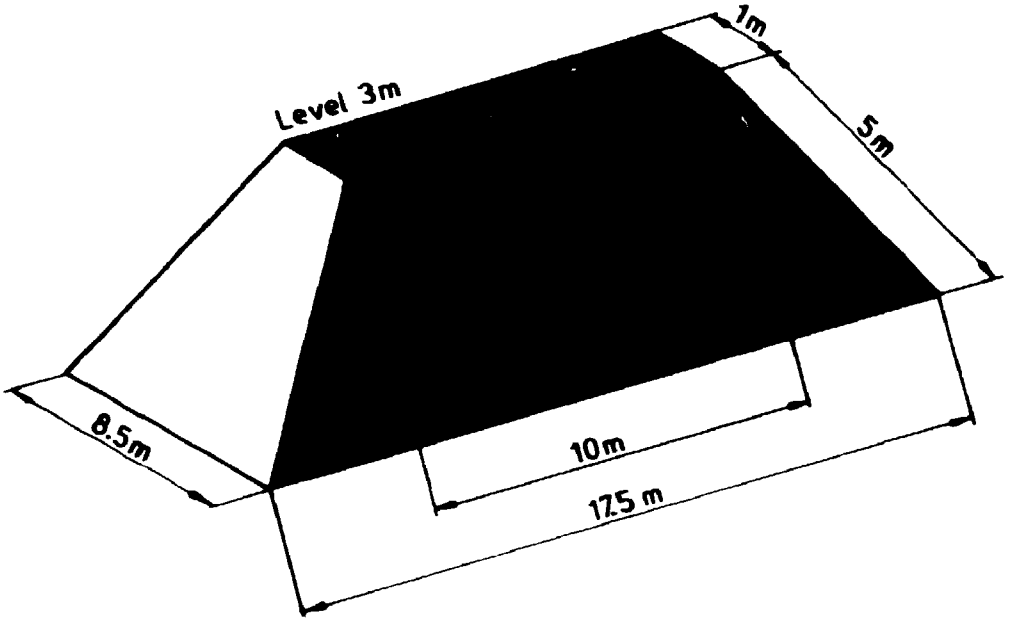

Fig. 3.8.1. Geometry and dimensions of the obstacle.

The obstacle is located at a distance of 30 m from the explosion center.

Fig. 3.8.2 gives an impression of the topography on the test site.

Fig. 3.8.2. Topography of the test site.

3.8.1. EXPERIMENTAL SETUP

The experimental setup for the actual tests is outlined in Fig. 3.8.1.1 below

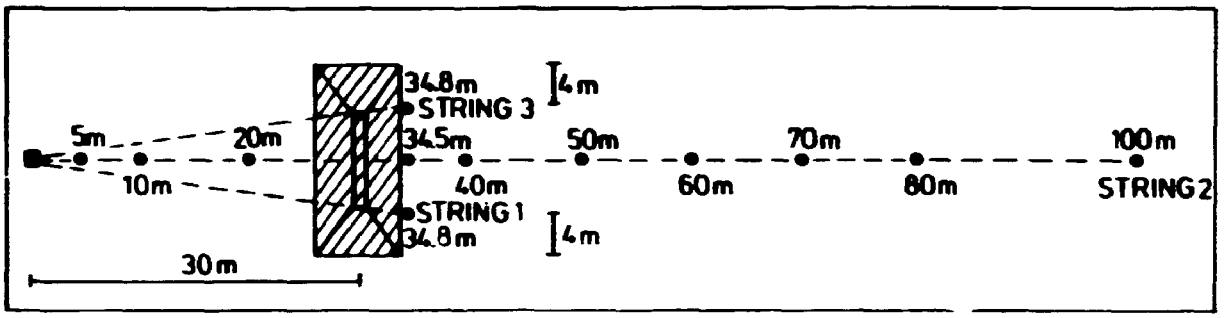

Fig. 3.8.1.1. The experimental setup.

As in the previous sections "■" symbolizes the source and "●" symbolizes the pressure-measuring points placed in different positions, all in a height of 1.8 m from the ground. The hatched area symbolizes the bank of earth. It is seen that the measurements have been performed in 3 different directions denoted by string 1, 2 and 3.

3.8.2. RESULTS

The experimental data and the data from the meteorological measurements are given in the following tables referring to experiment numbers 185 and 186.

The pressure measurement at string 3, shown in Fig. 3.8.1.1, was unfortunately lost due to an error in the measuring chain.

From pressure-time curves, which again are qualitatively similar to the ones obtained in the free-field tests, the normalized peak and the normalized peak-to-peak pressures are evaluated and given as a function of the distance from the center of the gas cloud in Figures 3.8.2.1-4.

No. 185

Date: 20/12-83

Time: 13.07

Purpose: To measure the pressure in front of, on and behind a bank of earth located at a distance of 30 m from the center of the explosion.

Atmosphere: neutral

Windspeed (m/sec) 2.0 m : 2.23
4.3 m : 2.62
8.5 m :

Wind direction (°from N): 211

Temperature (°C) 2.0 m : 4.0
8.5 m : 4.0

Direct measured temperature difference (°C): 0.00

Atmospheric pressure (mbar): 994.2

Balloon: 1100 g Delasson

Gas mixture (vol. %): CH_4 = 25, H_2 = 50, N_2 = 25

Volume (m^3): 10

Explosion max. pressure (mbar) 5.0 m : 177
pp. pressure (mbar) 5.0 m : 144

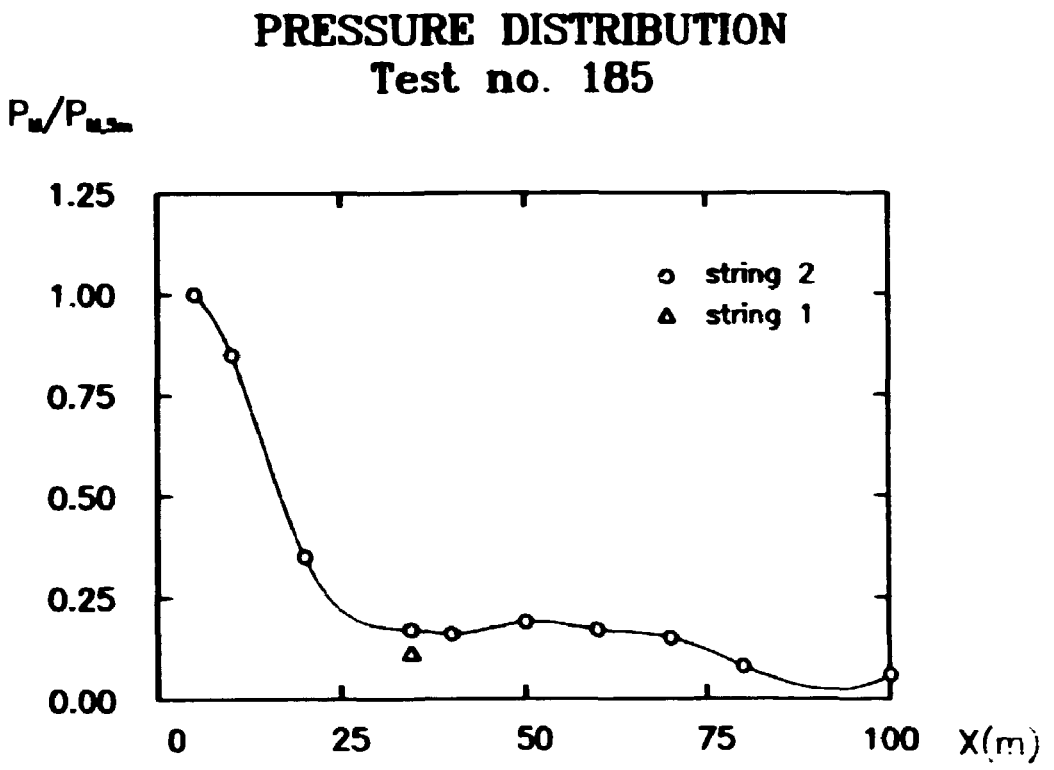

Fig. 3.8.2.1. Normalized peak pressure.

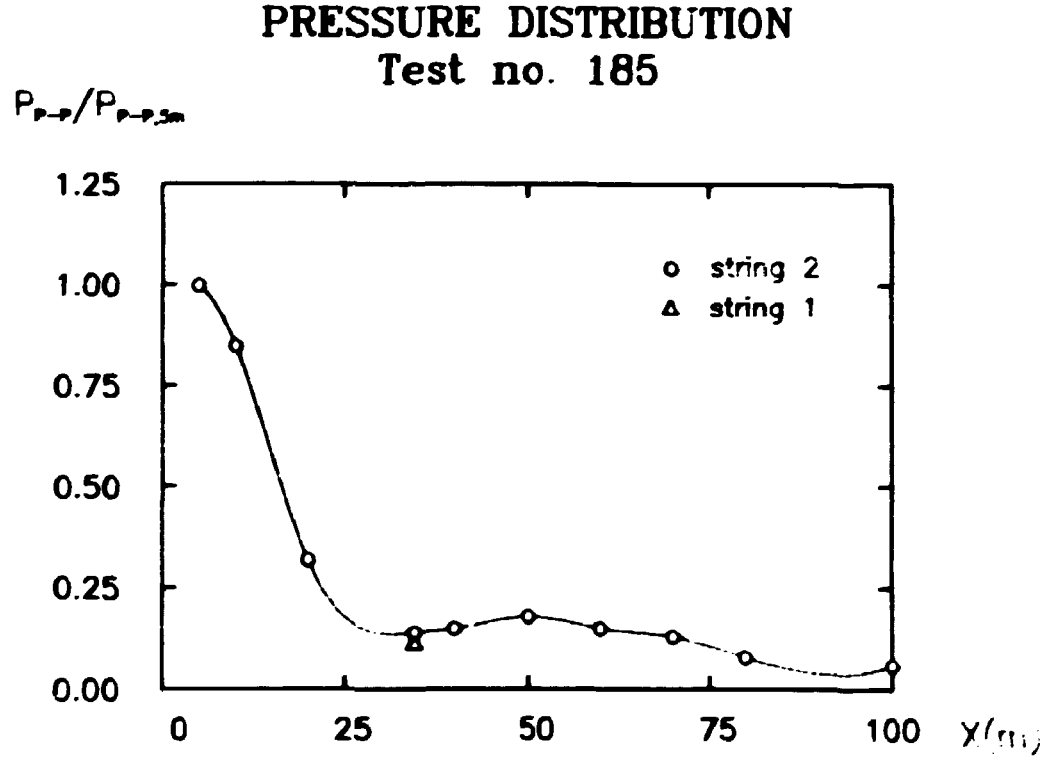

Fig. 3.8.2.2. Normalized peak-to-peak pressure.

No. 186

Date: 20/12-83

Time: 14.35

Purpose: To measure the pressure in front of, on and behind a bank of earth located at a distance of 30 m from the center of the explosion.

Atmosphere: stable

Windspeed (m/sec) 2.0 m : 1.96
4.3 m : 2.30
8.5 m :

Wind direction (°from N): 209

Temperature (°C) 2.0 m : 4.1
8.5 m : 4.1

Direct measured temperature difference (°C): 0.05

Atmospheric pressure (mbar): 994.6

Balloon: 1100 g Delasson

Gas mixture (vol. %): CH_4= 25, O_2= 50, N_2= 25

Volume (m^3): 7.5

Explosion max. pressure (mbar) 5.0 m : 9[illegible]
pp. pressure (mbar) 5.0 m : [illegible]

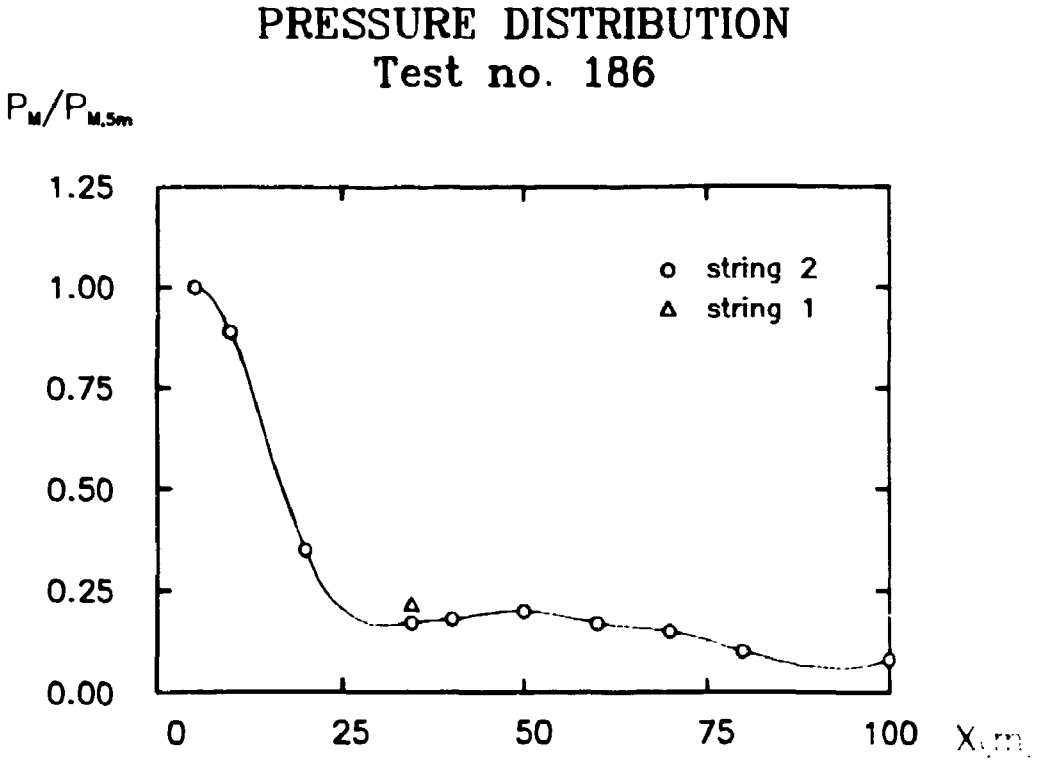

Fig. 3.8.2.3. Normalized peak pressure.

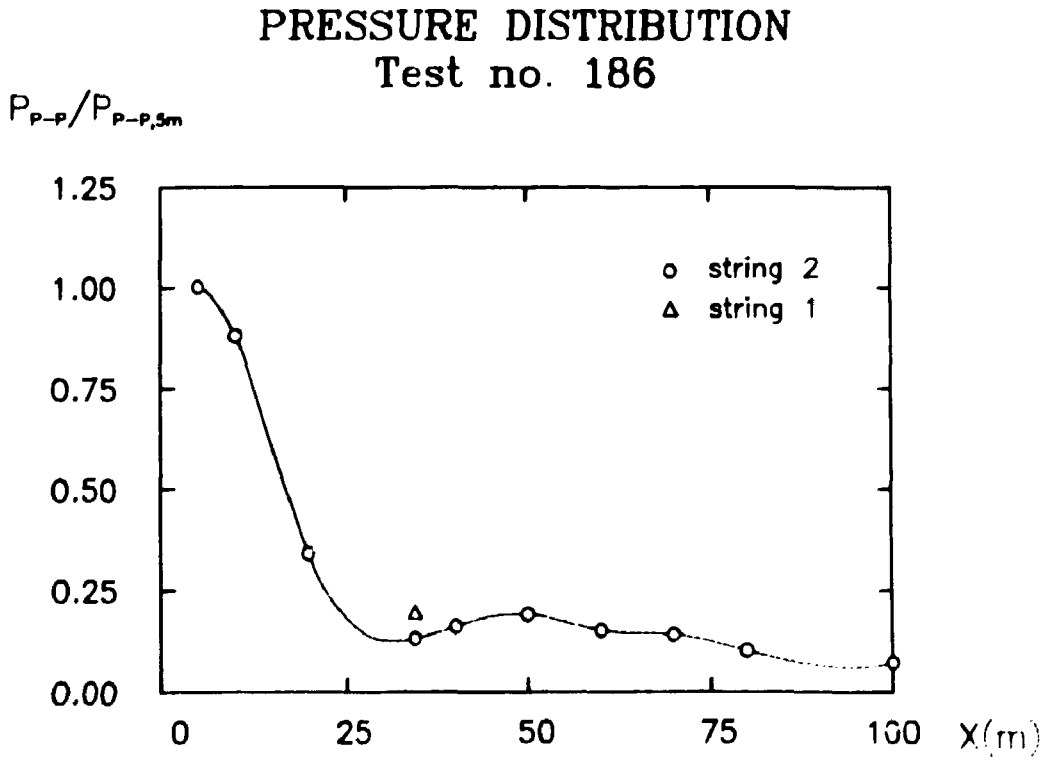

Fig. 3.8.2.4. Normalized peak-to-peak pressure.

3.8.3. EVALUATION OF THE RESULTS

The results obtained in test numbers 185 and 186 are mutually in agreement within the estimated uncertainties of the experiments, except for the string 1 measurement. The deviations in the string 1 measurements might be explained by turbulence effects at the end regions of the bank. Moreover, the results for string 2 presented in the Figures 3.8.2.1 - 4 are qualitatively in agreement with the corresponding results obtained from the free-field measurements, except for the measuring points just behind the bank (in 34.5 and 40.0 m distance from the source). Finally the regression analysis performed in the succeeding section 3.10 shows that these corresponding results, in this specific sense, are also quantitatively in agreement.

The conclusion is that the bank can be felt in a shade zone 15 m (corresponding to 5 times the height of the bank or 0.7 times the wavelength of the pressure pulse) behind the bank, whereas the pressure wave propagation at greater distances is uraffected by the presence of the obstacle. The measurements in the end region show considerable fluctuations, although the pressure level is of the same order of magnitude as the pressure level measured just behind the center of the bank.

In [5] a number of experiments with a 550 m long and 2.7 m high earth barrier have been described. The experiments have been performed with harmonic signals. Their experimental setup is in principle identical with the above described.

The measurements have been performed in 40, 70, 120, 170, 220 and 270 m distance from the source. These measurements seem to indicate that the transmission loss due to the earth barrier tends to zero for low frequencies (< 100 Hz). This is in agreement with the present results.

3.9. PRESSURE PROPAGATION IN THE PRESENCE OF A WALL

In the present section the pressure distribution on and around a simple building element is studied.

For this purpose a 10.0 m long, 3.3 m high and 0.1 m thick

light-weight concrete wall was built at a distance of 25 m from the center of the gas clouds, and perpendicular to the direction of the pressure propagation. The wall is shown in Fig. 3.9.1 below

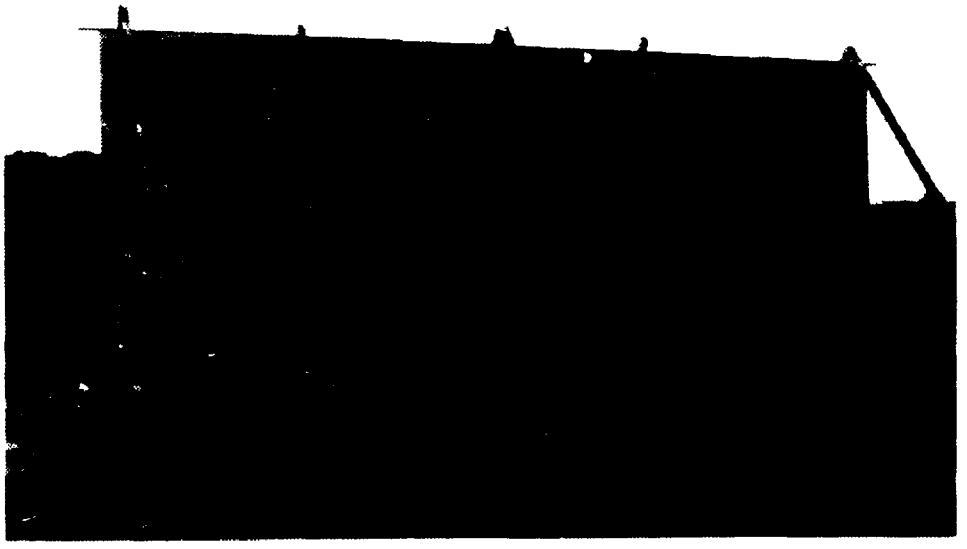

Fig. 3.9.1. Light-weight concrete wall at the test site.

3.9.1. PRESSURE DISTRIBUTION AROUND A WALL

The pressure distribution around the wall is studied in the experiments numbered 125 and 126.

3.9.1.1. EXPERIMENTAL SETUP

The experimental setup corresponding to these tests is outlined in Fig. 3.9.1.1.1.

As in the previous sections "■" symbolizes the source, whereas "●" symbolizes the pressure-measuring points placed in different distances from the source, all at a height of 1.8 m from the ground.

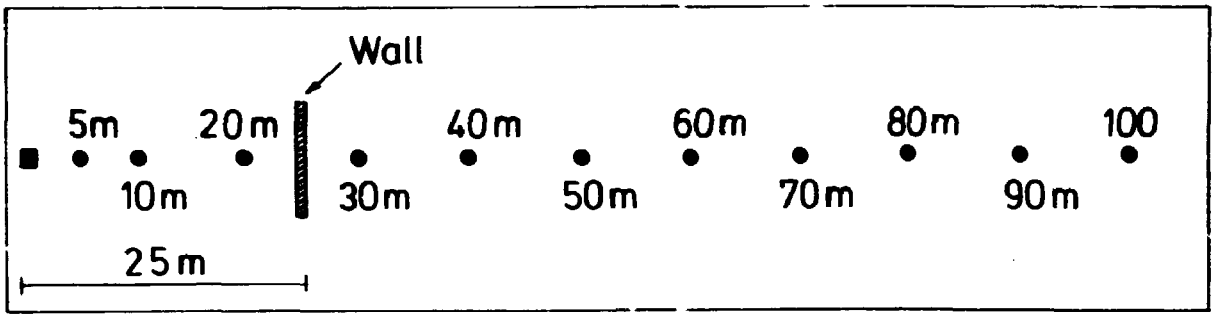

Fig. 3.9.1.1.1. The experimental setup.

3.9.1.2. RESULTS

In the following, the experimental data, and the data from the meteorological measurements are given in the tables referring to experiments numbers 125 and 126.

The pressure pulses recorded in these tests are qualitatively similar to the pulses recorded in the previous tests. The normalized peak and the normalized peak-to-peak pressures are evaluated and given as a function of the distance from the center of the gas cloud in the Figures 3.9.1.2.1-4.

No. 125

Date: 29/9-83

Time: 11.46

Purpose: To measure the pressure in front of and behind a light weight concrete wall located at a distance of 25 m from the center of the explosion.

Atmosphere: unstable

Windspeed (m/sec) 2.0 m : 0.84
4.3 m : 0.98
8.5 m : 1.15

Wind direction {°from N}: 98

Temperature {°C} 2.0 m : 10.7
8.5 m : 10.5

Direct measured temperature difference {°C}: -0.19

Atmospheric pressure {mbar}: 1022.3

Balloon: 1100 g Delasson

Gas mixture {vol. %}: CH_4= 25, O_2= 50, N_2= 25

Volume {m^3}: 10

Explosion max. pressure {mbar} 5.0 m : 41
pp. pressure {mbar} 5.0 m : 91

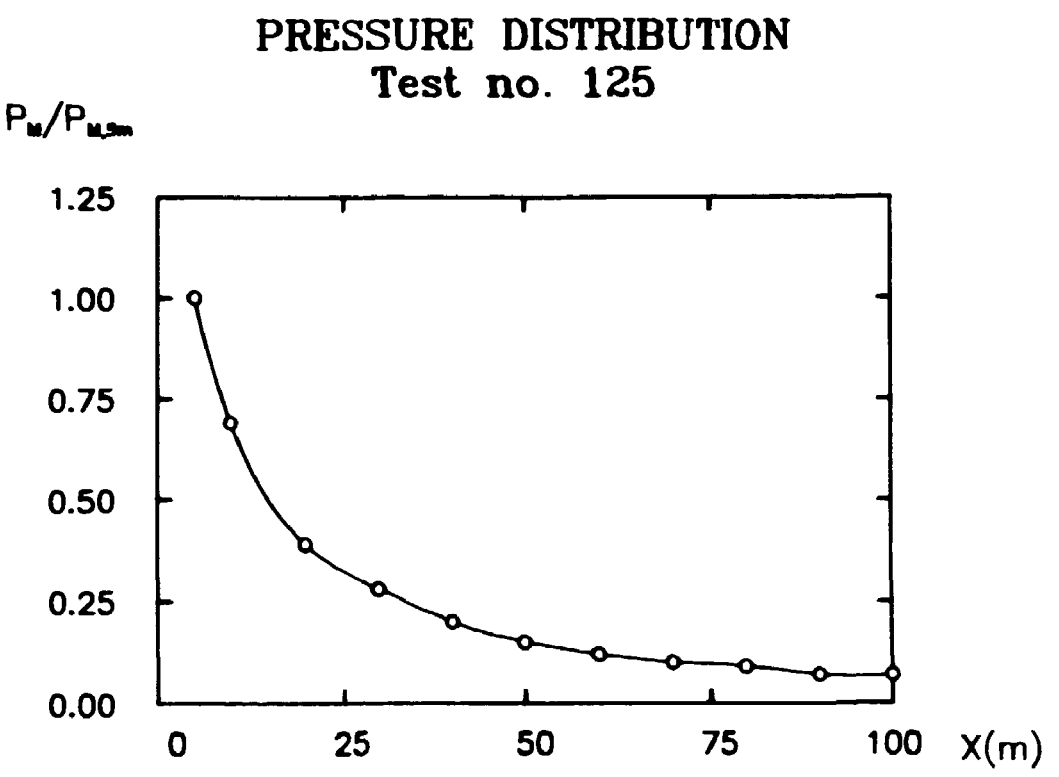

Fig. 3.9.1.2.1. Normalized peak pressure.

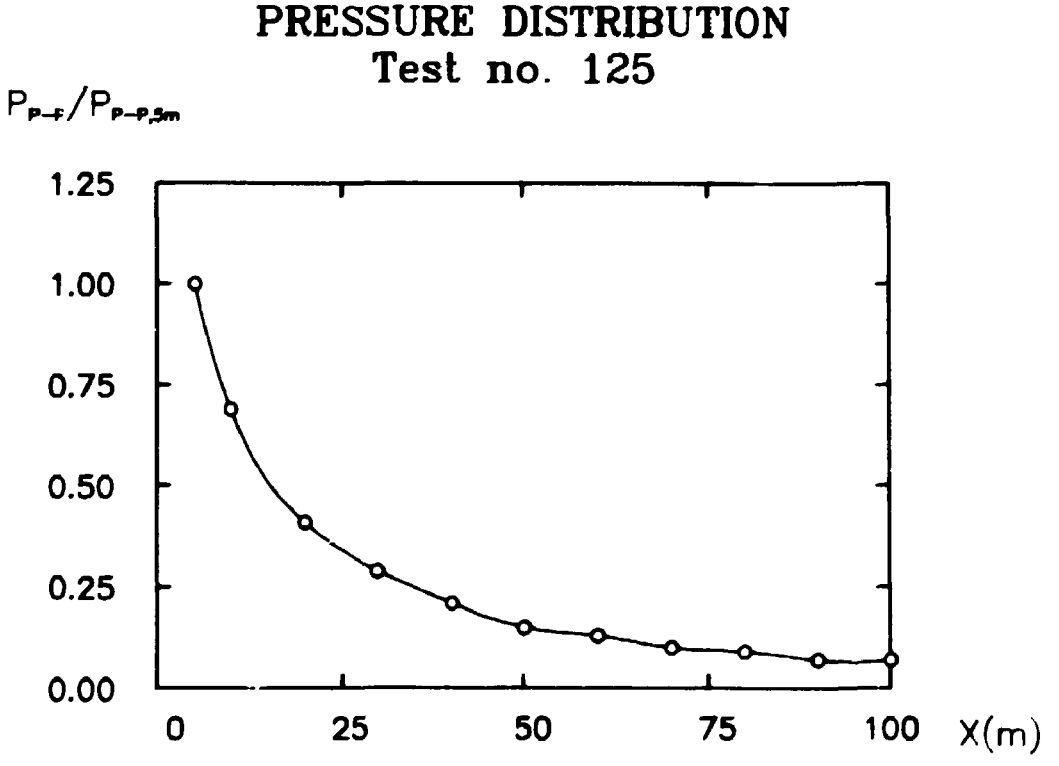

Fig. 3.9.1.2.2. Normalized peak-to-peak pressure.

No. 126

Date: 29/9-83

Time: 14.55

Purpose: To measure the pressure in front of and behind a light weight concrete wall located at a distance of 25 m from the center of the explosion.

Atmosphere: unstable

Windspeed (m/sec) 2.0 m : 0.39
4.3 m : 0.42
8.5 m : 0.60

Wind direction {°from N}: 83

Temperature {°C} 2.0 m : 10.5
8.5 m : 10.4

Direct measured temperature difference {°C}: -0.19

Atmospheric pressure {mbar}: 1020.6

Balloon: 1100 g Delasson

Gas mixture {vol. %}: CH_4= 25, O_2= 50, N_2= 25

Volume {m^3}: 10

Explosion max. pressure {mbar} 5.0 m : 146
pp. pressure {mbar} 5.0 m : 273

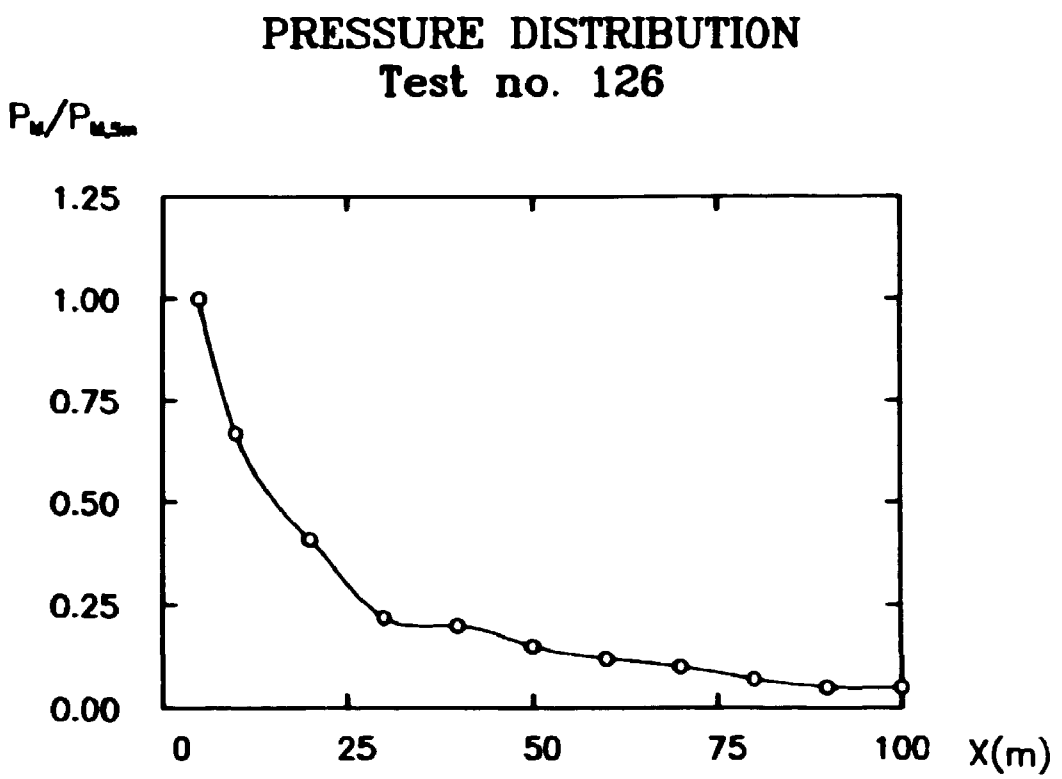

Fig. 3.9.1.2.3. Normalized peak pressure.

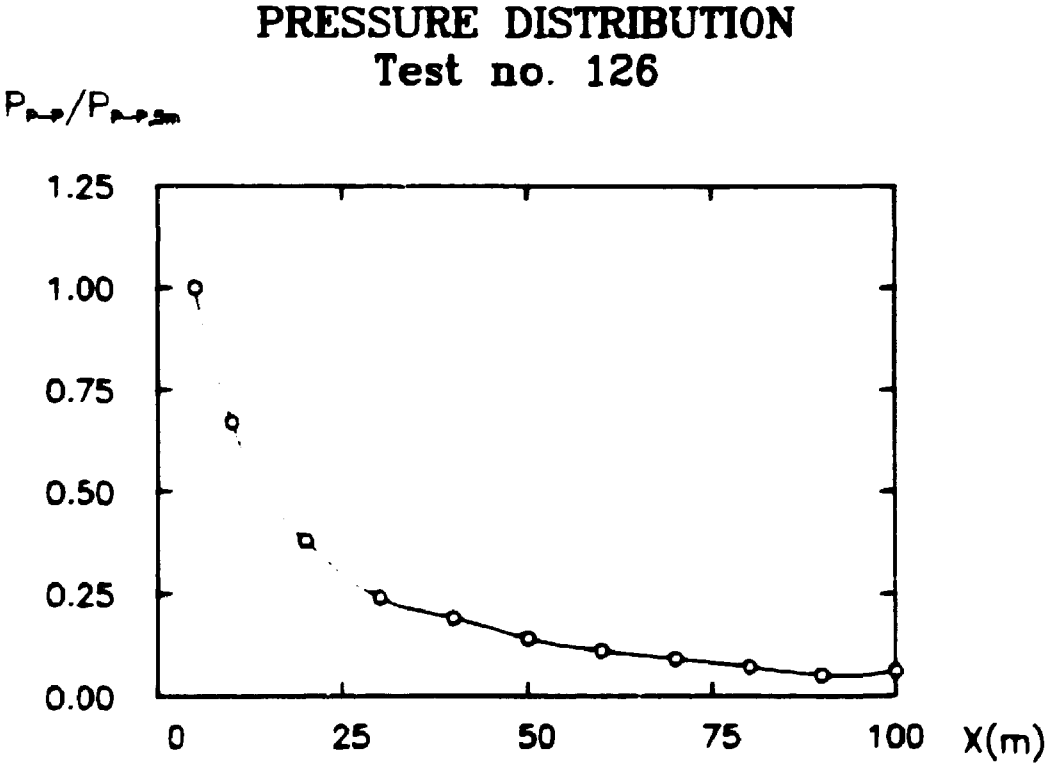

Fig. 3.9.1.2.4. Normalized peak-to-peak pressure.

3.9.1.3. EVALUATION OF THE RESULTS

It is seen that the results obtained in the present two tests are mutually in excellent agreement. Furthermore, it appears that the results presented in Figures 3.9.1.2.1 - 4 are qualitatively in agreement with the corresponding results obtained from the free-field measurements. Finally, the regression analysis performed in the succeeding section 3.10. shows, that the results, in this specific sense, are also quantitatively in good agreement.

The conclusion is that the overall pressure field is unaffected by the presence of the wall. This means that a possible shade zone must have an extension of less than 5 m (corresponding to one third of the wavelength of the signal) behind the wall.

3.9.2. PRESSURE DISTRIBUTION ON A WALL

In experiments number 127, 128, 129, 164, 165, 166, 167, 168 and 169 the pressure distribution on the front and back of the wall has been investigated.

3.9.2.1. EXPERIMENTAL SETUP

The experimental setup corresponding to these tests is outlined in Figures 3.9.2.1.1 and 3.9.2.1.2 below.

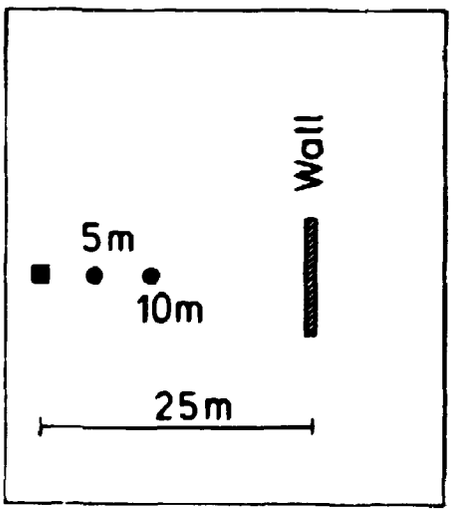

Fig. 3.9.2.1.1. Positions of the reference measuring points.

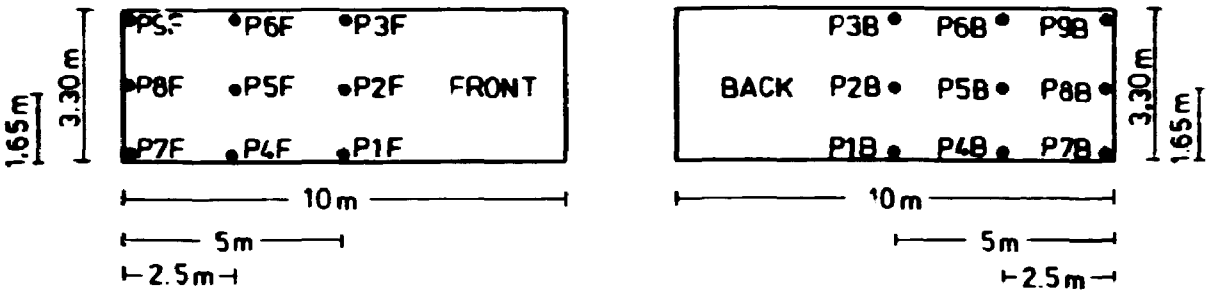

Fig. 3.9.2.1.2. Positions of the measuring points on the wall.

In Fig. 3.9.2.1.1 the positions of the reference measuring points ("●"), relative to the source ("■") and the wall, have been given. In Fig. 3.9.2.1.2 all the measuring positions on the front as well as on the back of the wall have been shown. The "F" and the "B" behind the number of the position refers to the front and to the back, respectively.

However, in a specific experiment, only a part of the measuring points given in Fig. 3.9.2.1.2 have been instrumented. A detailed survey giving the connection between the experiment number and the "active" measuring points, is presented in Table 3.9.2.1.1 below. Here "+" symbolizes an active measuring point.

EXPERIMENT NO.	P1F	P2F	P3F	P4F	P5F	P6F	P7F	P8F	P9F
127	X	X	X					X	
128		X	X				X		X
129	X								X
164	X	X	X				X	X	X
165									
166									
167	X	X	X				X	X	X
168	X	X	X	X	X	X			
169		X							

EXPERIMENT NO.	P1B	P2B	P3B	P4B	P5B	P6B	P7B	P8B	P9B
127									
128		X							
129		X							
164									
165	X	X	X				X	X	X
166	X	X	X				X	X	X
167									
168									
169	X			X	X	X			

Table 3.9.2.1.1. "Active" measuring points.

3.9.2.2. RESULTS

The experimental data, the reference pressures and the data concerning the meteorological measurements are in the following given in the tables referring to the experiments number 127, 128, 129, 164, 165, 166, 167, 168 and 169.

Typical examples of pressure pulses recorded on the wall are presented in Figures 3.9.2.2.1-2 below

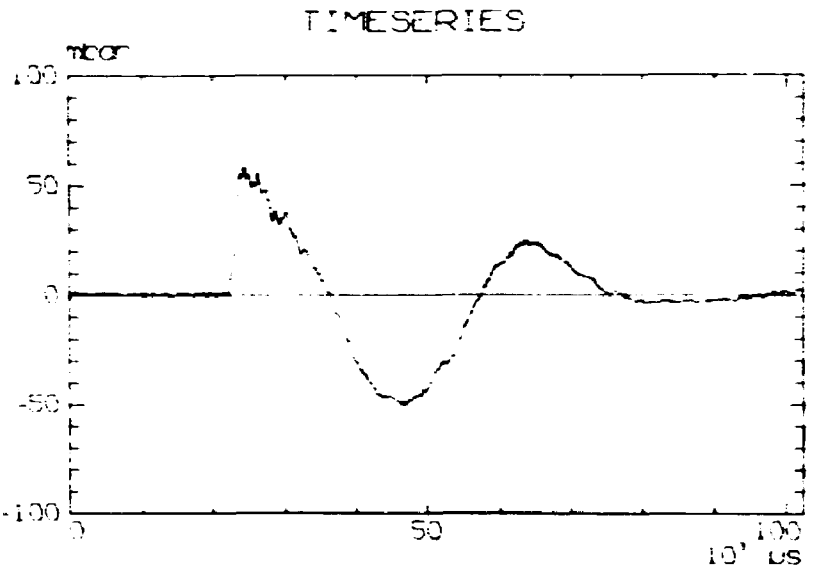

Fig. 3.9.2.2.1. Pressure pulse recorded at P1F in experiment no. 167.

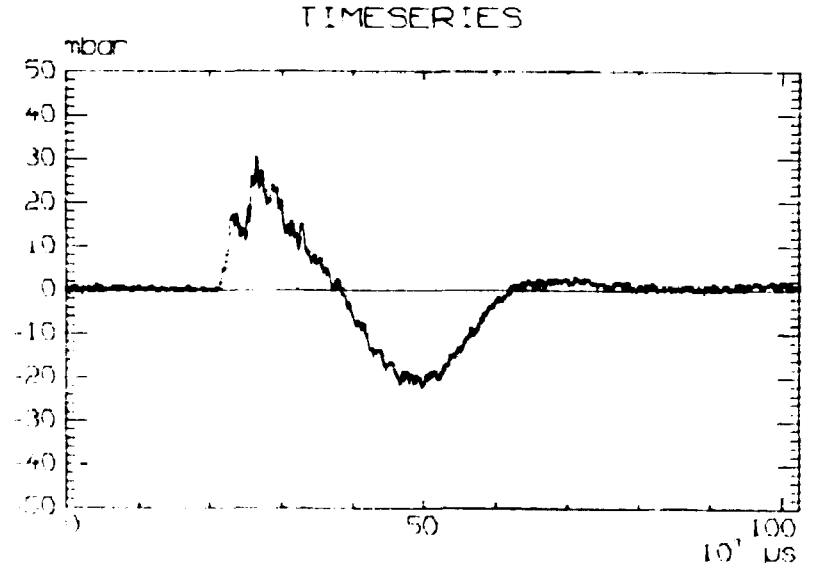

Fig. 3.9.2.2.2. Pressure pulse recorded at P9F in experiment no. 168.

From such pressure-time curves the normalized peak and the normalized peak-to-peak pressures measured on the wall have been evaluated. These are then in the following given as a function of the parameter $^{x}/_{H}$ in different sections of the wall. The sections and the $^{x}/_{H}$ parameter are explained in Fig. 3.9.2.2.3 below

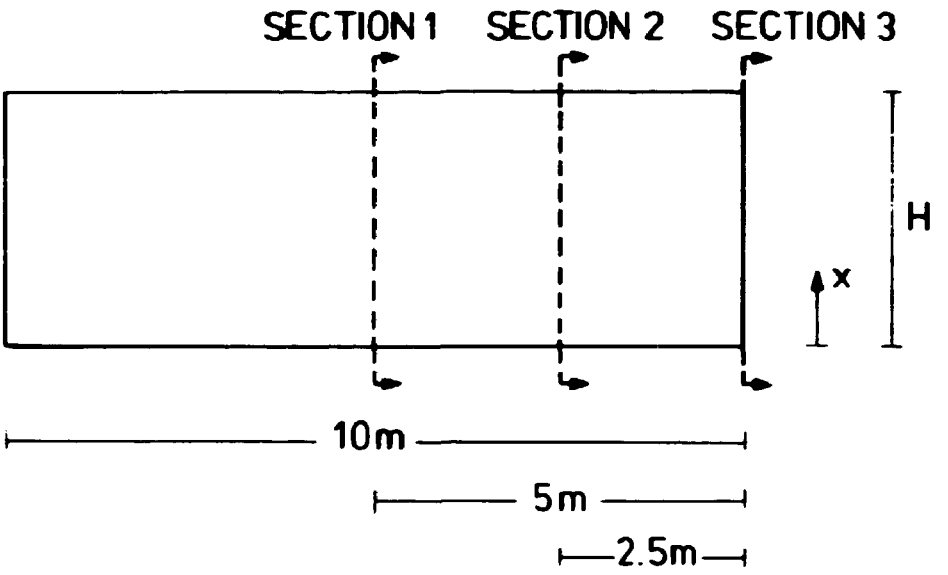

Fig. 3.9.2.2.3. Positions of the sections in the wall.

When a section number is succeeded by an "f" or "b", this will refer to the front and the back of the wall, respectively.

No. 127

Date: 30/9-83

Time: 11.08

Purpose: To measure the pressure distribution on a wall located at a distance of 25 m from the center of the explosion.

Atmosphere: unstable

Windspeed {m/sec} 2.0 m : 1.26
4.3 m : 1.36
8.5 m : 1.64

Wind direction {°from N}: 308

Temperature {°C} 2.0 m : 10.4
8.5 m : 10.0

Direct measured temperature difference {°C}: -0.52

Atmospheric pressure {mbar}: 1022.5

Balloon: 1100 g Delasson

Gas mixture {vol. %}: CH_4= 25, O_2= 50, N_2= 25

Volume {m^3}: 10

Explosion max. pressure {mbar} 5.0 m : 86
pp. pressure {mbar} 5.0 m : 164

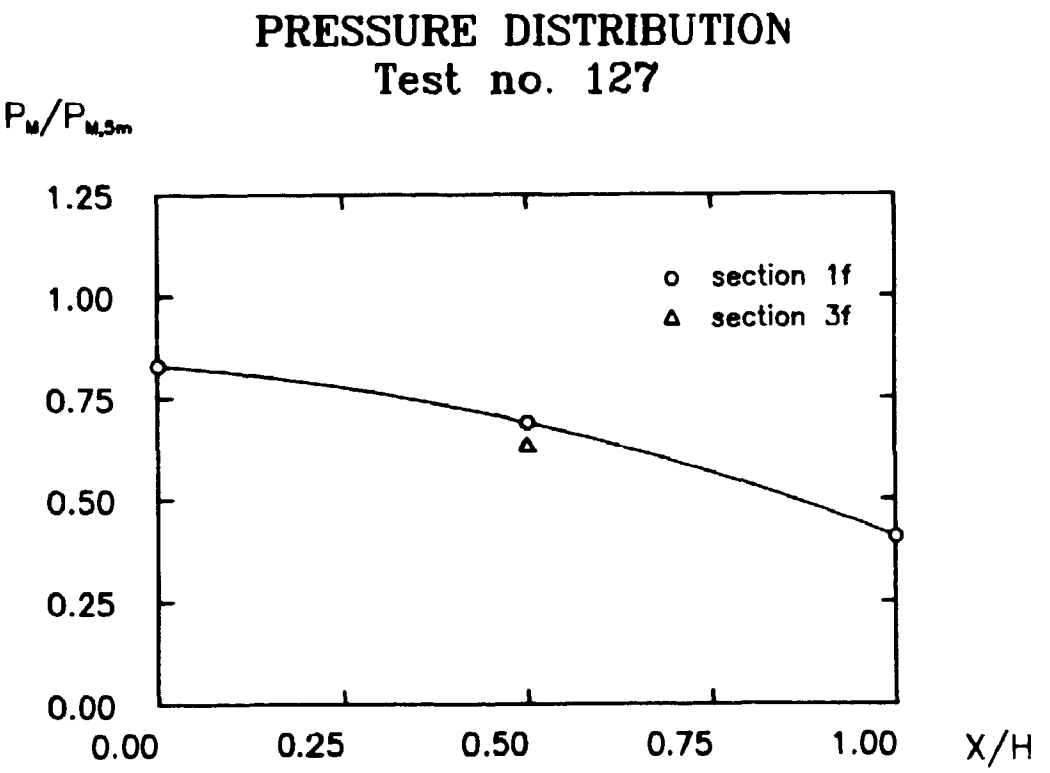

Fig. 3.9.2.2.4. Normalized peak pressure.

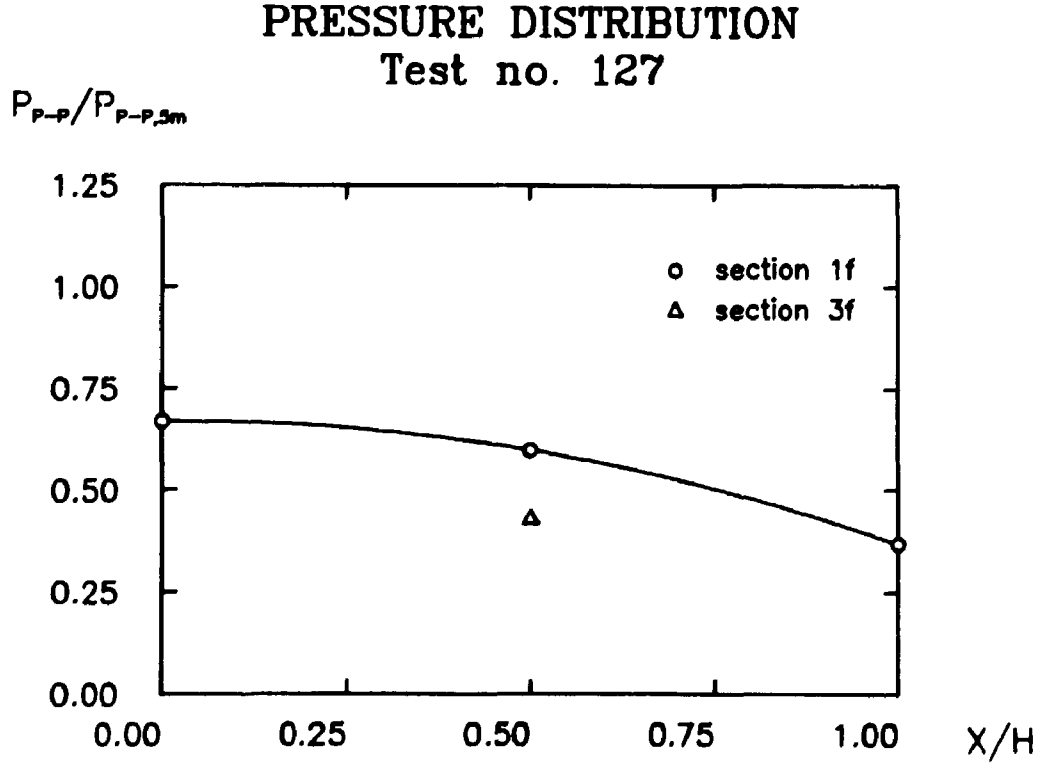

Fig. 3.9.2.2.5. Normalized peak-to-peak pressure.

No. 128

Date: 4/10-83

Time: 9.45

Purpose: To measure the pressure distribution on a wall located at a distance of 25 m from the center of the explosion.

Atmosphere: neutral

Windspeed {m/sec} 2.0 m : 2.06
4.3 m : 2.37
8.5 m : 2.69

Wind direction {°from N}: 209

Temperature {°C} 2.0 m : 13.4
8.5 m : 13.4

Direct measured temperature difference {°C}: -0.09

Atmospheric pressure {mbar}: 1012.7

Balloon: 1100 g Delasson

Gas mixture {vol. %}: CH_4= 25, O_2= 50, N_2= 25

Volume {m^3}: 10

Explosion max. pressure {mbar} 5.0 m : 138
pp. pressure {mbar} 5.0 m : 268

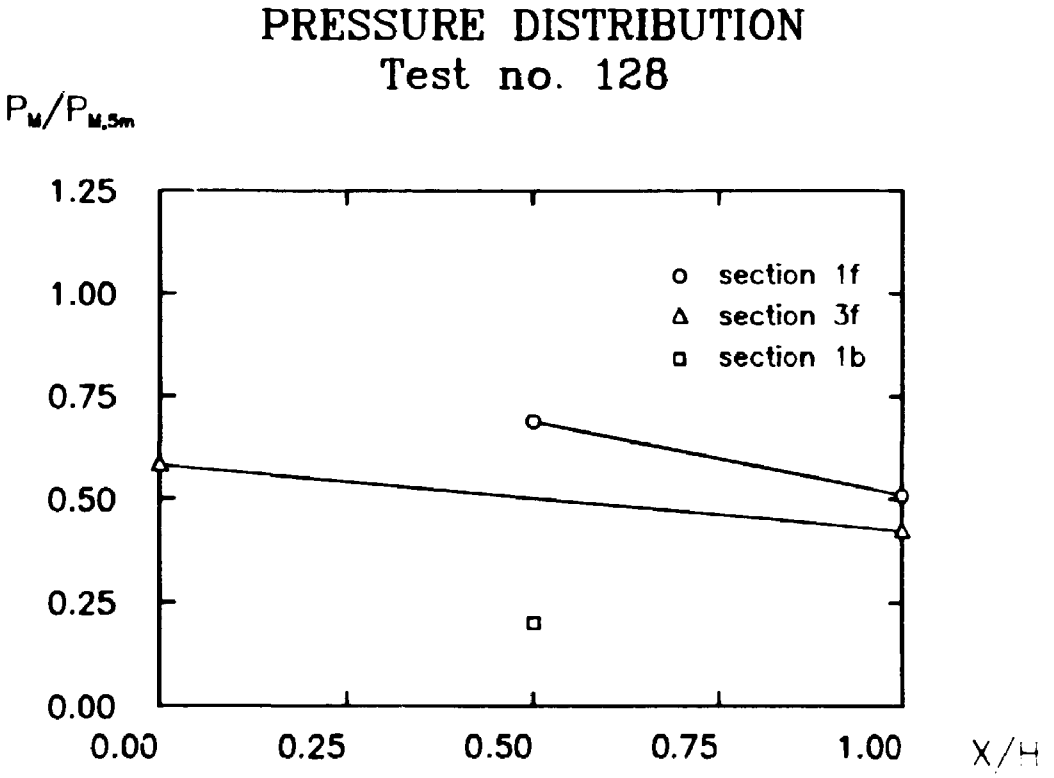

Fig. 3.9.2.2.6. Normalized peak pressure.

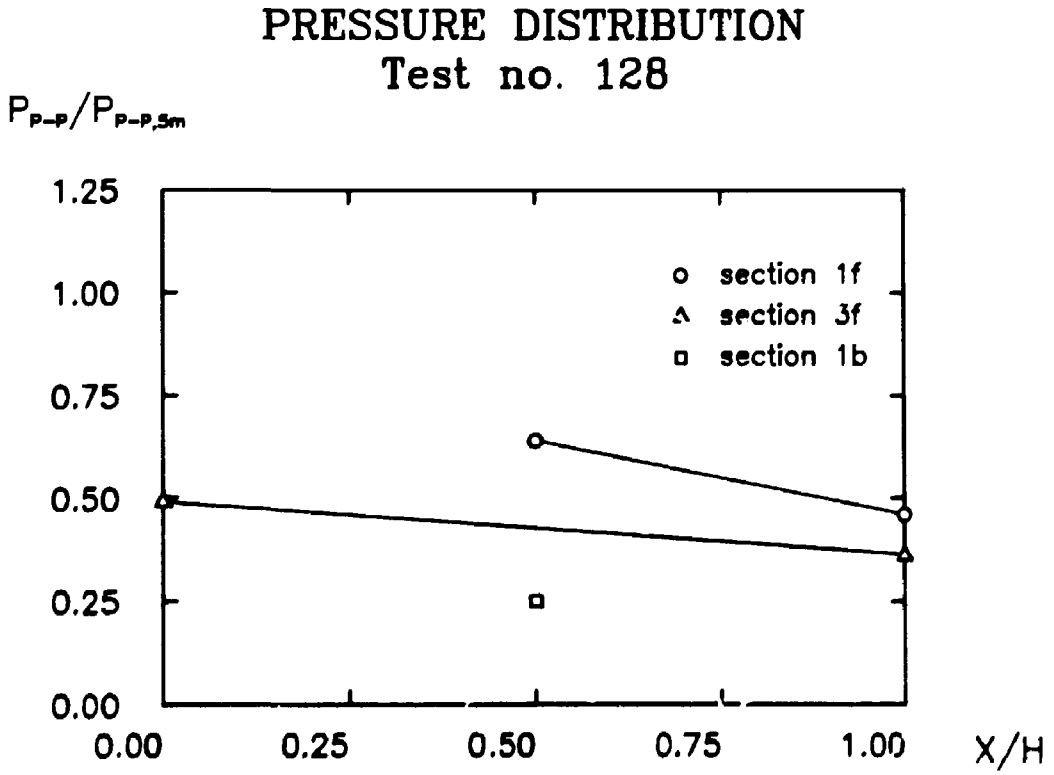

Fig. 3.9.2.2.7. Normalized peak-to-peak pressure.

No. 129

Date: 4/10-83

Time: 12.30

Purpose: To measure the pressure distribution on a wall located at a distance of 25 m from the center of the explosion.

Atmosphere: unstable

Windspeed {m/sec} 2.0 m : 2.30
4.3 m : 2.84
8.5 m : 3.42

Wind direction {°from N}: 197

Temperature {°C} 2.0 m : 15.5
8.5 m : 15.4

Direct measured temperature difference {°C}: -0.14

Atmospheric pressure {mbar}: 1011.6

Balloon: 600 g Delasson

Gas mixture {vol. %}: CH_4= 25, O_2= 50, N_2= 25

Volume {m^3}: 7

Explosion max. pressure {mbar} 5.0 m : 117
pp. pressure {mbar} 5.0 m : 190

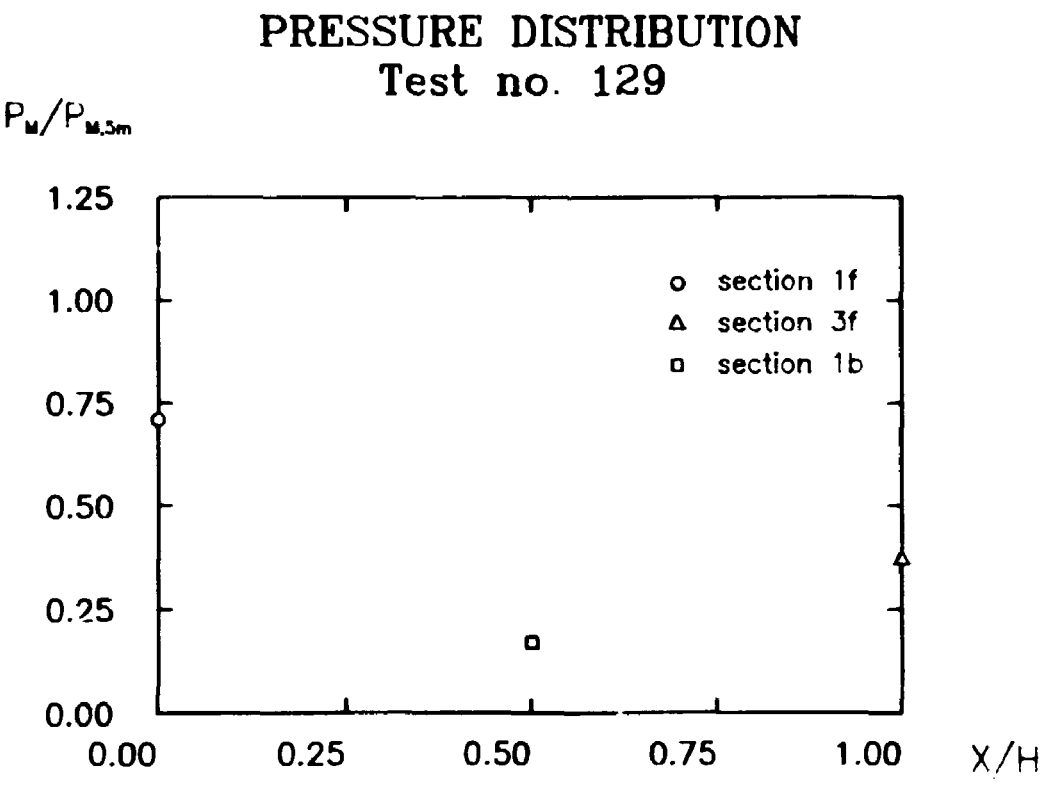

Fig. 3.9.2.2.8. Normalized peak pressure.

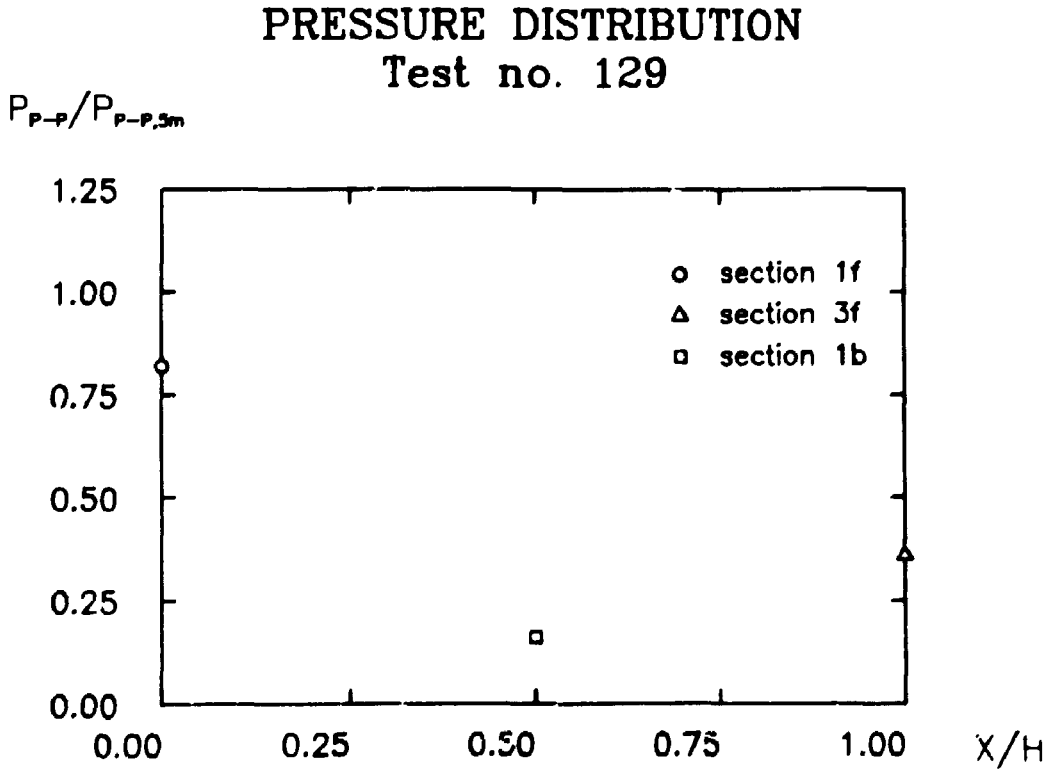

Fig. 3.9.2.2.9. Normalized peak-to-peak pressure.

No. 164

Date: 7/11-83

Time: 12.41

Purpose: To measure the pressure distribution on the front of a wall located at a distance of 25 m from the center of the explosion.

Atmosphere: neutral

Windspeed {m/sec} 2.0 m : 1.47
4.3 m : 1.78
8.5 m : 1.99

Wind direction {°from N}: 180

Temperature {°C} 2.0 m : 9.3
8.5 m : 9.3

Direct measured temperature difference {°C}: -0.05

Atmospheric pressure {mbar}: 1022

Balloon: 1100 g Delasson

Gas mixture {vol. %}: CH_4= 25, O_2= 50, N_2= 25

Volume {m^3}: 5

Explosion max. pressure {mbar} 5.0 m : 69
pp. pressure {mbar} 5.0 m : 144

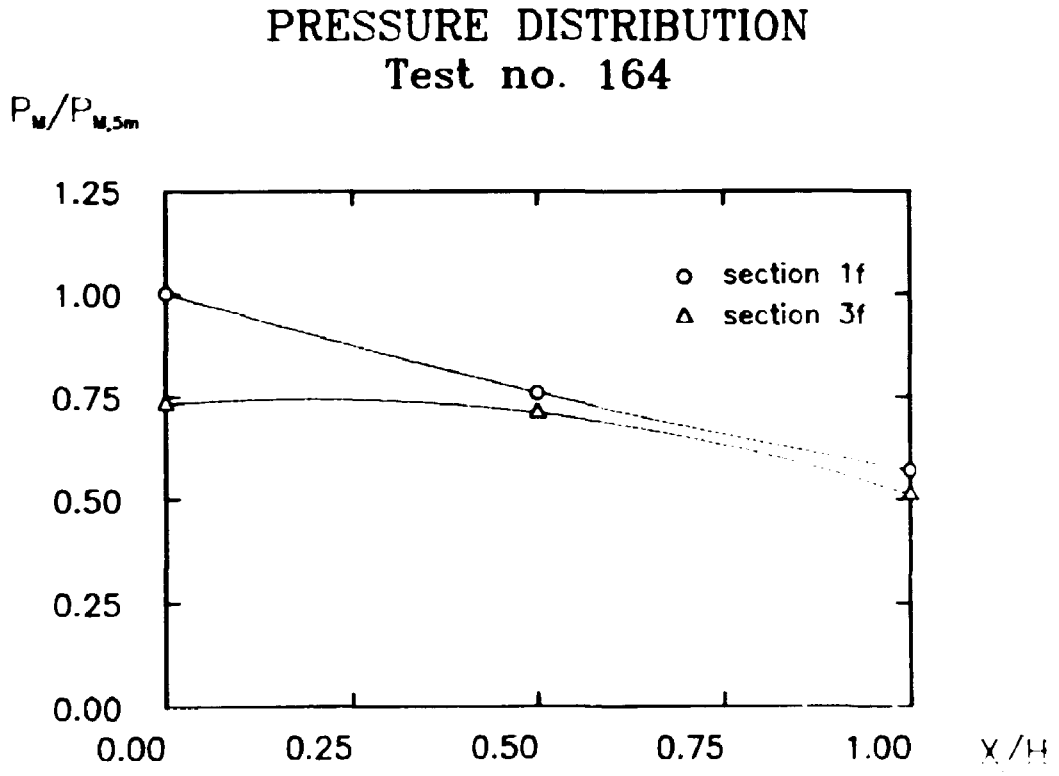

Fig. 3.9.2.2.10. Normalized peak pressure.

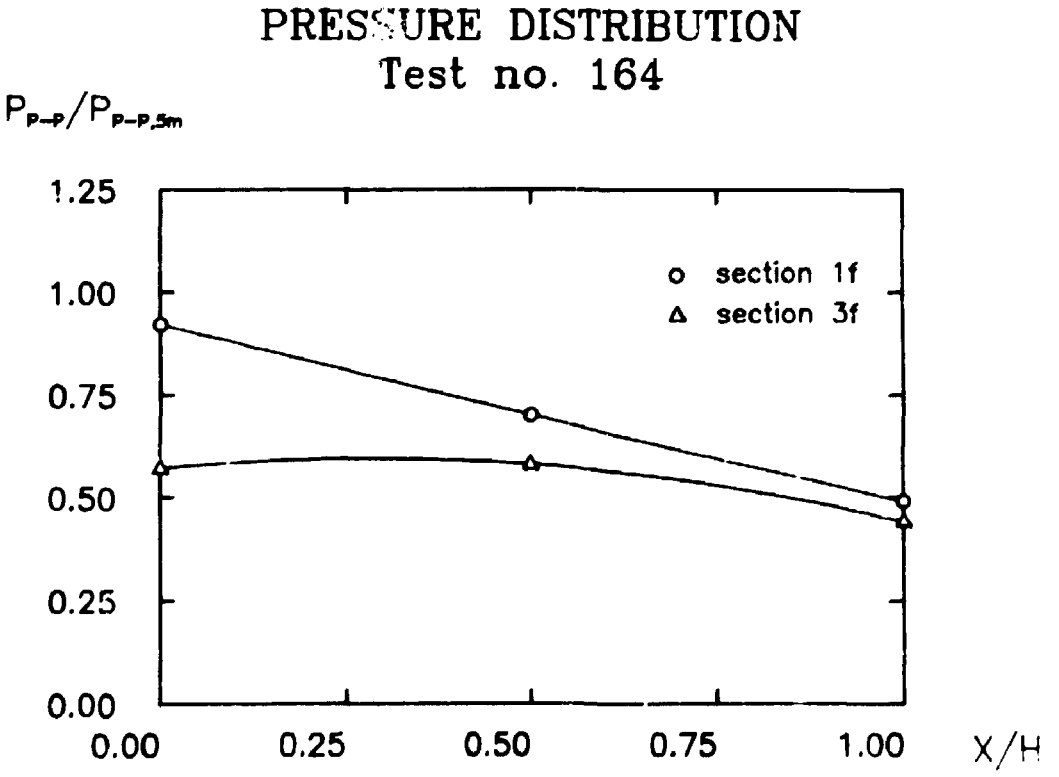

Fig. 3.9.2.2.11. Normalized peak-to-peak pressure.

No. 165

Date: 9/11-83

Time: 9.41

Purpose: To measure the pressure distribution on the back of a wall located at a distance of 25 m from the center of the explosion.

Atmosphere: unstable

Windspeed {m/sec} 2.0 m : 1.09
4.3 m : 1.36
8.5 m : 1.47

Wind direction {°from N}: 197

Temperature {°C} 2.0 m : 6.4
8.5 m : 6.3

Direct measured temperature difference {°C}: -0.23

Atmospheric pressure {mbar}: 1021.5

Balloon: 600 g Delasson

Gas mixture {vol. %}: CH_4= 25, O_2= 50, N_2= 25

Volume {m^3}: 5

Explosion max. pressure {mbar} 5.0 m : 68
pp. pressure {mbar} 5.0 m : 130

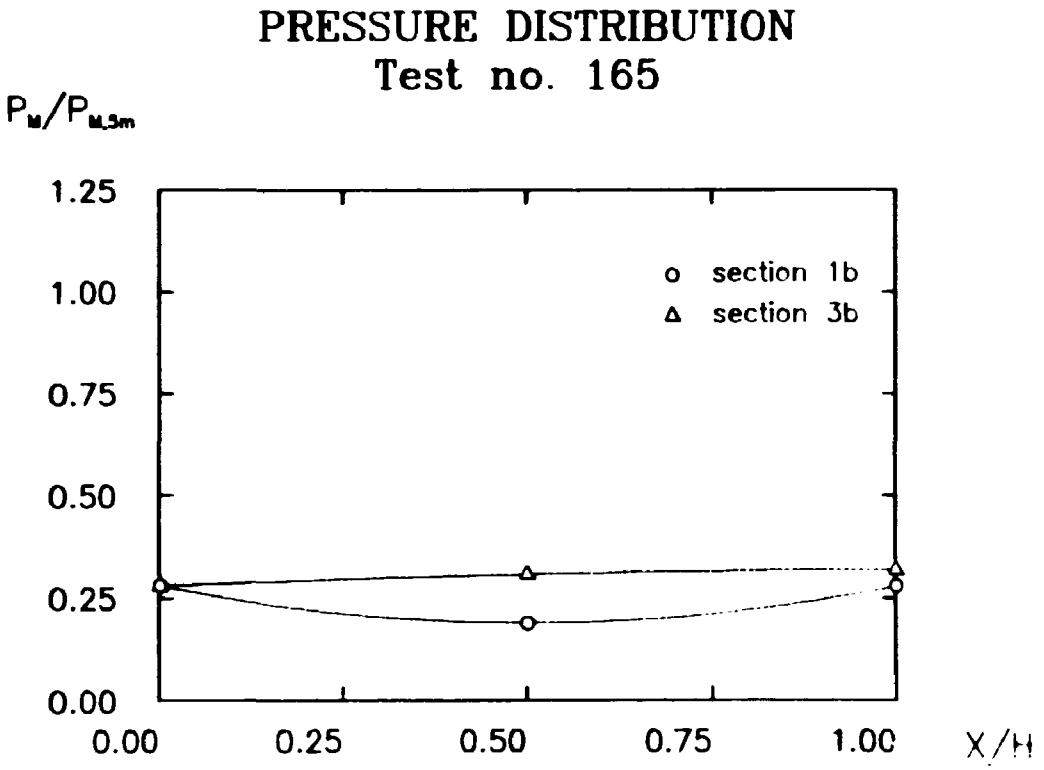

Fig. 3.9.2.2.12. Normalized peak pressure.

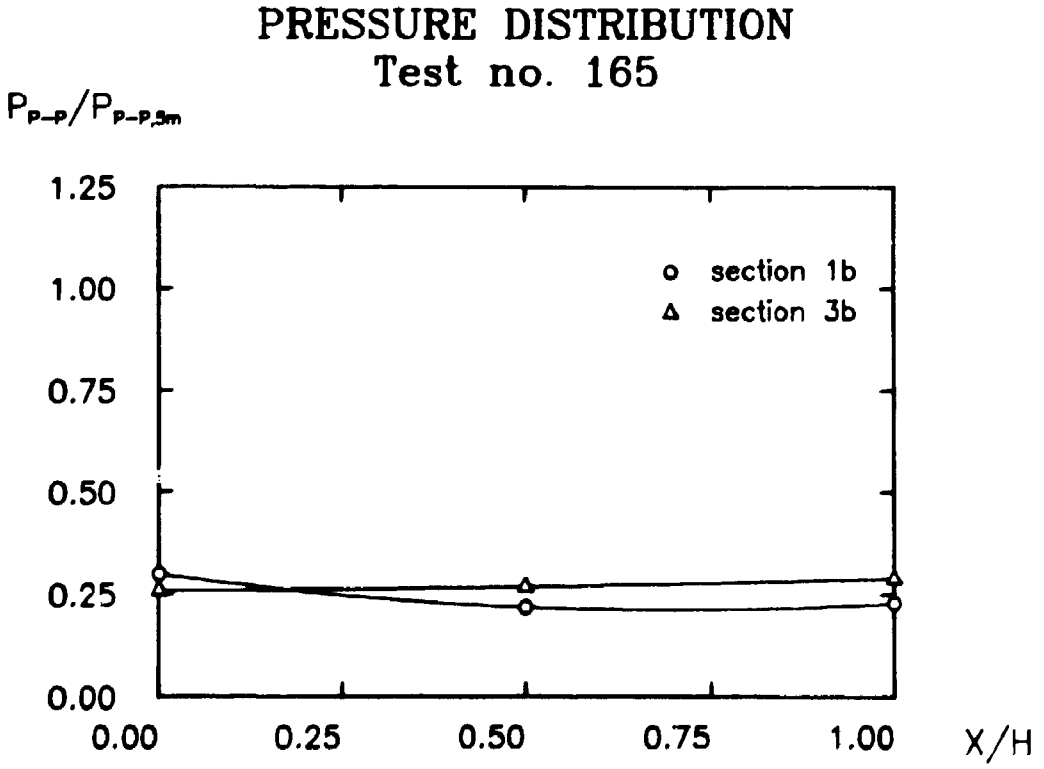

Fig. 3.9.2.2.13. Normalized peak-to-peak pressure.

No. 166

Date: 9/11-83

Time: 11.00

Purpose: To measure the pressure distribution on the back of a wall located at a distance of 25 m from the center of the explosion.

Atmosphere: unstable

Windspeed {m/sec} 2.0 m : 0.77
4.3 m : 0.95
8.5 m : 1.02

Wind direction {°from N}: 169

Temperature {°C} 2.0 m : 9.0
8.5 m : 8.5

Direct measured temperature difference {°C}: -0.23

Atmospheric pressure {mbar}: 1021.6

Balloon: 600 g Delasson

Gas mixture {vol. %}: CH_4= 25, O_2= 50, N_2= 25

Volume {m^3}: 5

Explosion max. pressure {mbar} 5.0 m : 30
pp. pressure {mbar} 5.0 m : 64

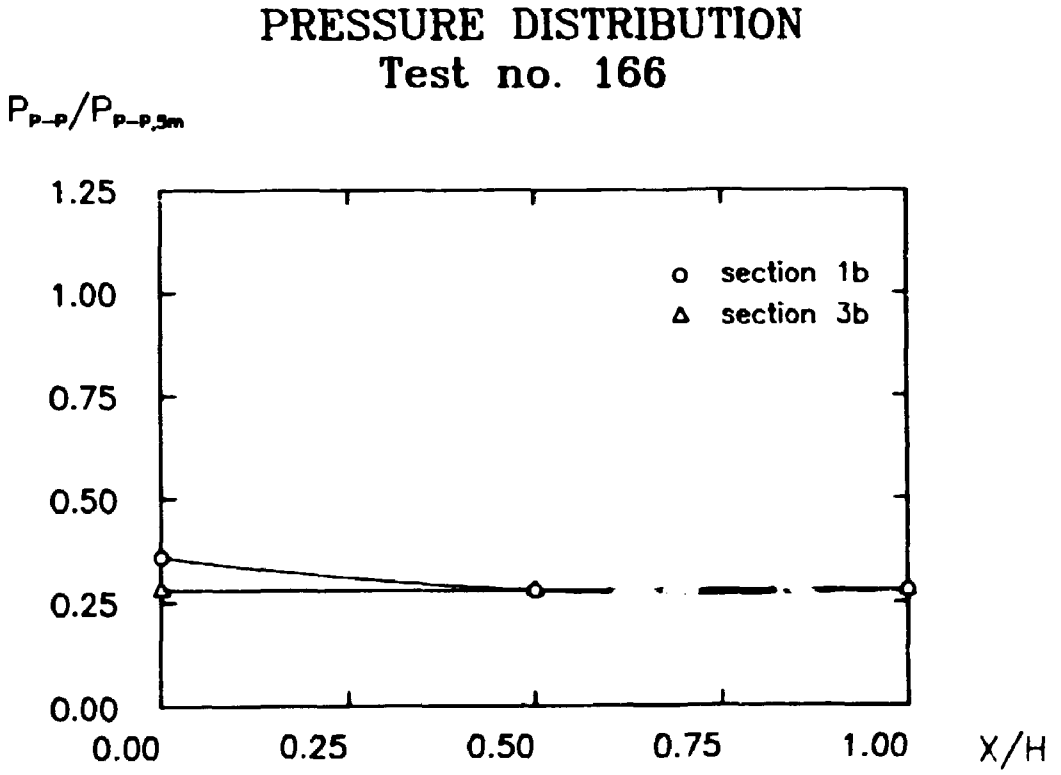

Fig. 3.9.2.2.14. Normalized peak pressure.

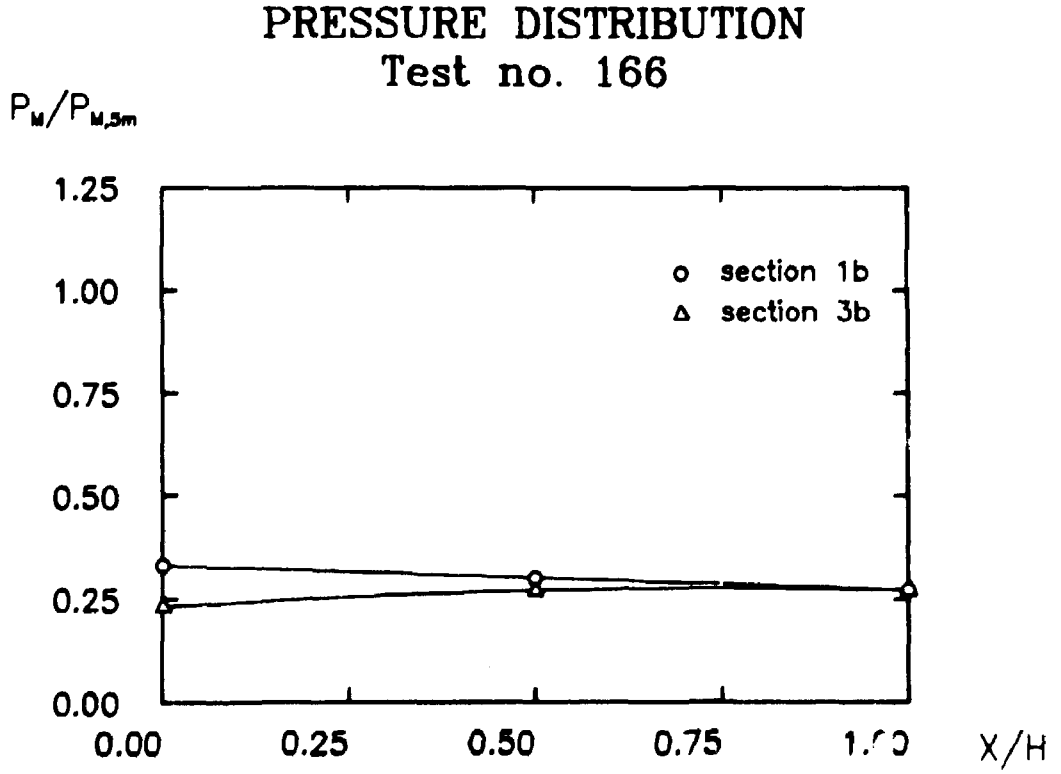

Fig. 3.9.2.2.15. Normalized peak-to-peak pressure.

No. 167

Date: 9/11-83

Time: 13.17

Purpose: To measure the pressure distribution on the front of a wall located at a distance of 25 m from the center of the explosion.

Atmosphere: unstable

Windspeed (m/sec) 2.0 m : 1.22
4.3 m : 1.47
8.5 m : 1.61

Wind direction (°from N): 205

Temperature (°C) 2.0 m : 9.0
8.5 m : 8.5

Direct measured temperature difference (°C): -0.47

Atmospheric pressure (mbar): 1021.5

Balloon: 600 g Delasson

Gas mixture (vol. %): CH_4= 25, O_2= 50, N_2= 25

Volume (m^3): 7.5

Explosion max. pressure (mbar) 5.0 m : 78
pp. pressure (mbar) 5.0 m : 148

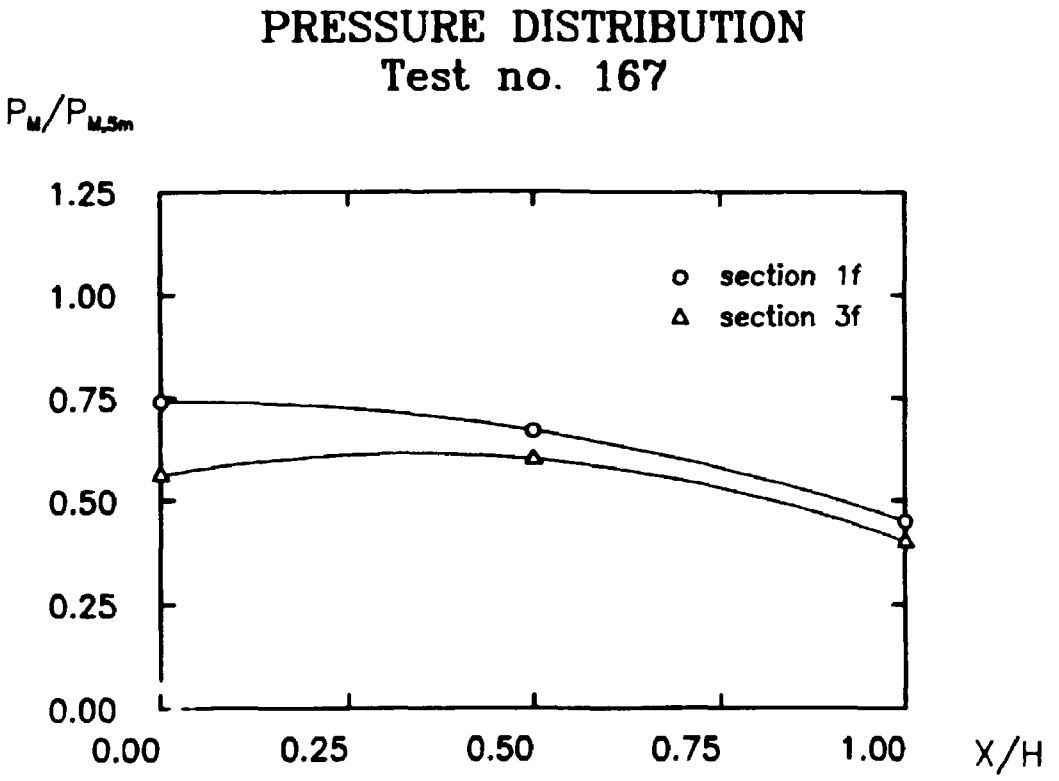

Fig. 3.9.2.2.16. Normalized peak pressure.

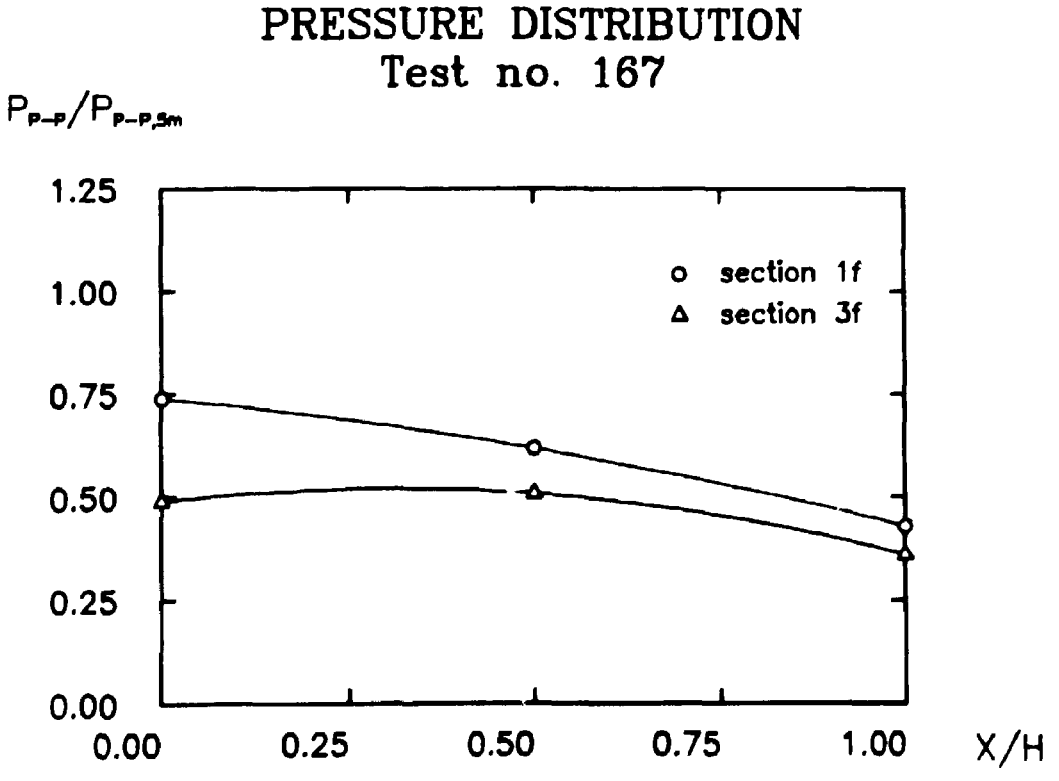

Fig. 3.9.2.2.17. Normalized peak-to-peak pressure.

No. 168

Date: 10/11-83

Time: 12.00

Purpose: To measure the pressure distribution on the front of a wall located at a distance of 25 m from the center of the explosion.

Atmosphere: unstable

Windspeed {m/sec} 2.0 m : 2.09
4.3 m : 2.44
8.5 m : 2.72

Wind direction {°from N}: 310

Temperature {°C} 2.0 m : 8.0
8.5 m : 7.9

Direct measured temperature difference {°C}: -0.09

Atmospheric pressure {mbar}: 1021.0

Balloon: 600 g Delasson

Gas mixture {vol. %}: CH_4= 25, O_2= 50, N_2= 25

Volume {m^3}: 5

Explosion max. pressure {mbar} 5.0 m : 129
pp. pressure {mbar} 5.0 m : 222

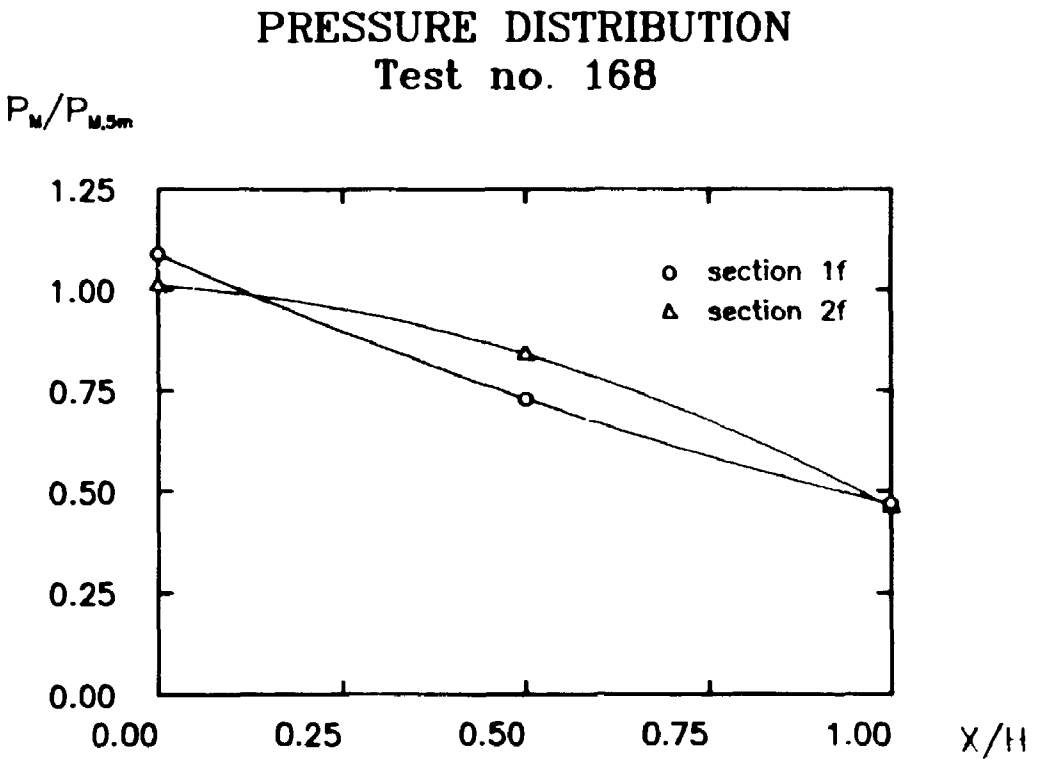

Fig. 3.9.2.2.18. Normalized peak pressure.

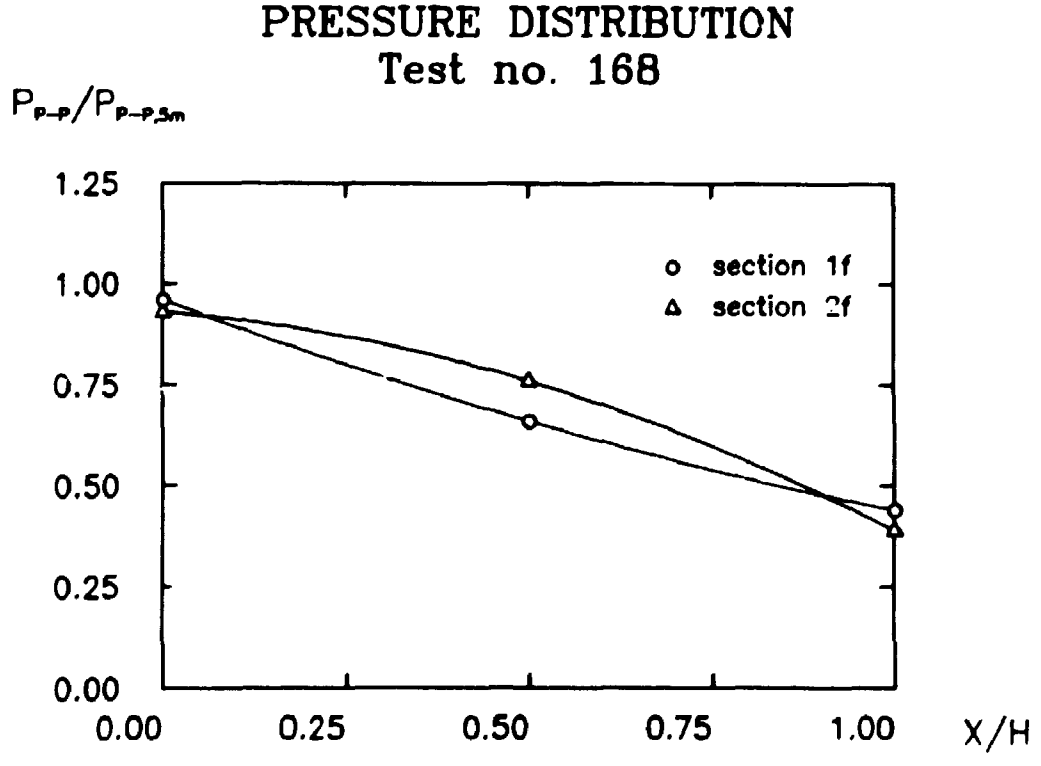

Fig. 3.9.2.2.19. Normalized peak-to-peak pressure.

No. 169

Date: 10/11-83

Time: 14.10

Purpose: To measure the pressure distribution on a wall located at a distance of 25 m from the center of the explosion.

Atmosphere: unstable

Windspeed {m/sec} 2.0 m : 2.16
4.3 m : 2.58
8.5 m : 2.79

Wind direction {°from N}: 295

Temperature {°C} 2.0 m : 8.5
8.5 m : 8.4

Direct measured temperature difference {°C}: -0.05

Atmospheric pressure {mbar}: 1019.7

Balloon: 600 g Delasson

Gas mixture {vol. %}: CH_4= 25, O_2= 50, N_2= 25

Volume {m^3}: 5

Explosion max. pressure {mbar} 5.0 m : 75
pp. pressure {mbar} 5.0 m : 140

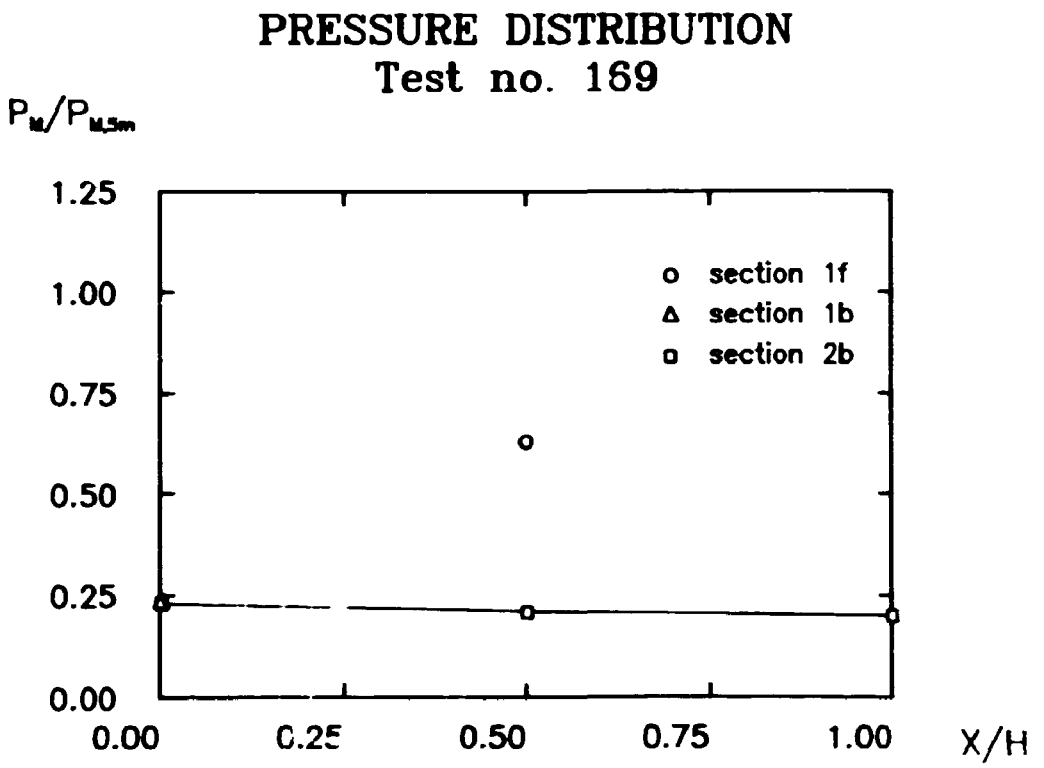

Fig. 3.9.2.2.20. Normalized peak pressure.

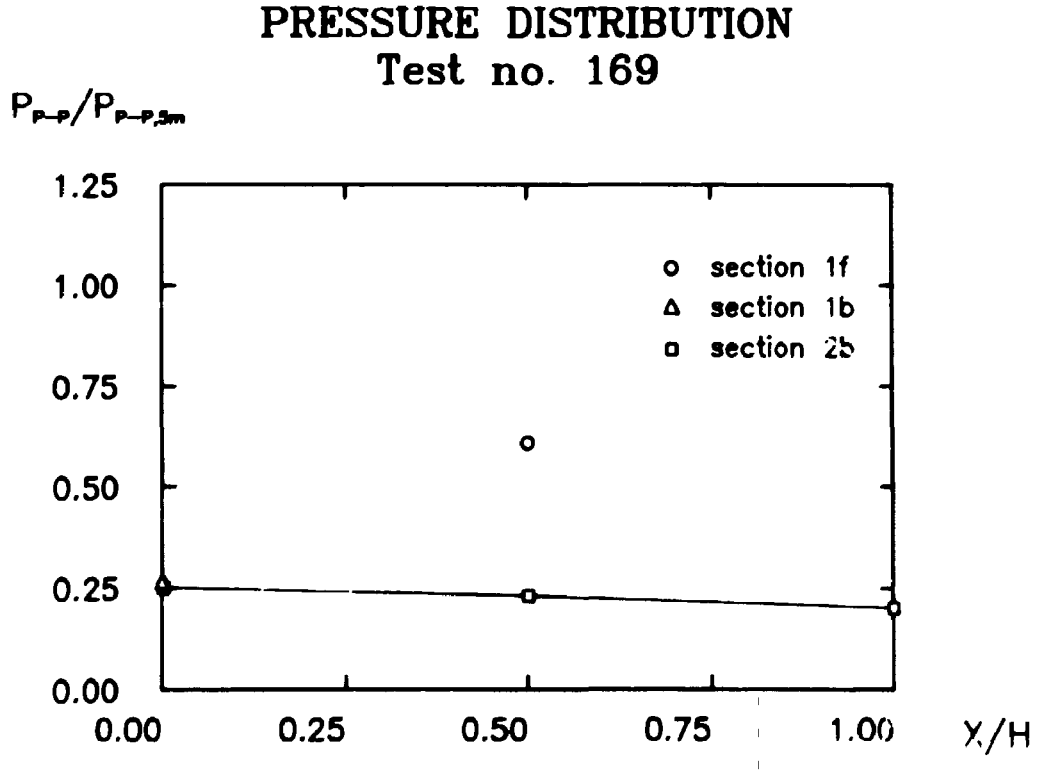

Fig. 3.9.2.2.21. Normalized peak-to-peak pressure.

3.9.2.3. EVALUATION OF THE RESULTS

The curves presented in the previous section contain, as expected, the following qualitative features

- the pressure build-up at the front is more pronounced at the bottom of the wall than at its top,
- the pressure build-up at the front is less at the edge of the wall than at its center,
- the pressure on the back of the wall is rather insensitive both to the distance from the bottom and the edge,
- the pressure level on the front of the wall is considerably higher than the pressure level on the back of the wall.

In order to give a more quantitative evaluation of the results, the "reflection factors" for all the measurements performed on the wall have been calculated on the basis of the P_M-values. The reflection factors have been computed as the ratio between the actual pressure measurement and pressure which would have been measured on the actual position in a undisturbed pressure field.

This is expressed in the formula

$$f_w = \frac{P_M / P_{M,5m}}{P_{M,5m} / P_{M,5m}} \quad \frac{25m}{5m}$$

$$= \frac{5\ P_M}{P_{M,5m}} \quad ,$$

where f_w denotes the reflection factor for the wall, P_M the actual peak pressure and $P_{M,5m}$ the reference peak pressure 5 m from the source. The geometric 1/R attenuation is assumed. The mean values of the computed reflection factors are given in Fig. 3.9.2.3.1 below, together with the standard deviation in percentage of the mean value. The standard deviation has not

been given for the section 2-values, as these are determined from a single measurement only.

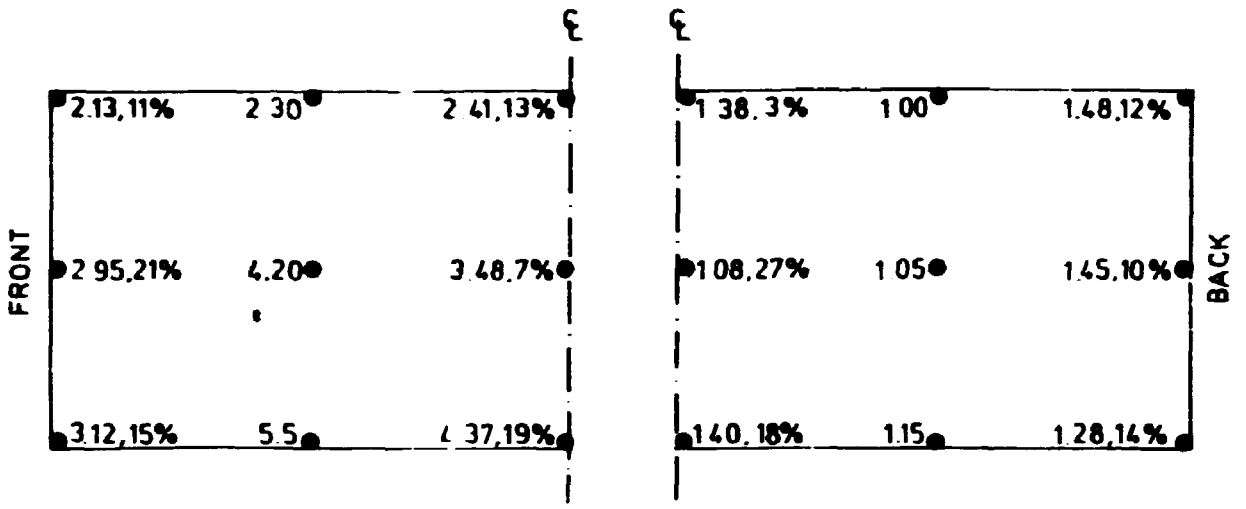

Fig. 3.9.2.3.1. Reflection factors, f_w, evaluated at different positions on the wall.

It is seen that the mean pressure over the front area is approximately 3.3 times that which would exist on the position without the wall present. In the region near the ground and the center of the wall, the pressure build-up is more pronounced ($f_W \simeq 4.5$) than in the outer region near the edge and near the top of the wall ($f_W \simeq 2.5$). For weak transients, the acoustic theory would give a reflection factor of 2 for a fully developed reflection. For stronger shocks, the enhancement of the reflected pressure will be increased. An upper limit often cited in the literature, f.ex. [8], is a reflection factor of 8, which is based on the asumption that the air behaves as a perfect gas even at high pressures and temperatures. This indicates that nonlinear effects have to be taken into account in a theoretical evaluation of the pressure/wall interaction.

The mean pressure over the back area is approximately 1.25 times the pressure which would exist in an undisturbed pressure field. It is remarkable that this factor is greater than 1 and also that none of the f_W - values on the back are less than 1, which would give a shade zone.

As f_W is directly proportional to the normalized peak pressure, the values given in Fig. 3.9.2.3.1 can also be interpreted as

mean values of the normalized pressures, except for a constant factor. Doing this it is seen that the mean pressure on the front is 2.6 times that on the back. The pressure differences are least at the boundary and largest in the central part of the wall, as expected.

Concerning the front, it is moreover seen, that, on the average, the pressure at the "center" is 1.2 times the pressure at the "edge", and the pressures at the "bottom" are 1.8 times those at the "top".

Finally, no clear demarcation of the end effects has been observed either in the vertical or horizontal directions, which means either that the measurements have insufficient resolution, or that the boundaries can be felt throughout the surface of the present wall.

The conclusion to be drawn from these experiments is that the wall is more heavily affected by the blast wave that would have been predicted by acoustic theory.

3.10. REGRESSION ANALYSIS

The maximum peak pressure P_M is proportional to the inverse of the distance R from the source, assuming acoustic theory. In order to evaluate how the measured values fits with an acoustic assumption, P_M is expressed by an equation of the form:

$$P_M = P_f/R^k \qquad (3.10.1)$$

where P_f is a constant and k the exponent, which for ideal conditions is equal to 1.0.

For some of the experiments, the measured data has been used to determine P_f and k in equation (3.10.1) by a least square regression analysis. The results are given in the following Table 3.10.1.

The analysis is performed for two different sets of data for each experiment: one with all data included, and one with the measurement performed in 5m distance from the source excluded. The values

of k are nominated k_5 and k_{10} respectively, indicating the closest measuring position included. For tests no.185 and 186 the values measured immediately behind the bank were furthermore excluded, see Figures 3.8.2.1-4, as they obviously are significantly affected by the presence of the obstacle.

EXPERIMENT NO.	PEAK PRESSURE {mbar} 5m	10m	k_5	k_{10}
125	41	28	0.77	0.93
126	146	98	0.79	0.98
185	122	103	1.09	1.01
186	95	75	0.71	1.02
187	48	39	0.80	1.11
188	100	87	0.74	1.05
189	40	35	0.77	1.11
190	119	124	0.84	1.25
191	55	43	0.83	1.14

Table 3.10.1. Calculated exponents k_5 and k_{10} for equation (3.10.1.)

From Table 3.10.1 it is seen, that the acoustic assumption is valid for pressure measured at distances greater than 10m from the source, even for the cases with obstacles present. When a measurement closer to the source is included, the 5 m measurement, the k-values is less than 1.0 in most cases. It is resonable, that very close measurements will result in k-values less than 1.0 as the acoustic theory contains a singularity at zero distance, where as the pressure in the physical situation has a limited value here.

The average values of k for all tests are:

$$\langle k_5 \rangle = 0.82$$
$$\langle k_{10} \rangle = 1.07$$

For some of the experiments, the impulse $I(t) = \int_0^t p(t)dt$ was calculated at the different measuring distances. An example of this calculated impulse is given in Fig. 3.10.1 and 3.10.2 for

5, respectively 50 m distance for one of the free field tests, exp. no. 190.

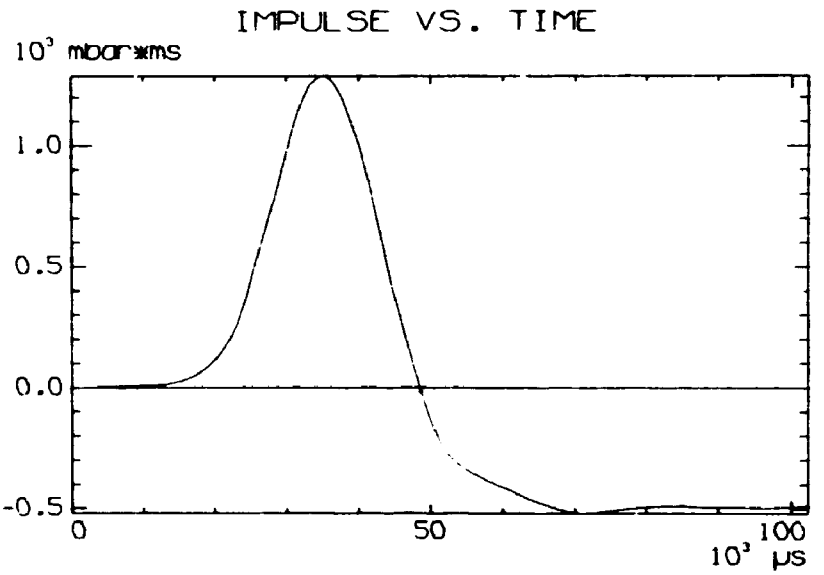

Fig. 3.10.1. Typical impulse history 5 m from the center of the source.

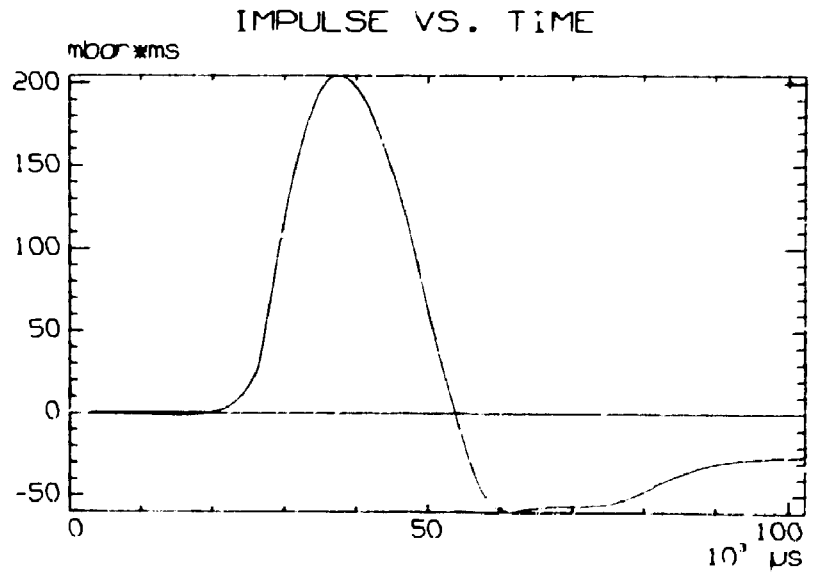

Fig. 3.10.2. Typical impulse history 50 m from the center of the source.

The curves are smooth, and it is seen that the time shift for zero impulse is small compared to the total duration of the pulse. This indicates, that the shape of the pulse is only slightly modified with increasing distance. This observation is further confirmed by the regression analysis made for max. impulse, calculated for the different distances, Table 3.10.2. It is here assumed, that a similar relationship exists between the max. impulse at different distances as for the positive peak pressure, i.e. $I(R)=I_{RO}/R^k$. The exponent k has been calculated for selected experiments, and from Table 3.10.2 it is seen, that the deviation between the values calculated for impulse and pressure for a particular experiment is less than the deviation between the k-values for different experiments. For all practical purposes it is thus allowable to assume the same attenuation of the peak impulse as for the peak pressure.

EXPERIMENT	OBSTACLE	EXPONENT k_{10} FOR IMPULSE	EXPONENT k_{10} FOR PEAK PRESSURE
125	wall	0.91	0.93
186	bank	1.16	1.02
188	forest	1.11	1.05
189	free field	1.17	1.11
190	free field	1.20	1.25

Table 3.10.2. Calculated exponents for max. impulse and for positive peak pressure.

3.11. PRESSURE AND ACCELERATION MEASUREMENTS AROUND A GROUP OF HOUSES.

In the first part of these experiments, consisting of experiments number 170, 171, 172, 173, 174, 175, 176 and 177, the center of the balloon was positioned 30 m from an empty farmhouse belonging to an earlier small holding. In these experiments the direction of the pressure propagation was perpendicular to the longitudinal direction of the house. In Fig. 3.11.1 below the farmhouse is seen from the position of the balloon.

Fig. 3.11.1. The face of the farmhouse seen from south.

The measurements were performed on as well as inside the building, and they consisted of both pressure and vibration recordings. All the pressure measurements were performed with hydrophones. The acceleration measurements were done with accelerometers.

In all the experiments (except one) the pressure at the distances 5 and 10 m from the balloon were measured. These values were used to normalize the explosion levels.

The second part of these experiments consists of the experiments number 178, 179, 180, 181, 182, 183 and 184. In these tests the source was placed inside a courtyard enclosed by the farmhouse and a wing. The courtyard is shown in the Figures 3.11.2-3 below.

Fig. 3.11.2. The farm seen from west.

Fig. 3.11.3. The court with the mast for the balloons.

In these experiments the distance between the center of the explosion and the buildings was reduced to the order of magnitude 10 m. In order to spare the buildings the strength of the source has been reduced too.

As in the first part, these measurements consisted of both pressure and vibration measurements. The pressure at 5 m's distance from the center of the explosion has been recorded in all these tests. This measurement was used to normalize the explosion levels.

3.11.1. DETAILS OF THE EXPERIMENTAL SETUP

In this section details of the experimental setup for both the part one and the part two experiments are given.

In the first part of the experiments, 8 pressure measuring channels (apart from the reference measurements) have been utilized. The position of a specific pressure transducer is shown in the Figures 3.11.1.1-3. A cross represent a pressure transducer mounted outside, and a dot represents a pressure transducer mounted inside a building. Each of the positions are provided with a number indicating the channel number. The numbers attached to the arrows are distances given in meters. Moreover, each figure are provided with the test numbers corresponding to the actual setup.

In the second part of the experiments 6 pressure transducers (apart from the reference measurement) have been used. The positions of those are shown in Fig. 3.11.1.4. The notation is as described above. The measuring position which has not been provided with a number, is the reference measurement in 5 m's distance from the center of the source.

In the experiments no. 170 and 171, vibration measurements were performed at 9 positions on the farmhouse. The position of a specific accelerometer is shown in Fig. 3.11.1.5. Here a pair consisting of an integer and a set of small arrows symbolizes a vibration measuring point. The arrows indicate the directions of the acceleration measurements. The remaining notation is as previously described. In the experiments no. 172, 173, 174, 175, 176, 177, 178, 179, 180 and 181 acceleation measurements were performed at 8 positions. The position of a specific accelerometer is shown in the Figures 3.11.1.6-8. The notation is as described above, except that a "b" or a "c" attached to the measuring point number indicate, that the actual measuring is performed inside the house.

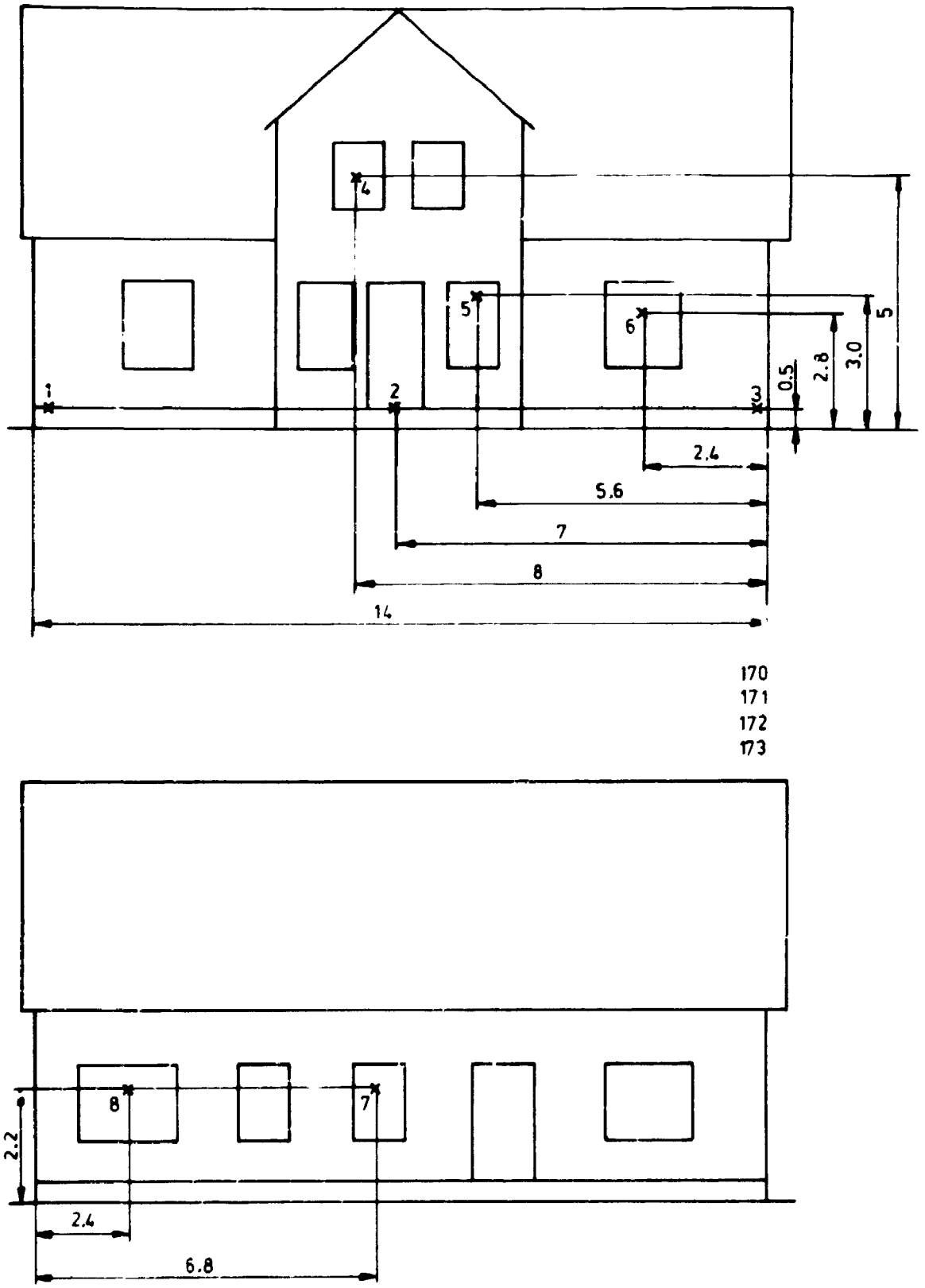

Fig. 3.11.1.1. Hydrophone positions on the farmhouse in experiments no. 170, 171, 172 and 173. House seen from south and from north.

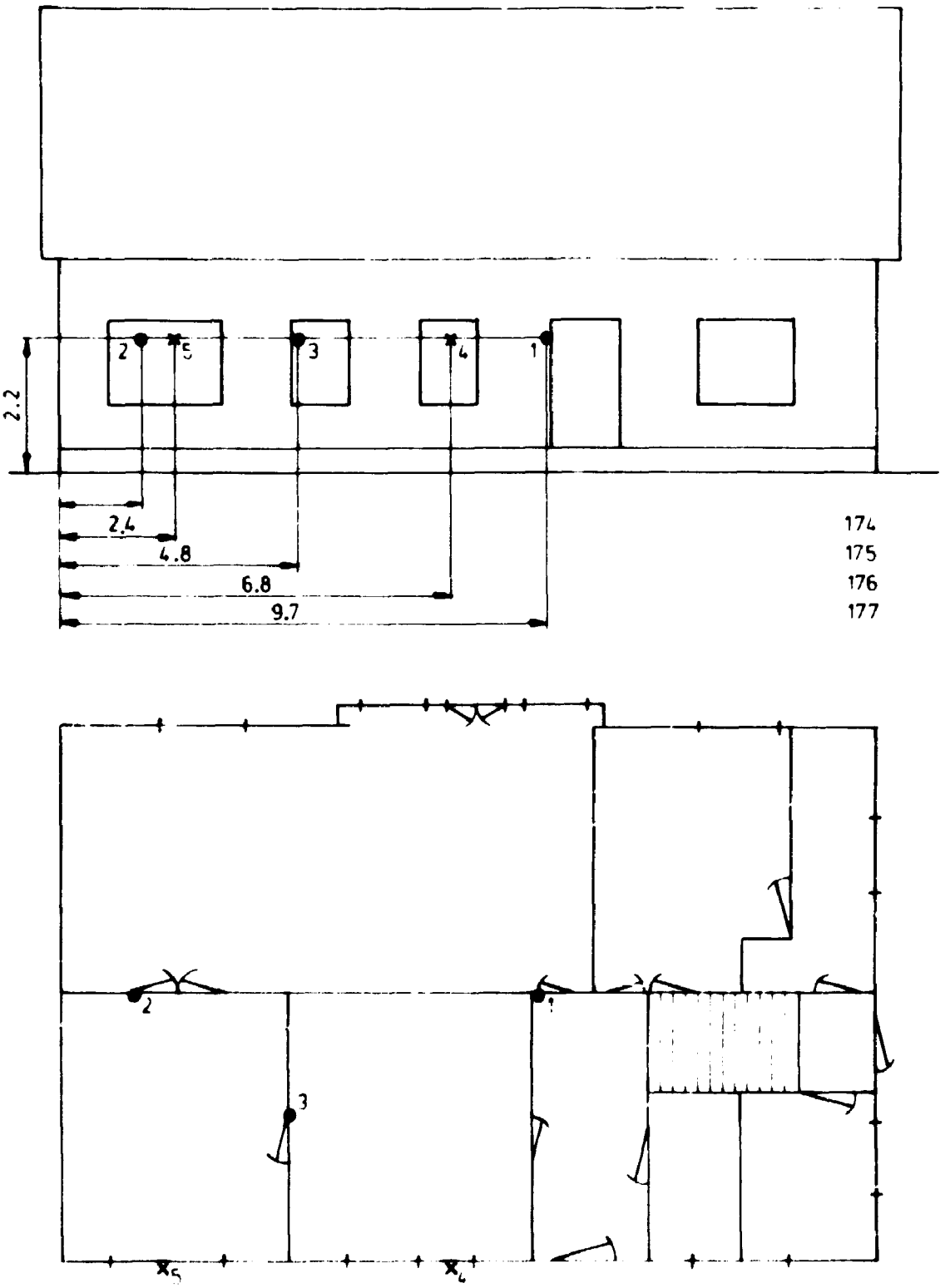

Fig. 3.11.1.2. Hydrophone positions on and inside the farmhouse in experiments no. 174, 175, 176 and 177. House seen from south and from above.

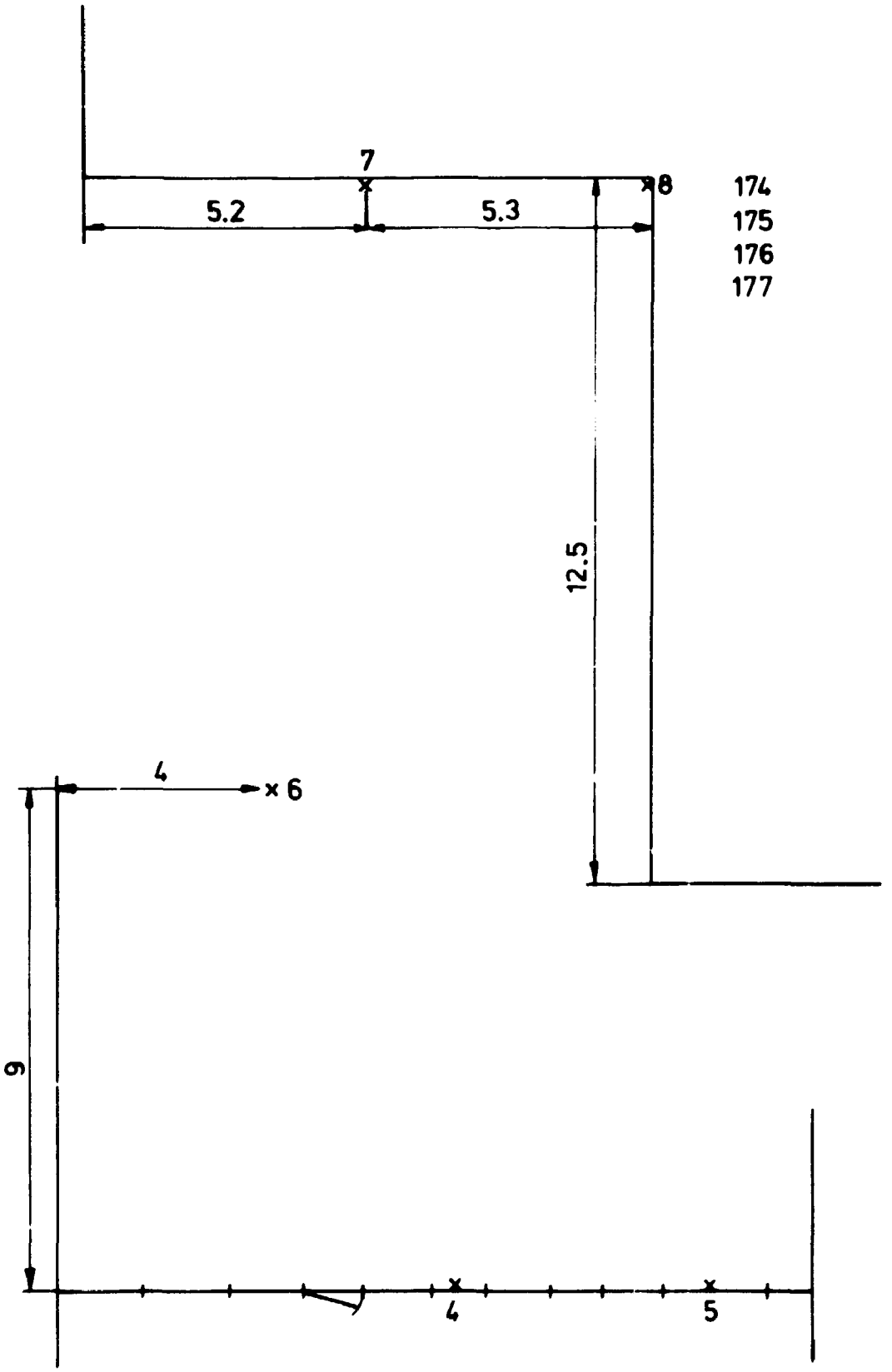

Fig. 3.11.1.3. Hydrophone positions in the court and on the buildings in experiments no. 174, 175, 176 and 177. Court seen from above.

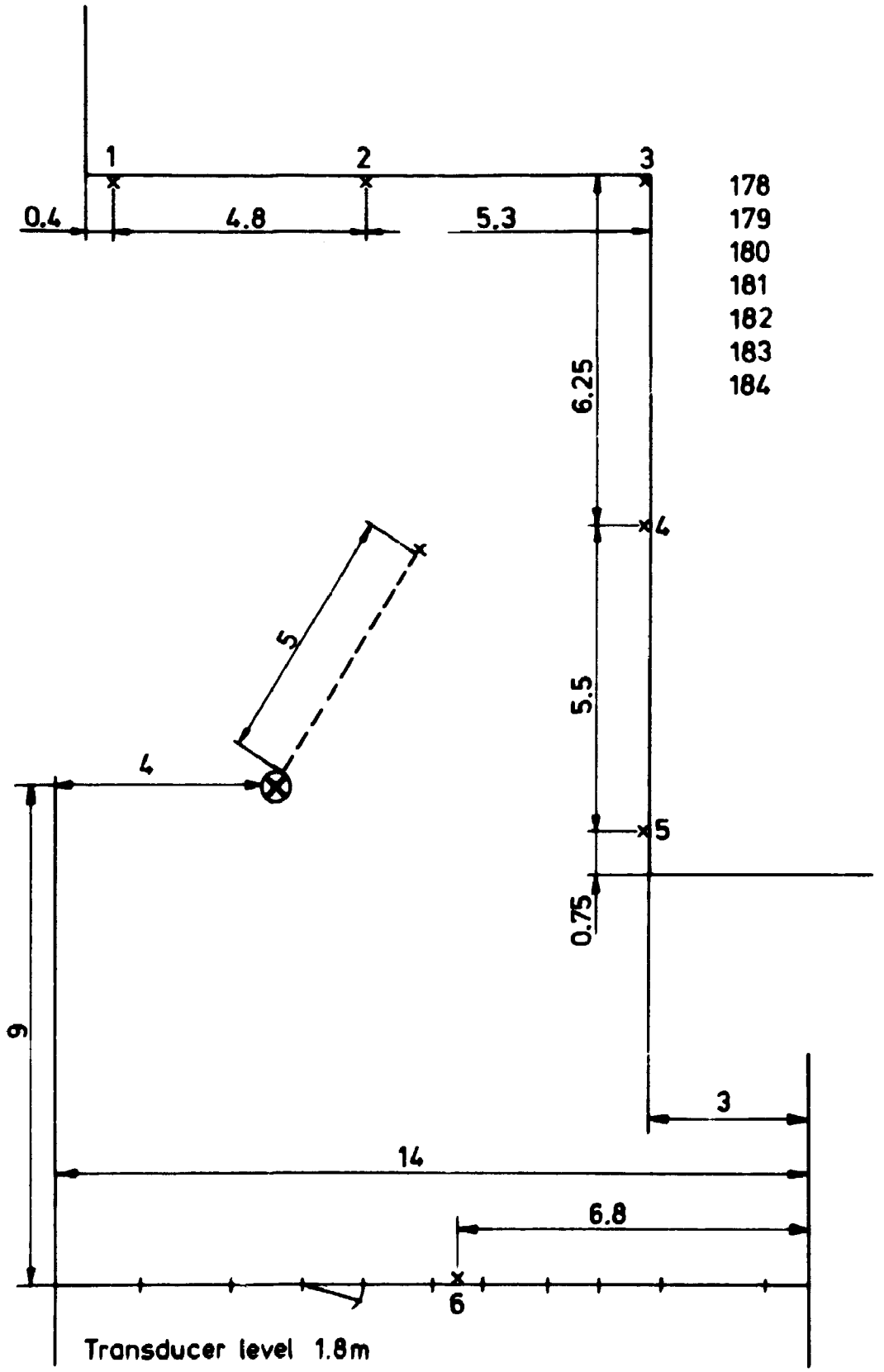

Fig. 3.11.1.4. Hydrophone positions in experiments no. 178, 179, 180, 181, 182, 183 and 184. Court seen from above.

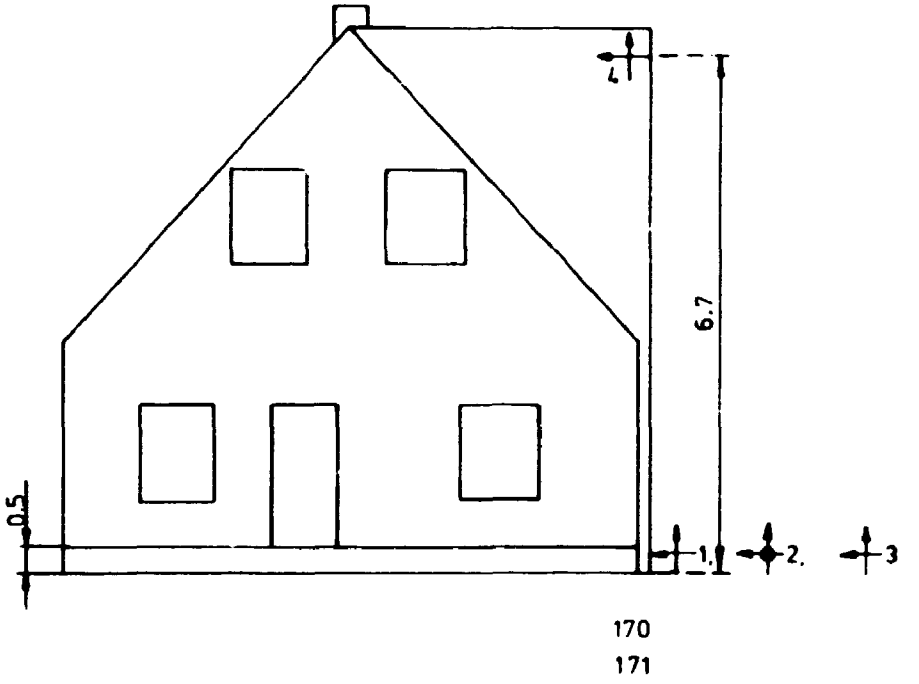

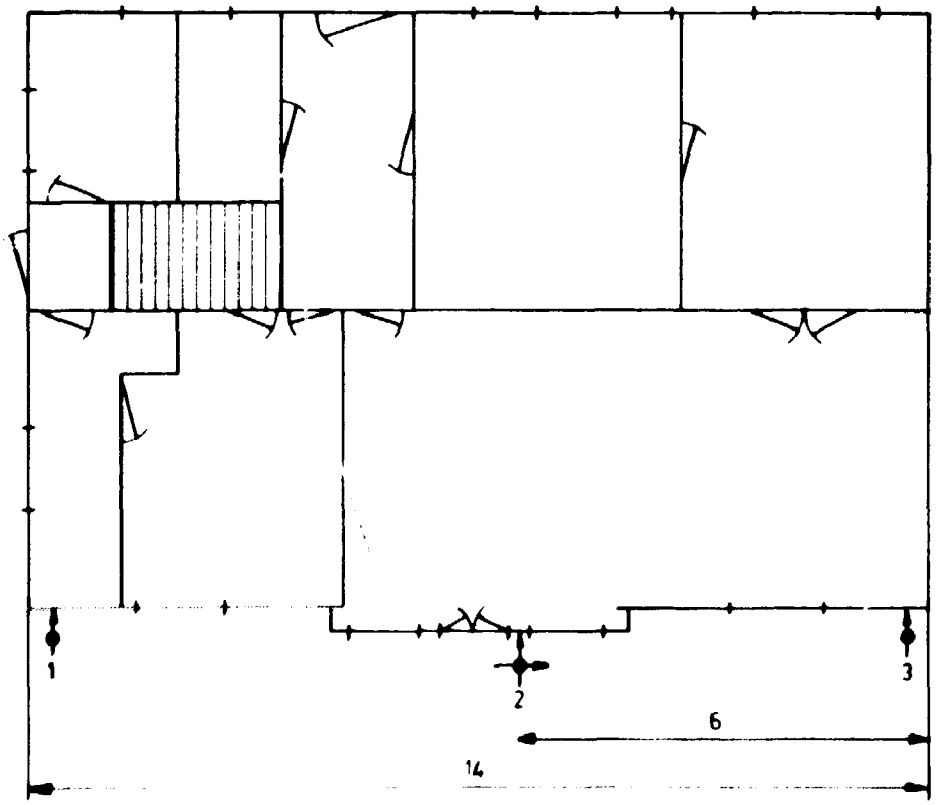

Fig 3.11.1.5. Accelerometer positions in experiments no. 170 and 171. House seen from west and from above.

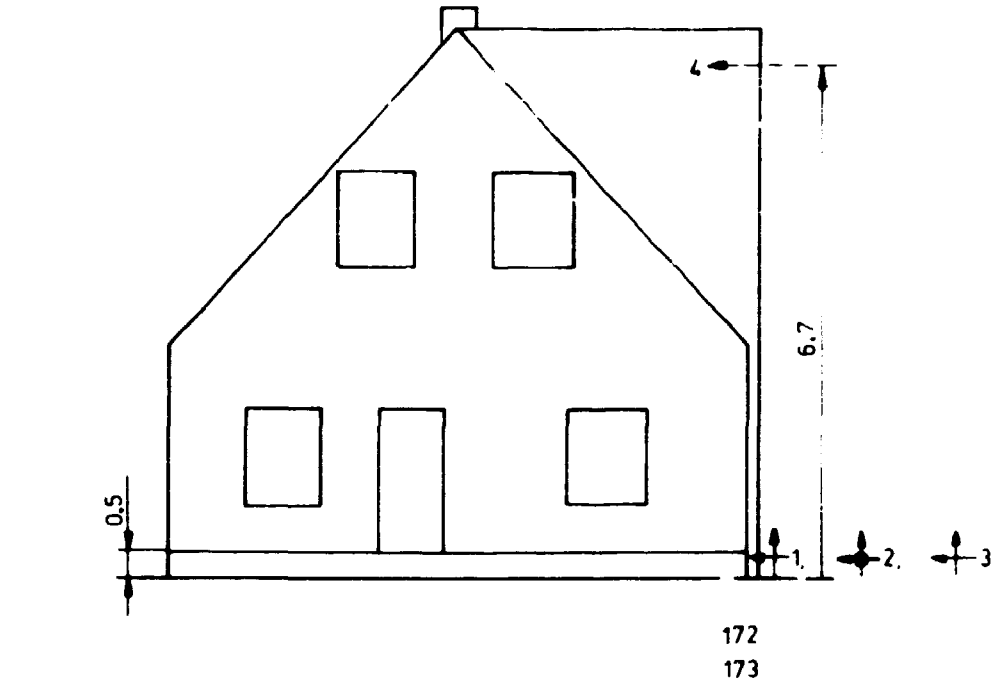

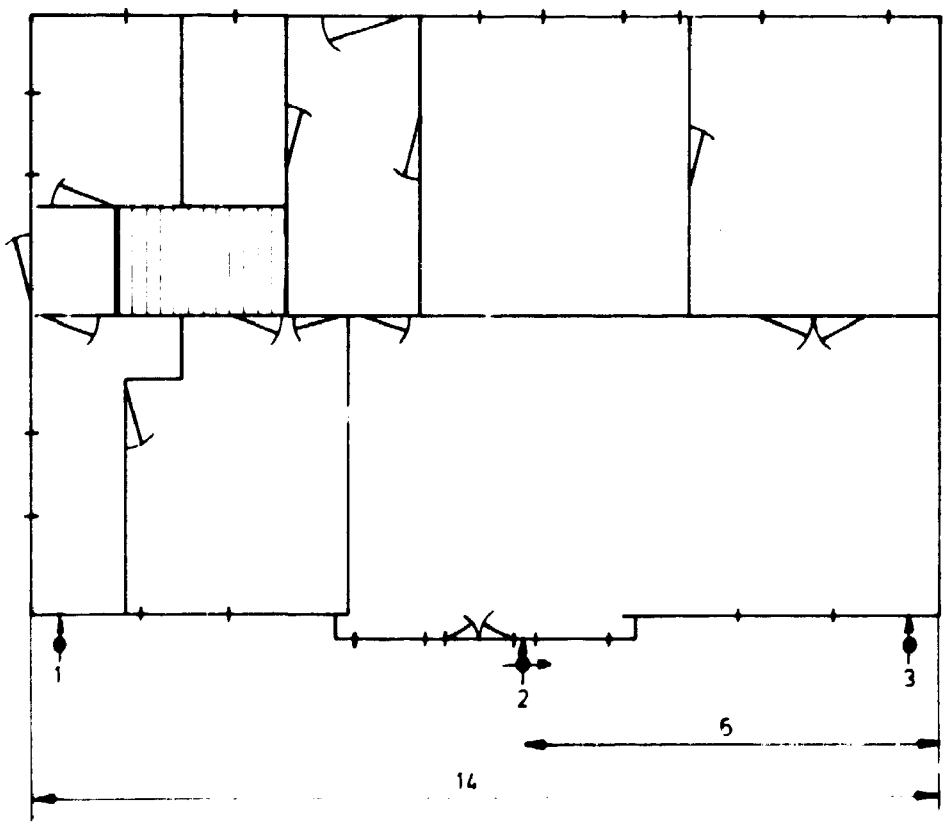

Fig. 3.11.1.6. Accelerometer positions in experiments no. 172 and 173. House seen from west and from above.

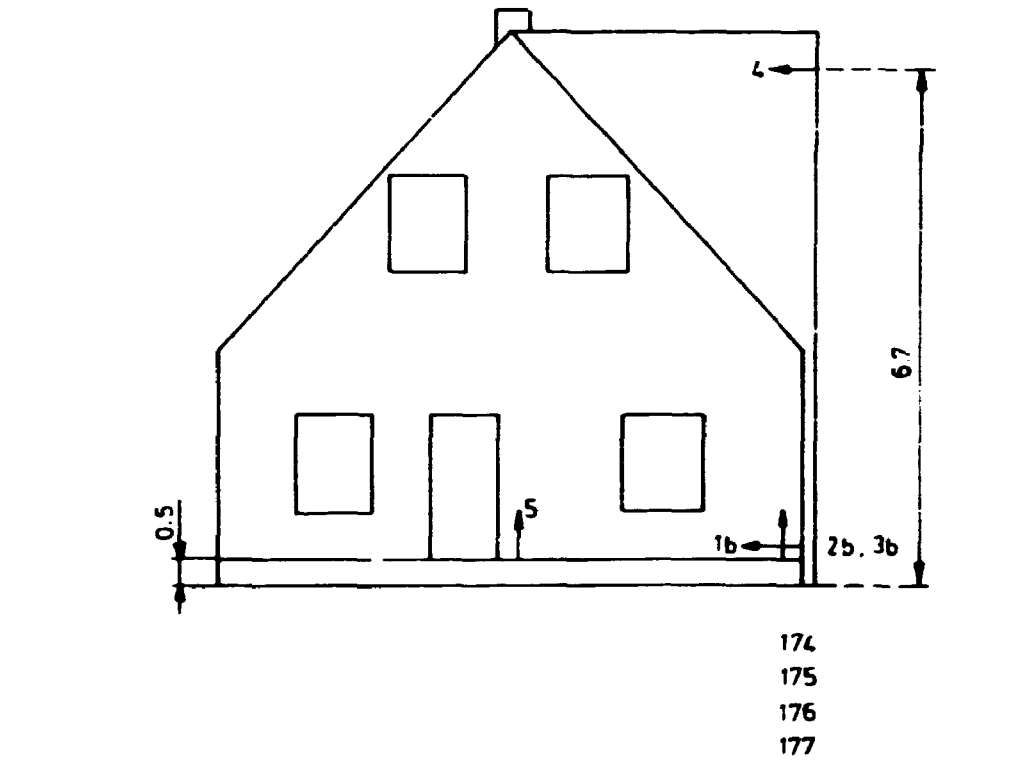

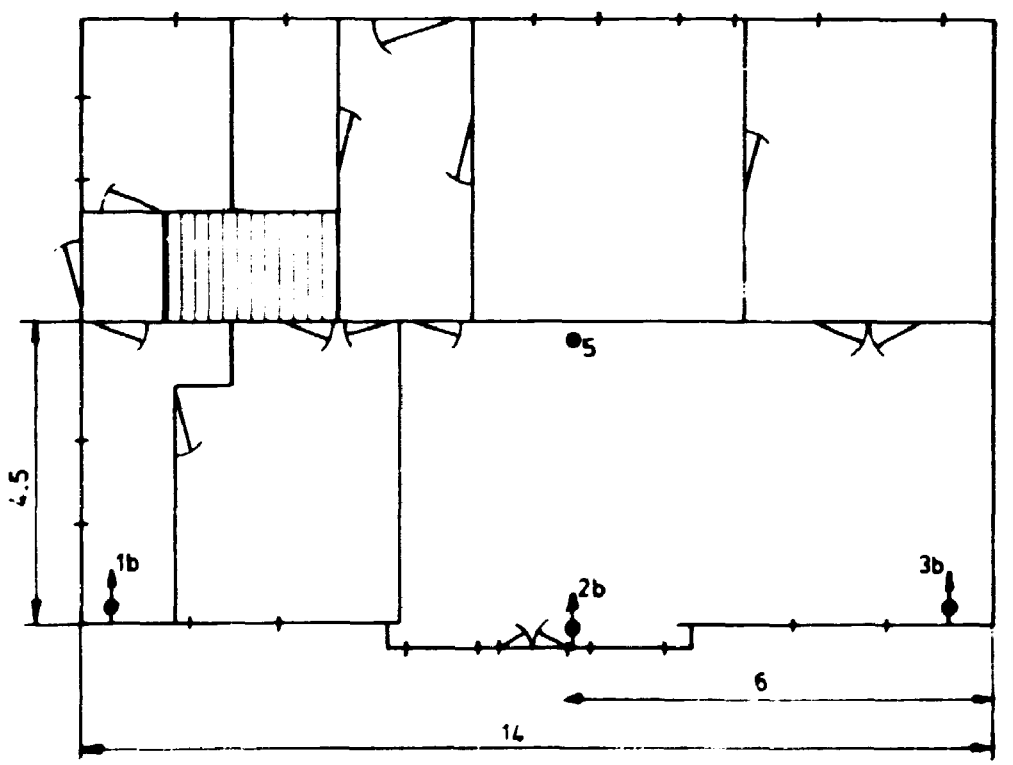

Fig. 3.11.1.7. Accelerometer positions in experiments no. 174, 175, 176 and 177. House seen from west and from above.

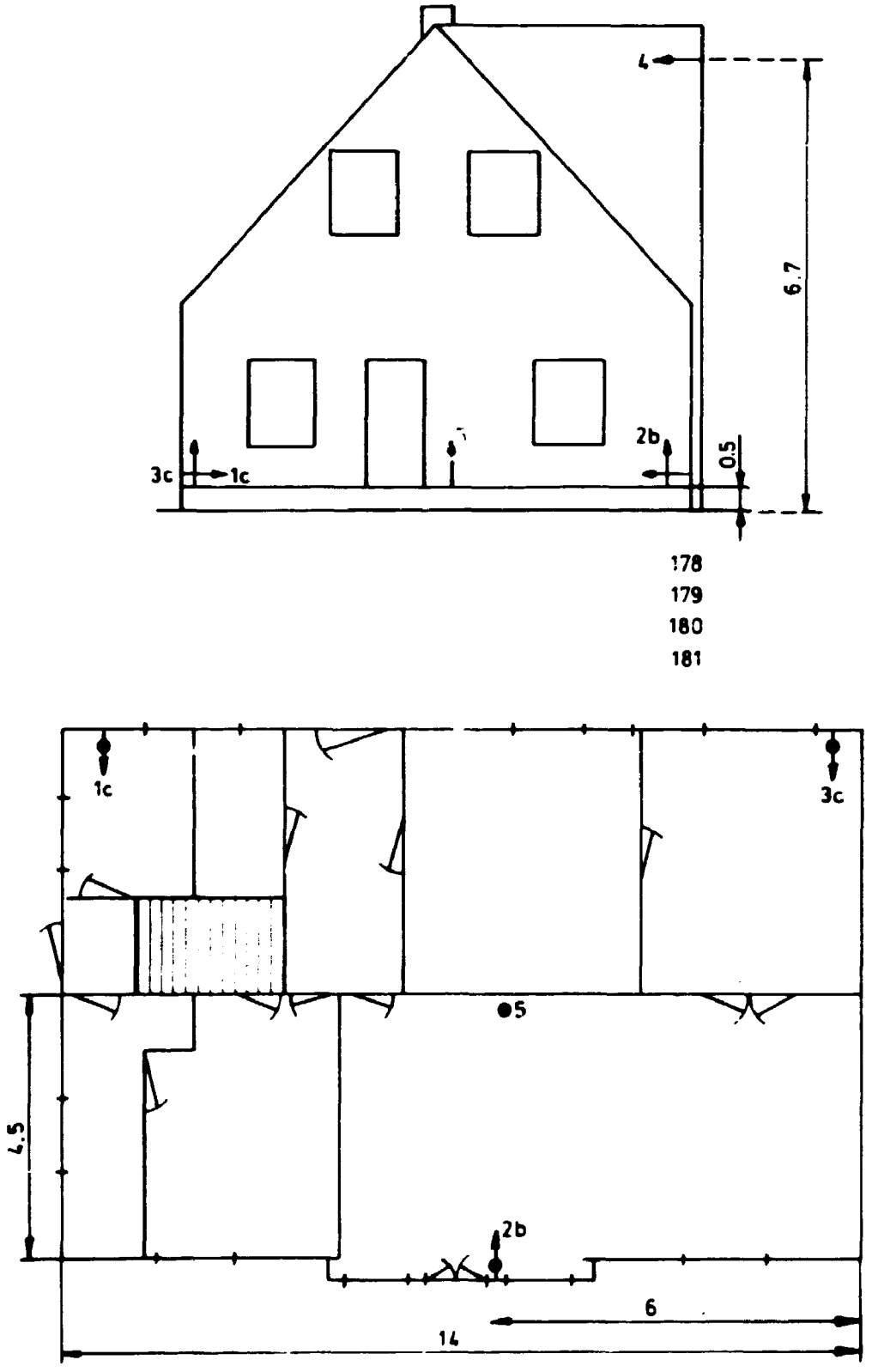

Fig. 3.11.1.8. Accelerometer positions in experiments no. 178, 179, 180 and 181. House seen from west and from above.

No. 170

Date: 14/11-83

Time: 14.10

Purpose: To measure the pressure distribution on, as well as the vibrations of a building located at a distance of 30 m from the center of the explosion.

Atmosphere: unstable

Windspeed (m/sec) 2.0 m : 2.89
4.3 m : 3.42
8.5 m : 3.73

Wind direction (°from N): 273

ature (°C) 2.0 m : 4.9
8.5 m : 4.8

Direct measured temperature difference (°C): -0.9

Atmospheric pressure (mbar): 1022.4

Balloon: 600 g Delasson

Gas mixture (vol. %): CH_4= 25, O_2= 50, N_2= 25

Volume (m^3): 5

Explosion max. pressure (mbar) 5.0 m : -
pp. pressure (mbar) 5.0 m : -

No. 171

Date: 14/11-83

Time: 16.00

Purpose: To measure the pressure distribution on, as well as the vibrations of a building located at a distance of 30 m from the center of the explosion.

Atmosphere: neutral

Windspeed (m/sec) 2.0 m : 2.96
4.3 m : 3.56
8.5 m : 3.94

Wind direction (°from N): 278

Temperature (°C) 2.0 m : 4.9
8.5 m : 4.9

Direct measured temperature difference (°C): -0.00

Atmospheric pressure (mbar): 1020.1

Balloon: 600 g Delasson

Gas mixture (vol. %): CH_4= 25, O_2= 50, N_2= 25

Volume (m^3): 5

Explosion max. pressure (mbar) 5.0 m : 30
pp. pressure (mbar) 5.0 m : 70

No. 172

Date: 17/11-83

Time: 11.55

Purpose: To measure the pressure distribution on, as well as the vibrations of a building located at a distance of 30 m from the center of the explosion.

Atmosphere: unstable

Windspeed (m/sec) 2.0 m : 1.22
4.3 m : 1.43
8.5 m : 1.57

Wind direction (°from N): 5

Temperature (°C) 2.0 m : 1.4
8.5 m : 1.3

Direct measured temperature difference (°C): -0.14

Atmospheric pressure (mbar): 1015.5

Balloon: 600 g Delasson

Gas mixture (vol. %): CH_4= 25, O_2= 50, N_2= 25

Volume (m^3): 5

Explosion max. pressure (mbar) 5.0 m : 88
pp. pressure (mbar) 5.0 m : 178

No. 173

Date: 17/11-83

Time: 13.47

Purpose: To measure the pressure distribution on, as well as the vibrations of a building located at a distance of 30 m from the center of the explosion.

Atmosphere: unstable

Windspeed (m/sec) 2.0 m : 0.88
4.3 m : 1.05
8.5 m : 1.02

Wind direction (°from N): 308

Temperature (°C) 2.0 m : 1.9
8.5 m : 1.7

Direct measured temperature difference (°C): -0.23

Atmospheric pressure (mbar): 1016.0

Balloon: 1100 g Delasson

Gas mixture (vol. %): CH_4= 25, O_2= 50, N_2= 25

Volume (m^3): 5

Explosion max. pressure (mbar) 5.0 m : 142
pp. pressure (mbar) 5.0 m : 280

No. 174

Date: 18/11-83

Time: 12.16

Purpose: To measure the pressure distribution around a group of buildings as well as the vibrations of one of them.

Atmosphere: neutral

Windspeed (m/sec) 2.0 m : 3.66
4.3 m : 4.22
8.5 m : 4.63

Wind direction (°from N): 297

Temperature (°C) 2.0 m : 6.5
8.5 m : 6.5

Direct measured temperature difference (°C): -0.00

Atmospheric pressure (mbar): 1008.7

Balloon: 600 g Delasson

Gas mixture (vol. %): CH_4= 25, O_2= 50, N_2= 25

Volume (m^3): 5

Explosion max. pressure (mbar) 5.0 m : 57
pp. pressure (mbar) 5.0 m : 105

No. 175

Date: 18/11-83

Time: 14.21

Purpose: To measure the pressure distribution around a group of buildings as well as the vibrations of one of the houses.

Atmosphere: neutral

Windspeed {m/sec} 2.0 m : 3.03
4.3 m : 3.56
8.5 m : 4.39

Wind direction {°from N}: 348

Temperature {°C} 2.0 m : 6.4
8.5 m : 6.4

Direct measured temperature difference {°C}: -0.05

Atmospheric pressure {mbar}: 1009.7

Balloon: 600 g Delasson

Gas mixture {vol. %}: CH_4= 25, O_2= 50, N_2= 25

Volume {m^3}: 5

Explosion max. pressure {mbar} 5.0 m : 37
pp. pressure {mbar} 5.0 m : 64

No. 176

Date: 23/11-83

Time: 13.15

Purpose: To measure the pressure distribution around a group of buildings as well as the vibrations of one of the houses.

Atmosphere: unstable

Windspeed (m/sec) 2.0 m : 1.15
4.3 m : 1.40
8.5 m : 1.47

Wind direction (°from N): 306

Temperature (°) 2.0 m : 2.1
8.5 m : 1.8

Direct measured temperature difference (°C): -0.23

Atmospheric pressure (mbar): 1018.4

Balloon: 1100 g Delasson

Gas mixture (vol. %): CH_4= 25, O_2= 50, N_2= 25

Volume (m^3): 10

Explosion max. pressure (mbar) 5.0 m : 125
pp. pressure (mbar) 5.0 m : 219

No. 177

Date: 23/11-83

Time: 14.08

Purpose: To measure the pressure distribution around a group of buildings as well as the vibrations of one of the houses.

Atmosphere: unstable

Windspeed (m/sec) 2.0 m : 1.19
4.3 m : 1.43
8.5 m : 1.64

Wind direction (°from N): 236

Temperature (°C) 2.0 m : 1.9
8.5 m : 1.8

Direct measured temperature difference (°C): -0.18

Atmospheric pressure (mbar): 1018.6

Balloon: 1100 g Oelasson

Gas mixture (vol. %): CH_4= 25, O_2= 50, N_2= 25

Volume (m^3): 5

Explosion max. pressure (mbar) 5.0 m : 110
pp. pressure (mbar) 5.0 m : 189

No. 178

Date: 29/11-83

Time: 12.35

Purpose: To measure the pressure distribution around a group of buildings as well as the vibrations of one of the houses.

Atmosphere: neutral

Windspeed {m/sec} 2.0 m : 0.95
4.3 m : 1.26
8.5 m :

Wind direction {°from N}: 147

Temperature {°C} 2.0 m : -1.1
8.5 m : -1.1

Direct measured temperature difference {°C}: -0.05

Atmospheric pressure {mbar}: 1005.9

Balloon: 600 g Delasson

Gas mixture {vol. %}: CH_4= 25, O_2= 50, N_2= 25

Volume {m^3}: 1

Explosion max. pressure {mbar} 5.0 m : 8.9
pp. pressure {mbar} 5.0 m : 16.8

No. 179

Date: 29/11-83

Time: 13.15

Purpose: To measure the pressure distribution around a group of buildings as well as the vibrations of one of the houses.

Atmosphere: neutral

Windspeed {m/sec} 2.0 m : 1.09
4.3 m : 1.36
8.5 m :

Wind direction {°from N}: 189

Temperature {°C} 2.0 m : -0.9
8.5 m : -1.0

Direct measured temperature difference {°C}: -0.14

Atmospheric pressure {mbar}: 1005.5

Balloon: 600 g Delasson

Gas mixture {vol. %}: CH_4= 25, O_2= 50, N_2= 25

Volume {m^3}: 2.7

Explosion max. pressure {mbar} 5.0 m : 69
pp. pressure {mbar} 5.0 m : 107

No. 180

Date: 29/11-83

Time: 14.10

Purpose: To measure the pressure distribution around a group of buildings as well as the vibrations of one of the houses.

Atmosphere: unstable

Windspeed {m/sec} 2.0 m : 0.42
4.3 m : 0.60
8.5 m :

Wind direction {°from N}: 111

Temperature {°C} 2.0 m : -1.3
8.5 m : -1.4

Direct measured temperature difference {°C}: -0.09

Atmospheric pressure {mbar}: 1005.4

Balloon: 600 g Delasson

Gas mixture {vol. %}: CH_4= 25, O_2= 50, N_2= 25

Volume {m^3}: 2.7

Explosion max. pressure {mbar} 5.0 m : 49
pp. pressure {mbar} 5.0 m : 99

No. 181

Date: 29/11-83

Time: 14.45

Purpose: To measure the pressure distribution around a group of buildings as well as the vibrations of one of the houses.

Atmosphere: unstable

Windspeed {m/sec} 2.0 m : 0.7
4.3 m : 0.91
8.5 m :

Wind direction {°from N}: 146

Temperature {°C} 2.0 m : -1.2
8.5 m : - 1.3

Direct measured temperature difference {°C}: -0.14

Atmospheric pressure {mbar}: 1005.4

Balloon: 600 g Delasson

Gas mixture {vol. %}: CH_4= 25, O_2= 50, N_2= 25

Volume {m^3}: 1

Explosion max. pressure {mbar} 5.0 m : 54
pp. pressure {mbar} 5.0 m : 100

No. 182

Date: 6/12-83

Time: 11.40

Purpose: To measure the pressure distribution around a group of buildings.

Atmosphere:

Windspeed {m/sec} 2.0 m :
4.3 m :
8.5 m :

Wind direction {°from N}:

Temperature {°C} 2.0 m :
8.5 m :

Direct measured temperature difference {°C}:

Atmospheric pressure {mbar}: 1010.1

Balloon: 100 g Phillips

Gas mixture {vol. %}: CH_4= 25, O_2= 50, N_2= 25

Volume {m^3}: 0.524

Explosion max. pressure {mbar} 5.0 m : 62
pp. pressure {mbar} 5.0 m : 100

No. 183

Date: 6/12-83

Time: 12.55

Purpose: To measure the pressure distribution around a group of buildings.

Atmosphere:

Windspeed {m/sec} 2.0 m :
4.3 m :
8.5 m :

Wind direction {°from N}:

Temperature {°C} 2.0 m :
8.5 m :

Direct measured temperature difference {°C}:

Atmospheric pressure {mbar}: 1010.3

Balloon: 100 g Phillips

Gas mixture {vol. %}: CH_4= 14, O_2= 57, N_2= 29

Volume {m^3}: 0.458

Explosion max. pressure {mbar} 5.0 m : 4
pp. pressure {mbar} 5.0 m : 15

No. 184

Date: 6/12-83

Time: 13.15

Purpose: To measure the pressure distribution around a group of buildings.

Atmosphere:

Windspeed {m/sec} 2.0 m :
4.3 m :
8.5 m :

Wind direction {°from N}:

Temperature {°C} 2.0 m :
8.5 m :

Direct measured temperature difference {°C}:

Atmospheric pressure {mbar}: 1009.3

Balloon: 100 g Phillips

Gas mixture {vol. %}: CH_4= 14, O_2= 57, N_2= 29

Volume {m^3}: 0.458

Explosion max. pressure {mbar} 5.0 m : 3
pp. pressure {mbar} 5.0 m : 10

As usual the results have been normalized with respect to a reference measurement. In the Tables 3.11.2.1-4 the normalized peak and the normalized peak-to-peak pressure have been given for each measuring position. Moreover the reference pressures for each experiment have been presented. The normalized accelerations are presented in Table 3.11.2.5.

NORMALIZED PRESSURES

EXPERIMENT	170		171		172		173	
	$P_M/P_{M,5m}$	$P_{P-P}/P_{P-P,5m}$	$P_M/P_{M,5m}$	$P_{P-P}/P_{P-P,5m}$	$P_M/P_{M,5m}$	$P_{P-P}/P_{P-P,5m}$	$P_M/P_{M,5m}$	$P_{P-P}/P_{P-P,5m}$
POS. 1	0.43	0.32	0.43	0.36	0.59	0.46		
POS. 2	0.57	0.46	0.57	0.46			0.70	0.57
POS. 3					0.73	0.56		
POS. 4	0.24	0.24	0.37	0.33			0.37	0.37
POS. 5	0.34	0.27	0.40	0.39			0.52	0.51
POS. 6							0.63	0.68
POS. 7							0.06	0.06
POS. 8							0.06	0.06

REFERENCE PRESSURES

EXPERIMENT	170		171		172		173	
	P_M[mbar]	P_{P-P}[mbar]	P_M[mbar]	P_{P-P}[mbar]	P_M[mbar]	P_{P-P}[mbar]	P_M[mbar]	P_{P-P}[mbar]
5m	104*)	206*)	30	70	88	172	142	291
10m			22	47	60	114	100	187

*) These values are estimated from the measurements in experiment no. 171, by forcing the normalized values corresponding to pos. 2 to be identical for experiment nos. 170 and 171.

Tabel 3.11.2.1. Pressure measured external on the main building. Explosion source 30 m from the building.

NORMALIZED PRESSURES

EXPERIMENT	174		175		176		177	
	$P_M/P_{M,5m}$	$P_{P-P}/P_{P-P,5m}$	$P_M/P_{M,5m}$	$P_{P-P}/P_{P-P,5m}$	$P_M/P_{M,5m}$	$P_{P-P}/P_{P-P,5m}$	$P_M/P_{M,5m}$	$P_{P-P}/P_{P-P,5m}$
POS. 1			0.12	0.10			0.03	0.04
POS. 2			0.10	0.11	0.04	0.04	0.04	0.06
POS. 3			0.09	0.13	0.06	0.08	0.08	0.08
POS. 4			0.07	0.08				
POS. 5			0.07	0.10				
POS. 6	0.18	0.21	0.08	0.10				
POS. 7			0.12	0.13			0.08	0.10
POS. 8	0.15	0.16	0.13	0.12			0.11	0.13

REFERENCE PRESSURES

EXPERIMENT	174		175		176		177	
	P_M[mbar]	P_{P-P}[mbar]	P_M[mbar]	P_{P-P}[mbar]	P_M[mbar]	P_{P-P}[mbar]	P_M[mbar]	P_{P-P}[mbar]
5m	52	105	37	65	125	219	110	189
10m	32	64	23	41	89	143	63	116

Table 3.11.2.2. External and internal (pos. 1,2,3) pressures at main building. Explosion source 30 m from the building.

NORMALIZED PRESSURES

EXPERIMENT	178		179		180		181	
	$P_M/P_{M,5m}$	$P_{P-P}/P_{P-P,5m}$	$P_M/P_{M,5m}$	$P_{P-P}/P_{P-P,5m}$	$P_M/P_{M,5m}$	$P_{P-P}/P_{P-P,5m}$	$P_M/P_{M,5m}$	$P_{P-P}/P_{P-P,5m}$
POS. 1	0.77	0.83						
POS. 2			1.16	1.50	1.33	1.70	1.13	1.36
POS. 3			1.97	2.13	1.72	1.66	2.06	2.29
POS. 4	1.04	1.21						
POS. 5								
POS. 6								

REFERENCE PRESSURES

EXPERIMENT	178		179		180		181	
	P_M[mbar]	P_{P-P}[mbar]	P_M[mbar]	P_{P-P}[mbar]	P_M[mbar]	P_{P-P}[mbar]	P_M[mbar]	P_{P-P}[mbar]
5m	8.9	16.8	68.9	107.0	48.8	98.6	53.9	99.6

Tabel 3.11.2.3. External pressures due to explosion source in the courtyard.

NORMALIZED PRESSURES

EXPERIMENT	182		183		184	
	$P_M/P_{M,5m}$	$P_{P-P}/P_{P-P,5m}$	$P_M/P_{M,5m}$	$P_{P-P}/P_{P-P,5m}$	$P_M/P_{M,5m}$	$P_{P-P}/P_{P-P,5m}$
POS. 1	1.13	1.48	0.83	0.89	0.71	0.71
POS. 2			1.60	1.14	1.28	1.43
POS. 3			1.14	1.44	1.20	1.21
POS. 4			1.30	1.19	0.88	0.93
POS. 5					0.78	0.85
POS. 6						

REFERENCE PRESSURES

EXPERIMENT	182		183		184	
	P_M[mbar]	P_{P-P}[mbar]	P_M[mbar]	P_{P-P}[mbar]	P_M[mbar]	P_{P-P}[mbar]
5m	61.5	105.5	4.4	14.7	3.13	10.06

Fig. 3.11.2.4. External pressures due to explosion source in the courtyard.

NO.	1 VERT	1 LONG	3 VERT	3 LONG	2 VERT	2 LONG	CEILING VERT	POS 4 LONG	2 TRANS	POS 5		
170	0.010	0.027	0.017	0.068								
171	0.016	0.021	0.023	0.046	0.179	0.14	0.089	0.097				
172	0.039	0.067	0.057	0.064	0.028	0.098		0.067	0.04			
173	0.019	0.050	0.022	0.054	0.019	0.108		0.056	0.04			
	1 VERT B	1 LONG B	3 VERT B	3 LONG B	2 VERT B	2 LONG B						
174	0.015	0.022	0.019	0.037	0.034	0.079		0.062		0.017		
175	0.012	0.024	0.017	0.035	0.023	0.064		0.055		0.014		
176	0.020	0.050	0.016	0.032	0.031	0.086		0.039				
177	0.015	0.038	0.019	0.032	0.021	0.069		0.042				
	1 VERT C	1 LONG C									3 LONG C	3 VERT C
178					0.033	0.057		0.198			0.100	0.066
179	0.035	0.09			0.013	0.026		0.100			0.196	0.065
180	0.032	0.066			0.019	0.037		0.124			0.247	0.076
181	0.079	0.179		0.129	0.015	0.037		0.056			0.129	0.043

Table 3.11.2.5. Accelerations normalized with respect to $P_{M,5}$.

3.11.3. EVALUATION OF THE PRESSURE MEASUREMENTS

For reference purposes, the pressure was measured as previously at distances 5 and 10 m from the source. However, due to the short distance between the buildings in the courtyard, the 5 m reference pressure was chosen in this case for normalizing the pressure at the individual measuring positions.

The transducer positions were kept the same in the first four experiments. One of the transducers, located close to the corner at the ground of the building, showed a very poor reproducibility, which is believed to be due to turbulence or diffraction phenomenae at this specific position.

As for the measurements performed at the free-standing wall, a reflection factor can be calculated for the different measuring positions at the buildings. The reflection factor is defined as the ratio between the actual measured pressure at the position and the corresponding pressure in the undisturbed pressure field, see section 3.9.2.3. For the reason given above, the 5m reference pressure is chosen, and an exponent equal to unity is assummed for the acoustic damping. This assumption may understimate the calculated free field pressure and thus overestimate the reflection factors. However, the source size utilized in this series of tests is less than the size used for regression analysis, and the 5 m reference pressure may be a more valid reference pressure in this case.

The calculated reflection coefficients are given in Table 3.11.3.1 below, where also the corresponding free field pressure, calculated as stated above, are given. As expected, there is a varation over the height of the building for the central part, as observed for the free-standing wall, and the reflection coefficients at ground level (0.5 m) and at the internal corner corresponds to the values obtained for the free-standing wall, see Fig. 3.9.2.3.1. The two small values for the internal corner for the very low pressures 3, respectively 4 mbar are measured for explosions performed outside the courtyard, and the main building may thus still give some shielding effect, i.e. the calculated reference pressure may be too high in this case.

MEASUR. POSITION		REFL. COEFF.	CALCUL. FREE FIELD PEAK PRESSURE (mbar)
Central part of building.	Level:0.5 (m)	3.4 3.4 4.2	17 5 24
	2-3	2.0 2.2 3.2 3.8 1.7* 2.6 2.0 2.5 2.5 3.6 2.2 2.8 1.5*	17 5 24 24 3 30 21 24 28 ~2 ~2 ~2 ~2
	5.0	1.4 2.4 2.2	17 5 24
External corner		2.6 2.6 3.5-4.2 1.8 1.9 1.6-1.1	17 5 15 3 ~2 ~2
Internal corner		1.7 1.5 5.1 4.5 5.4	4 3 30 21 24
		* measured on wall not perpendicular to wave propagation.	

Table 3.11.3.1. Reflection coefficients measured on buildings.

3.11.4. EVALUATION OF THE VIBRATION MEASUREMENTS

In order to compare the pressure measurements with the vibrations of the buildings, the accelerations were measured in several positions. They gave a very complicated picture since they consisted of contributions from the direct pressure-wave-initiated vibrations and from the waves which have been transmitted through the ground. As the accelerometers have been exposed to the direct pressure wave, spurious high-frequency components may be present in the signals.

All the vibration measurements have been treated by an analogue 2nd-order Butterworth filter with a band width of 1-156Hz, since vibrations above this frequency are without importance for buildings owing to their low content of energy. As a general feature the longitudinally measured accelerations have a higher frequency and a higher peak than those that are vertically measured. This suggests that the vertical accelerations are caused by tremors alone and longitudinal accelerations from both tremors and direct action. In order to compare the experiments mutually the accelerations have been normalized with regard to $P_{M,5}$.

There are several criteria for predicting how much vibration a building can stand [2]. A general rule applicable for frequencies higher than 5 Hz, is the following:

$v < 2$mm/sec	settings cracks can be expected
$2 < v < 5$mm/sec	cracks in the plaster
$5 < v < 12$mm/sec	cracks in the wall
$12 < v$	debilitation of concrete,

where v denotes the velocity.

All the measurements with accelerometers have been integrated with respect to time in order to find those velocities that best represent the loading on the building.

Some of the impulse curves show a linear drift due to a superimposed DC level. It is caused by insufficient resolution in the digitalisation of the small values registered. It is compensated by reference to an estimated drift.

The series consisting of experiments no. 170, 171, 172 and 173 are characterized by the mounting of the accelerometers outside the house. Therefore, besides the vibrations of the house, they were influenced by the pressure wave even though they were covered by a pail. (Those on the ceiling, marked 4, were inside the house). Some of the curves show velocities which can cause damage to the building, referring to the criteria stated above. Especially the accelerometers on the ceiling, pos. 4, have measured critical vibrations. An inspection of the building at this time showed that the wall above the door and the windows began to crack.

In the series consisting of experiments no. 174, 175, 176 and 177 all the transducers were placed inside the house. At this time eight roof plates were broken and the brickwork above the windows had been supported. Even though the windows were covered by shutters they were all broken. Several of the velocity curves show velocities of over 40 mm/sec during periods when they are harmful.

The experiments were made in the direction south of the house and, as mentioned, at a distance of 30 m from the explosion center. Besides, the experiments with the concrete wall were made at the same place and thus the building was exposed to other explosions than those just described.

The four explosions 178, 179, 180 and 181 were all performed in the courtyard with smaller amounts of gas (less than 2.5 m^3) owing to security considerations. Here it is again the measurements on the first floor which exhibit the most serious vibrations even though these were done on the opposite side of the building. It can be due to an already established crack in the extended piece of gable combined with the large exposed surface formed by the roof.

It is noted that the first eight series of results of the normalized accelerations cannot be compared with the last four since the distance from the explosion to the house is different.

The damage to the farmhouse is illustrated in the pictures below taken at different stages in the explosion program.

Fig. 3.11.4.1. The farmhouse after 5 explosions (seen from south).

Fig. 3.11.4.2. The farmhouse after 20 explosions.

Fig. 3.11.4.3. The part above the door after 20 explosions.

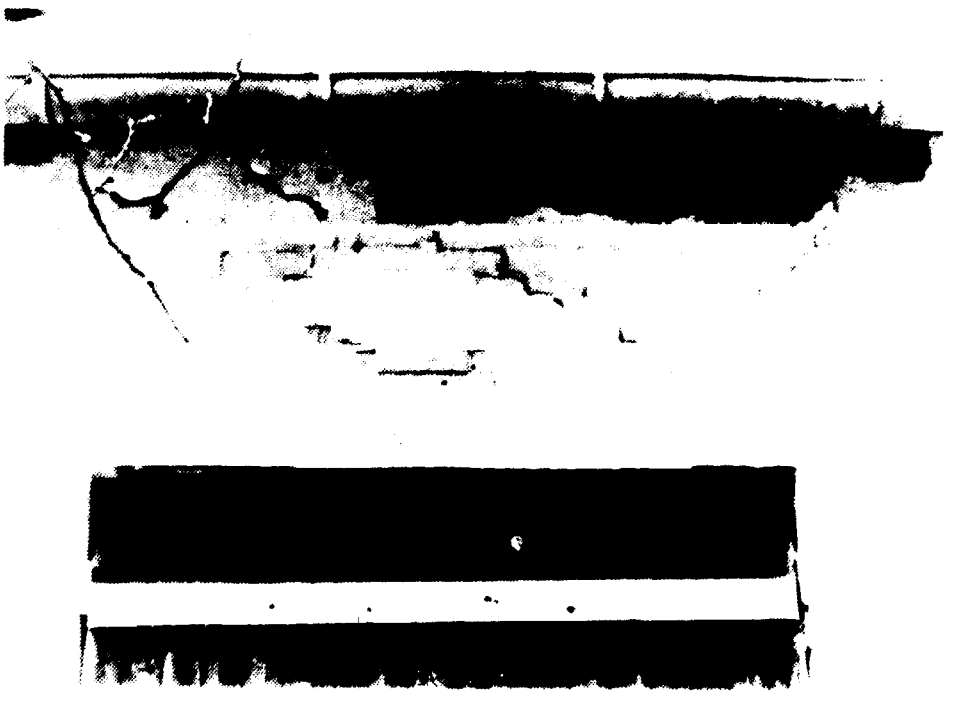

Fig. 3.11.4.4. The part above the right window after 20 explosions.

Fig. 3.11.4.5. The ceiling inside the farmhouse after 27 explosions.

4. SUMMARY

The measurements have been performed with blast waves arising from homogeneous and well-defined mixtures of methane, oxygen and nitrogen, contained within spherical balloons with controlled initial dimensions.

The explosion process has been recorded by a high-speed camera, and although the expansion of the gas cloud (at least in the film plane) looks reasonably symmetric, variations in the pressure level could indicate certain asymmetries. The variations in the pressure level are eliminated by normalising the pressure measurements with respect to a reference pressure that is characteristic of a particular experiment.

The scatter of the measurements is estimated for stable, neutral and unstable atmospheric conditions. The scatter is

seen to be accumulating in the sense that the scatter of measurements performed far from the source is larger than the scatter of measurements performed close to it. Moreover, it appears that atmospheres with a high content of turbulence give rise to more scatter of the measurements than atmospheric conditions containing no turbulence.

An attempt to determine the ground reflection factor has been performed with limited success, due to geometric and material inhomogeneities in the ground.

A number of reference experiments have been carried out on a plane area without vegetation. The pressure attenuation is observed to follow acoustic theory. A shock-up phenomenon has been observed in a few tests. The distance required to form the shock front is compared to theoretical predictions, and reasonable agreement is found.

The attenuation of the blast wave due to vegetation was investigated. No significant attenuation is observed for the forest studied and for the signals used. This is in agreement with other studies operating with harmonic signals [6].

The influence of obstacles as banks, walls and houses on the pressure field is also investigated.

It is observed, that the presence of a bank can be felt by the pressure waves in a shadow zone 15 m (corresponding to 5 times the height of the bank or 0.7 times the wavelength of the pressure pulse) behind the obstacle, whereas the pressure propagation at greater distances is unaffected. This is in agreement with the results given in [5] for harmonic signals.

The pressure build-up on the wall is more pronounced than predicted by the acoustic theory. The pressure varies with the distance from the boundaries and no clear demarcation of side diffraction effects, for the wavelength used and the dimensions of the obstacle studied, have been observed. The overall pressure field is seen to be unaffected by the presence of the wall.

The pressure build-up on the front of the house shows the same qualitative picture as the pressure build-up at the front of the wall. The reflection factor at the ground in the center of the house is around 3.5, whereas the reflection factor corresponding to the outer regions is of the order 1. The pressure inside the house and on the back of the house is of the same order of magnitude (and equal to 0.3 times the value that would be measured in a free field at the same distance). The pressure build-up in a corner is slightly more pronounced than the build-up in the center of a plane surface.

Finally the acceleration measurements on the house show that the longitudinal oscillations contain larger peaks and higher frequencies than the vertical ones. The measurements have been compared to a damage concept, which shows that structural failure should occur. This is in accordance with the observations.

5. REFERENCES

[1] Thomas, A., and Williams, G.T. (1966), Flame noise: sound emission from spark-ignited bubbles of combustible gas. Proc. R. Soc. London A294, 449-66.

[2] Lauritzen, E.K. (1978), Vibrationsskader på bygninger m.v. følge af konventionelle sprængninger. (Forsvarsakademiet, København). (in danish).

[3] Morse, P.M., and Ingard, K.U. (1968), Theoretical Acoustics, (McGraw - Hill, New York) 927pp.

[4] Strehlow, R.A., Luckritz, R.T., Adamczyk, A.A., and Shimpi, S.A. (1979), The blast wave generated by spherical flames, Combust. Flame 35, 297-310.

[5] de Jong, B.A., Moerkerken, A., and van der Toorn, J.D. (1983), Propagation of sound over grassland and over an earth barrier, Journal of Sound and Vibration, 86, 23-46.

[6] Fricke, F. (1984), Sound attenuation in forests, Journal of Sound and Vibration, 92, 149-158.

[7] Deshaies, B., and Leyer, J.C.(1981), Flow field induced by unconfined spherical accelerating flames. Combust. Flame, 40, 141-153.

[8] Baker, W.E.(1981), Explosions in Air. (University of Texas Press, Austin and London) 268pp.

[9] Essers, J.A.(1982), Characterization of the pressure wave origination in the explosion of an extended heavy gas cloud: critical analysis of the treatment of its propagation in air and interaction with obstacles. Von Karman Computational Fluid Dynamics Department, Belgium. ECI - 794 - 2651 - 81 - B.

[10] Landolt - Börnstein (1967), Zahlenwerte und Funktionen aus Physik - Chemie - Astronomie - Geophysik - Technik, Sechste Auflage, IV. Band, Technik, 4. Teil Wärmetechnik, Bandteil a, Springer, Berlin, 944pp.

[11] Larsen, G.(1984), Gas explosion characterization, wave propagation (small-scale experiments), CEC Contract No. 025 SR DK, Final Report, Risø-R-525, 144pp.

6. LIST OF SYMBOLS

The most important designations and symbols, used in the report, are listed and explained below.

A_i ; i = 1,2	The amplitude in the distance $R_i(X)$ from a point source.
H	The height of the wall.
I	The impulse.
I_{Ro}	The fictive max. impulse corresponding tc the fictive pressure in the center of the source.
P	The pressure.
P_f	The fictive maximum peak pressure at the center of the source.
$P_1(X)$	The pressure level in test number X.
P_M	The maximum peak pressure.
P_{P-P}	The peak-to-peak pressure.
P_{MI}	The minimum peak pressure.
PYF	The measuring position number Y at the front of the wall.
PYB	The measuring position number Y at the back of the wall.
R	The distance from the center of the source to the point of measuring.
R	The radius of the expanding gas cloud.
$R_1(X)$	The distance traveled by a "direct" signal.
$R_2(X)$	The distance traveled by a "reflected" signal.

T	The time.
U_f	The particle velocity corresponding to the flow at the end of the compression phase.
X	The horizontal distance between the point of measurement and the source.
X_1	The horizontal distance between the point of reflection and the source.
c_0	The speed of sound.
c_f	The speed of sound at the end of the compression phase.
$f(\theta)$	The reflection factor for the soil depending on the angle θ.
f_W	The reflection factor for the wall.
h	The level of the center of the source.
k	The exponent in the formula for pressure attenuation.
k_5	The exponent in the formula for pressure attenuation with 5 m as the closest measuring position.
k_{10}	The exponent in the formula for pressure attenuation with 10 m as the closest measuring position.
l	The level of the transducer.
$\bar{q}$	The dimensionless heat added by the flame.
t	The time.
Δt_c	The calculated time difference.
Δt_m	The measured time difference.
x	The level of a measuring point on the wall.

α	The expansion factor for the gasmixture.
β	The specific admittance of a surface.
γ	The heat capacity ratio.
γ_1	The heat capacity ratio of the unburned mixture.
γ_2	The heat capacity ratio of the burned mixture.
θ	The angle between a reflected beam and the normal to the surface.
θ	The time required for the shock formation.
λ	The distance required for complete shock formation.
$\sigma\%$	The standard deviation in percentage of the mean value.
τ	The time deserved from the start of a wave until it nas reached the maximum pressure.

SUBSCRIPT

$_0$	The ambient conditions.

SYMBOLS

■	The source.
●	A measuring point.
x	A measuring point.
<•>	A mean value operator.
→	A measuring direction.

APPENDIX 1

Print of high-speed film no. 3

In the following a print of high-speed film number 3 is given. This sequence represent every fourth picture of the original film. For each picture the time (t), taken from the ignition of the mixture, and the actual radius (R) of the exploding gas cloud have been given.

t = 0

R = 1.36 m

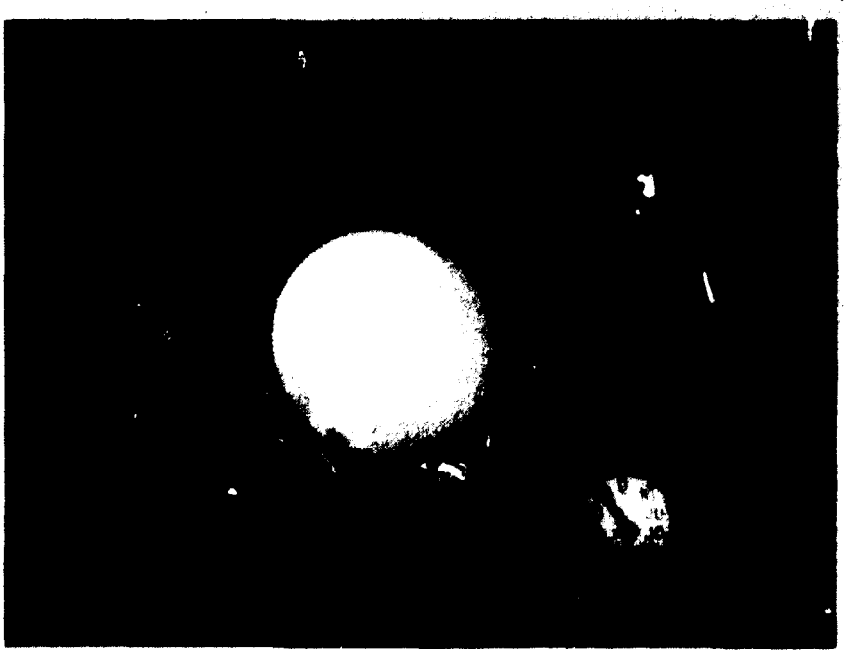

t = 1.23 ms

R = 1.38 m

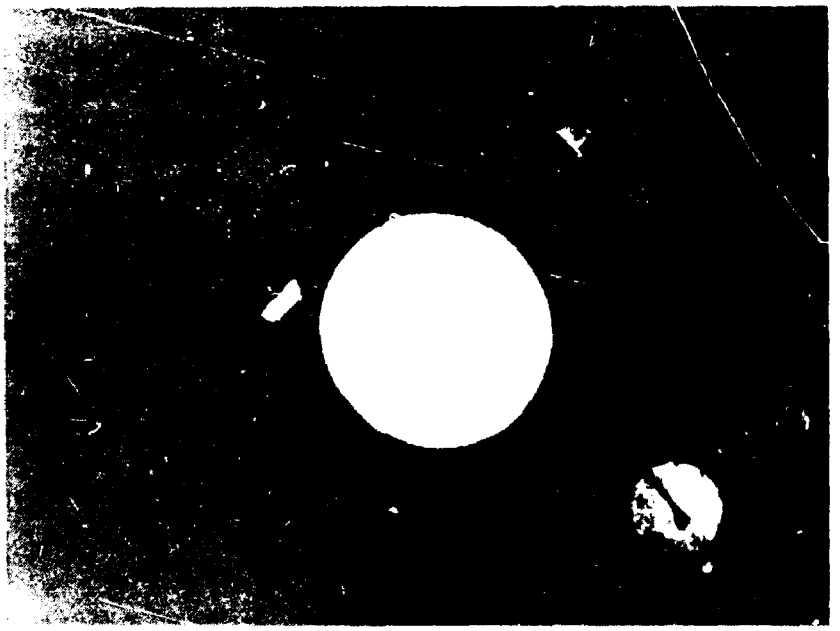

t = 2.47 mm

b = 1.40 m

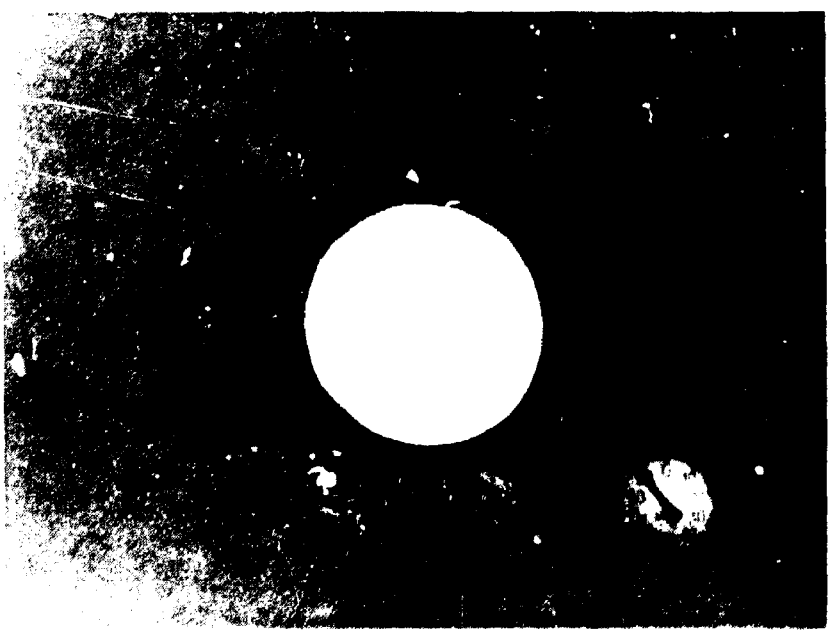

t = 3.[illegible] mm

b = 1.47 m

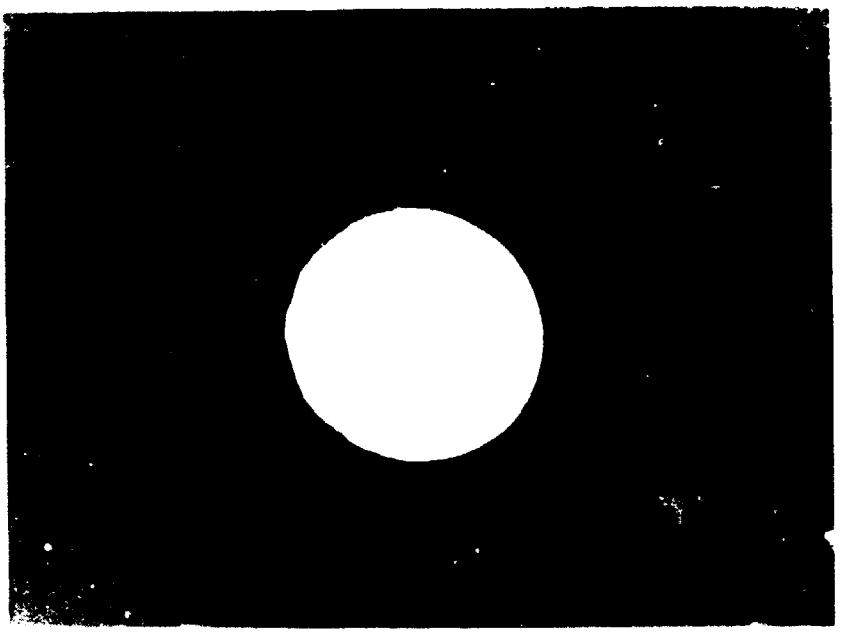

t = 4.94 ms

h = 1.54 m

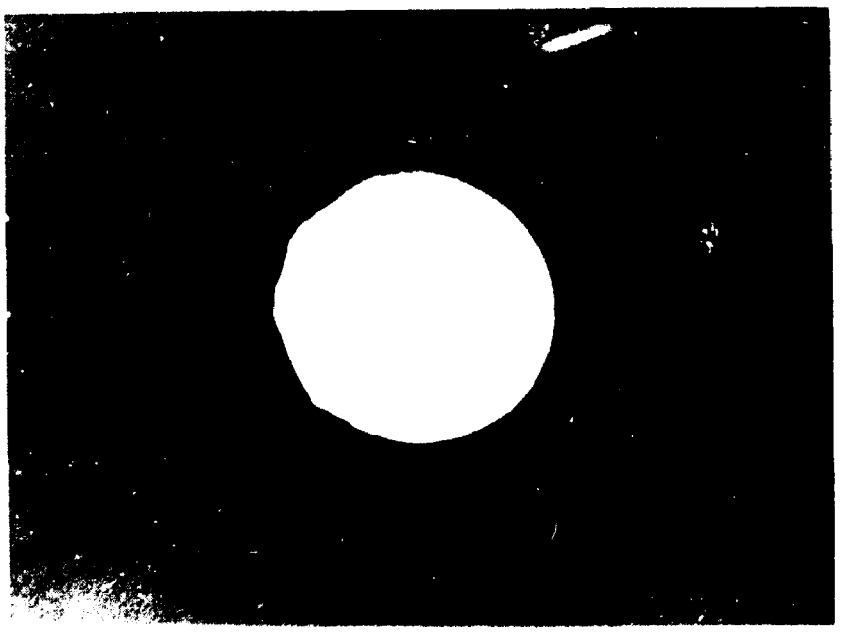

t = 6.17 ms

h = 1.67 m

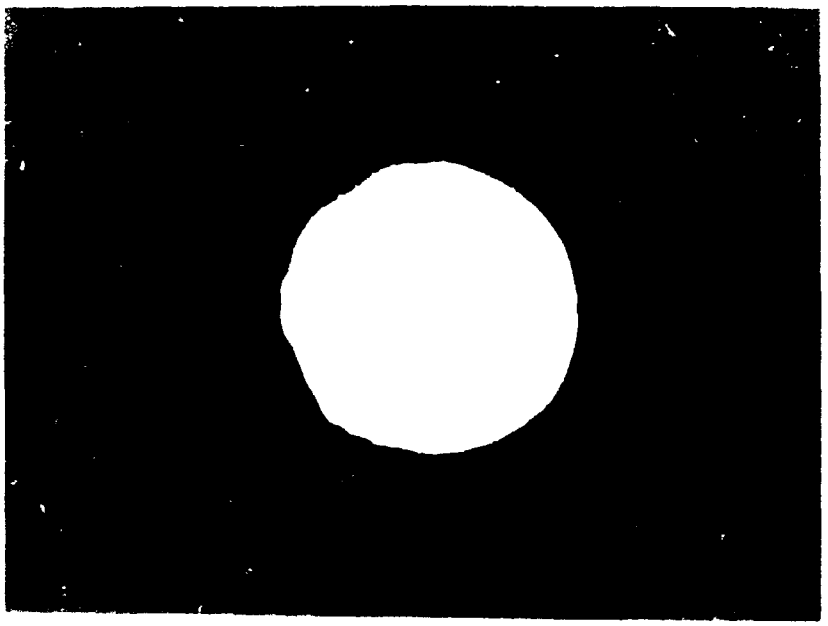

a 7.41 mm

b 1.[illegible] m

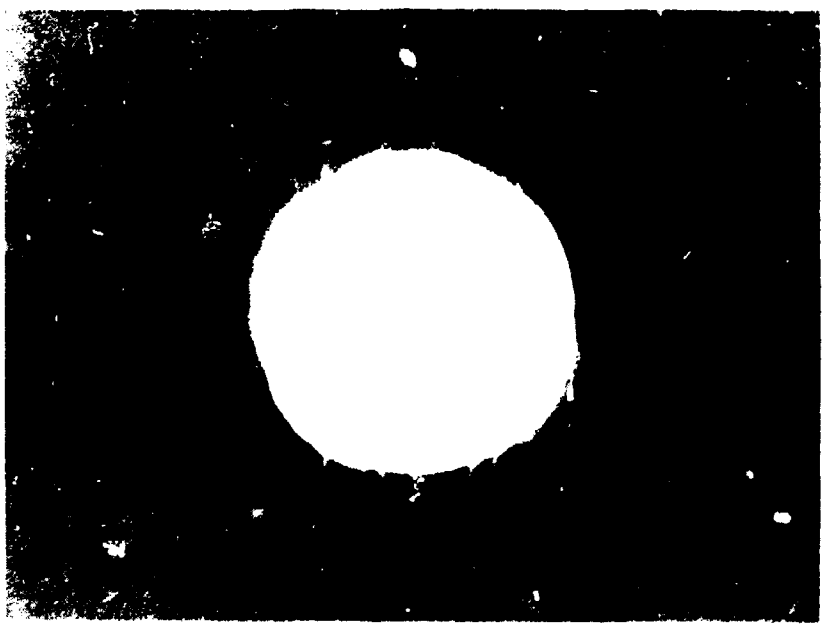

a [illegible] m

b 1.[illegible] m

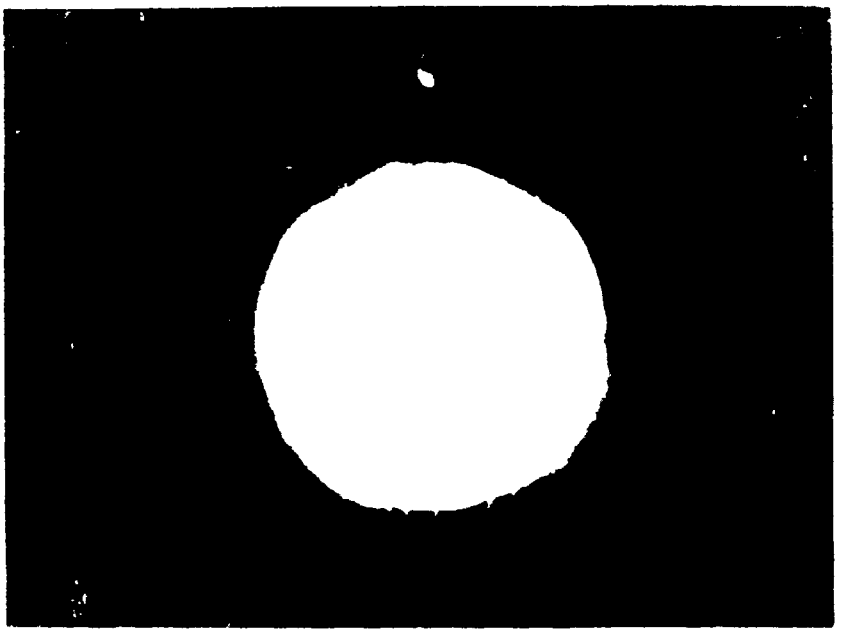

t = 9.88 ms

R = 2.11 m

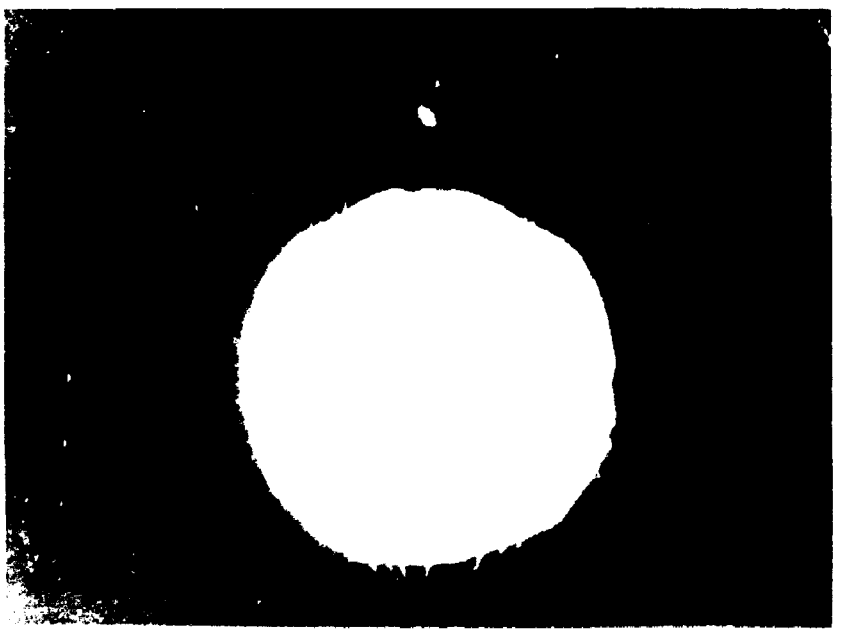

t = 11.11 ms

R = 2.24 m

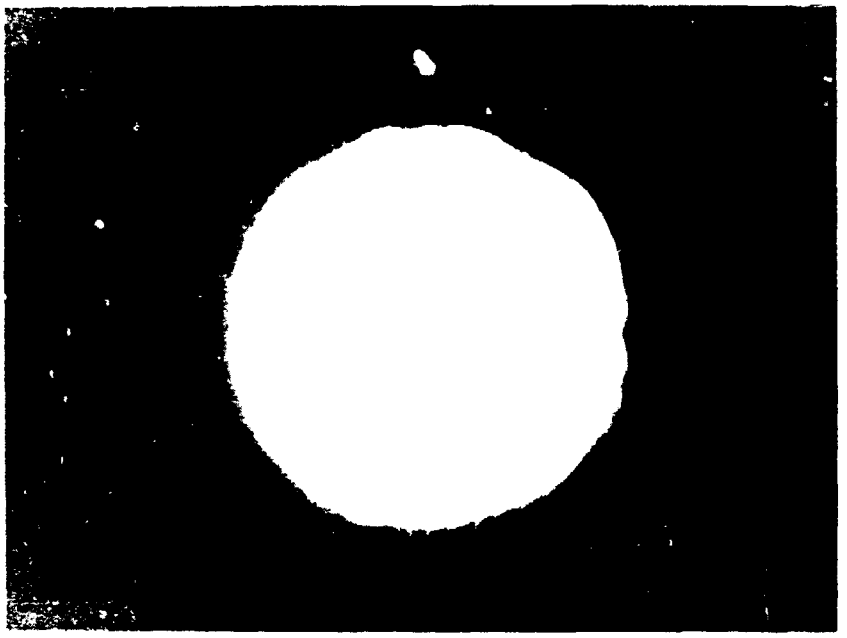

t = 12.35 ms

R = 2.37 m

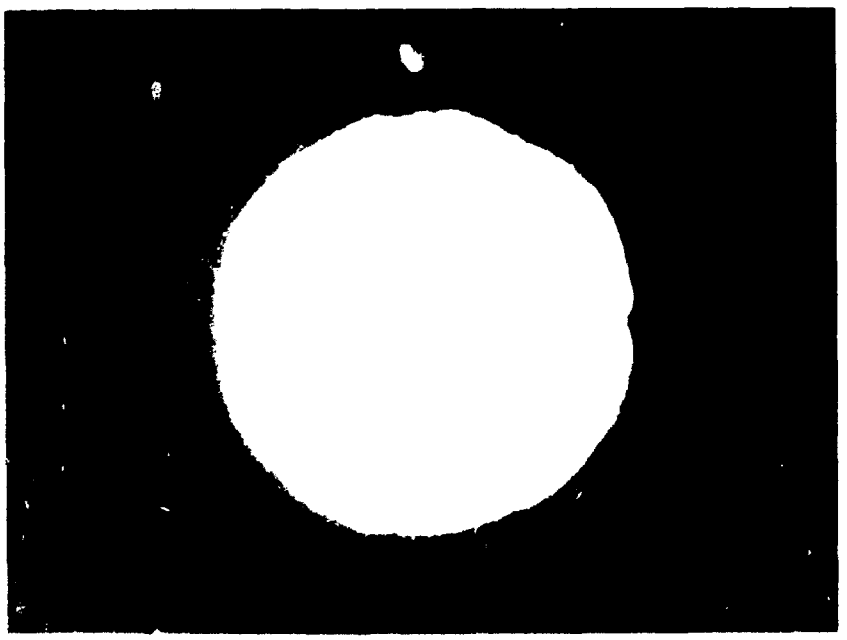

t = 13.58 ms

R = 2.50 m

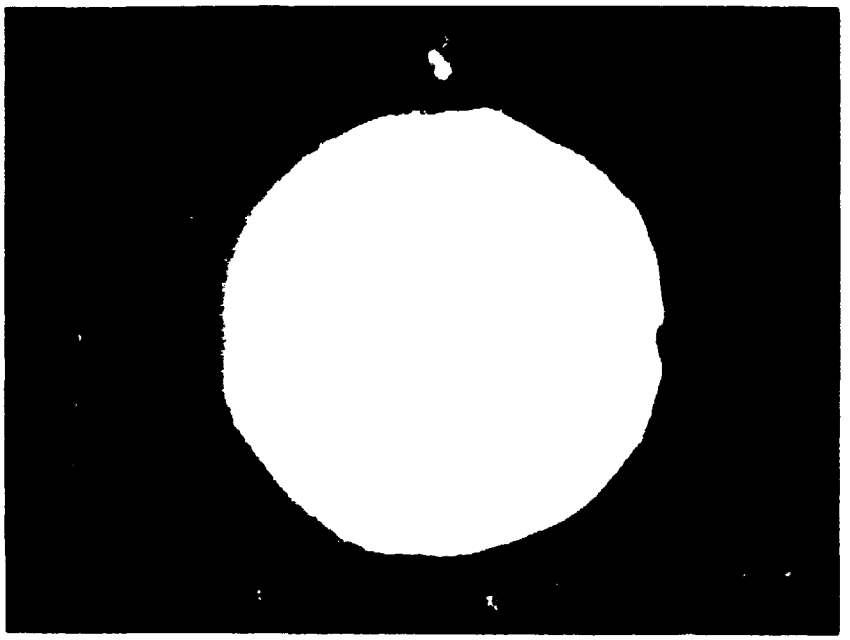

t = 14.81 ms

R = 2.63 m

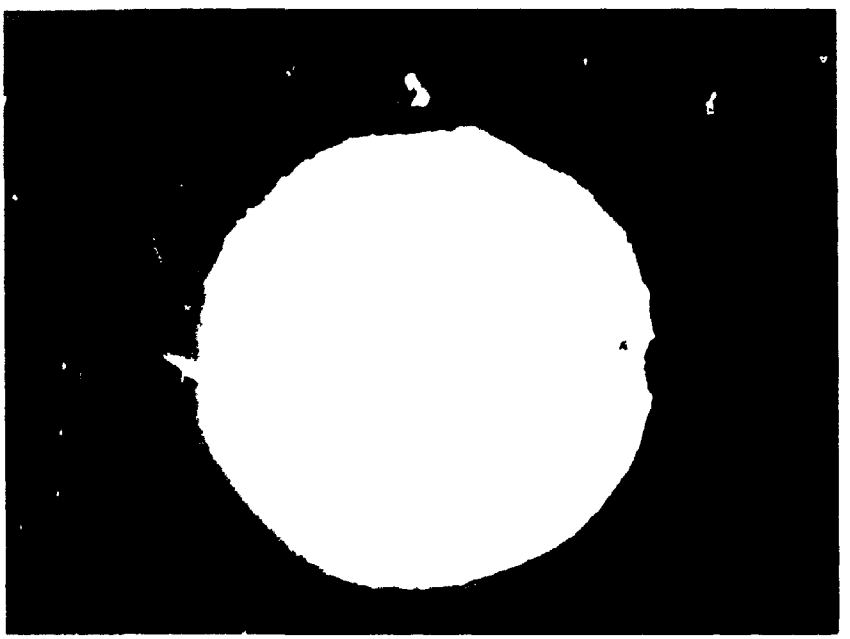

t = 16.05 ms

R = 2.72 m

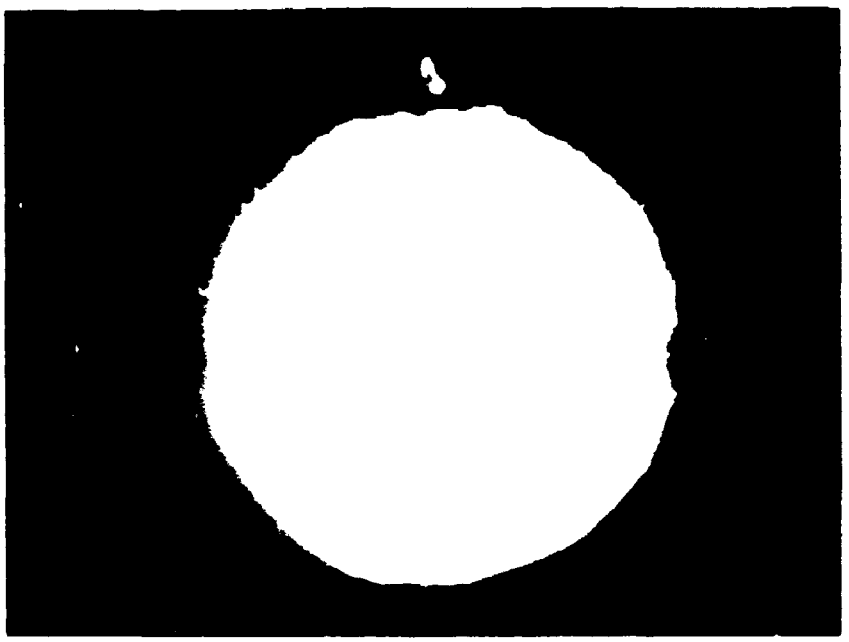

t = 17.28 ms

R = 2.81 m

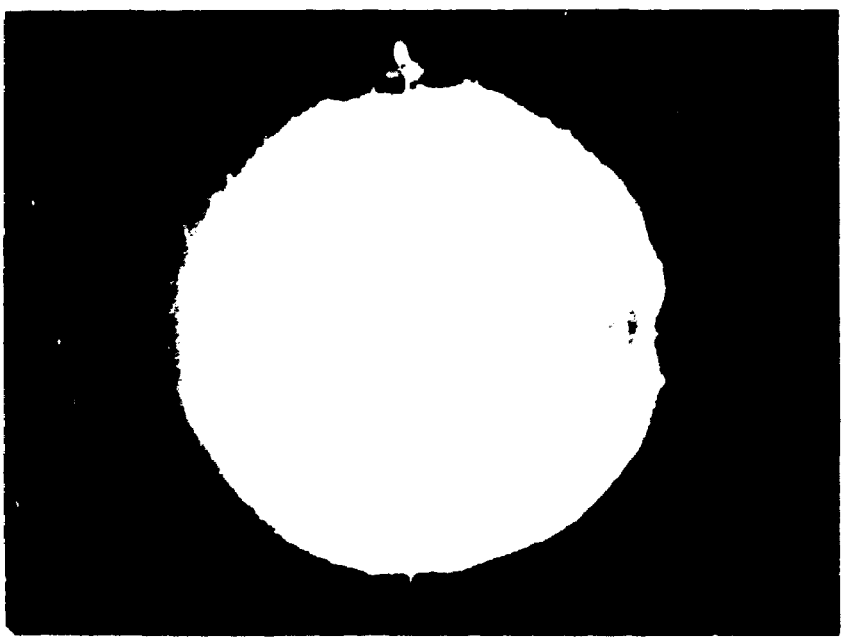

t = 18.52 ms

R = 2.90 m

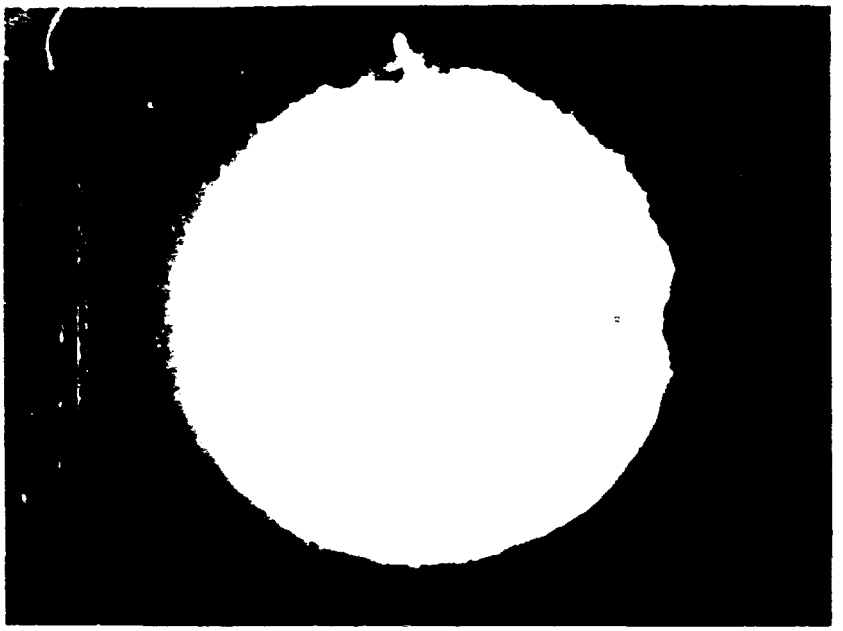

t = 19.75 ms

R = 2.98 m

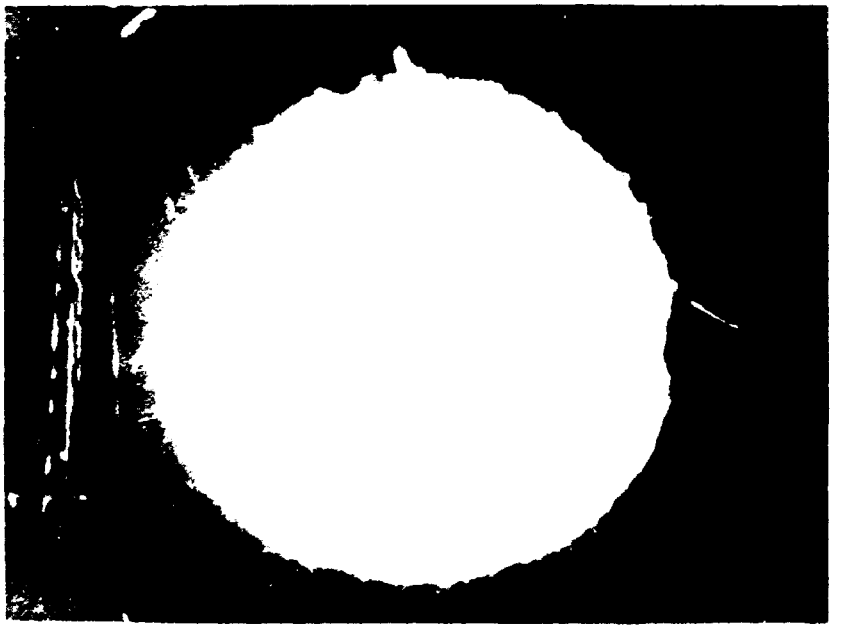

t = 20.99 ms

R = 3.07 m

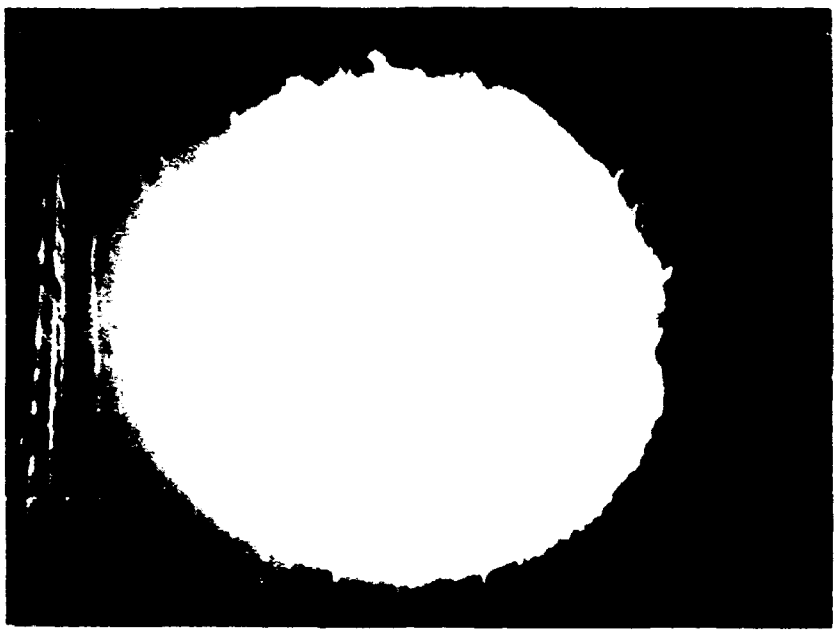

t = 22.22 ms

R = 3.11 m

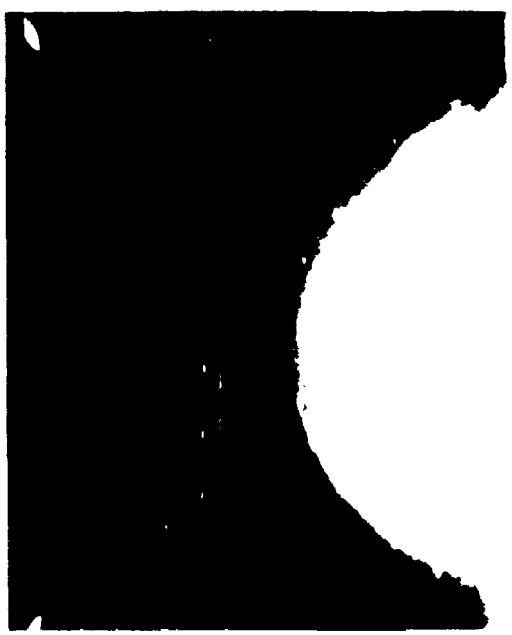

t = 23.46 ms

R = 3.14 m

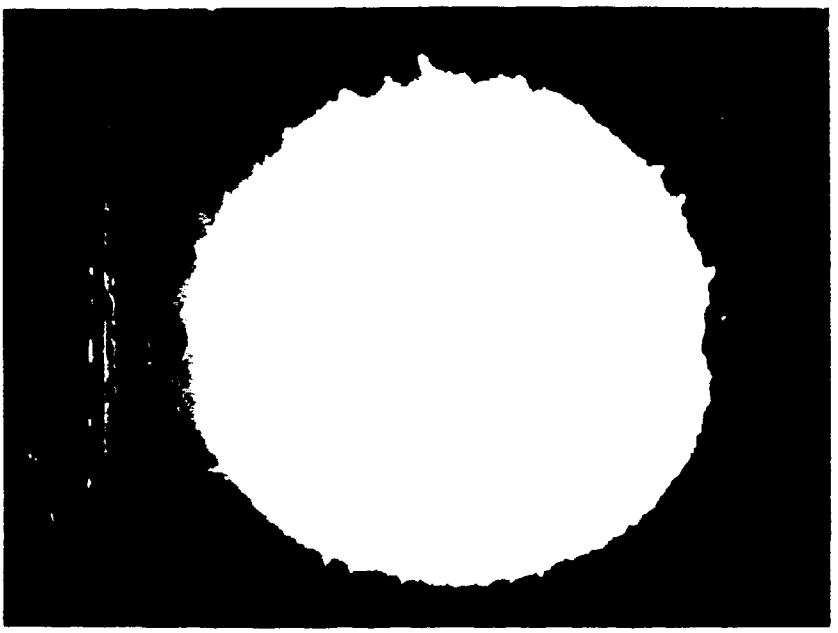

t = 24.69 ms

R = 3.16 m

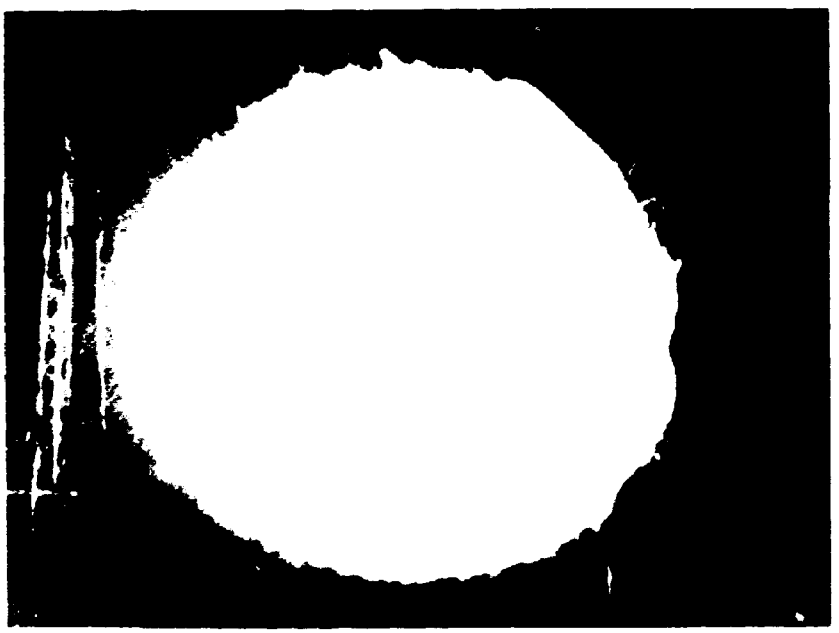

t = 25.93 ms

R = 3.20 m

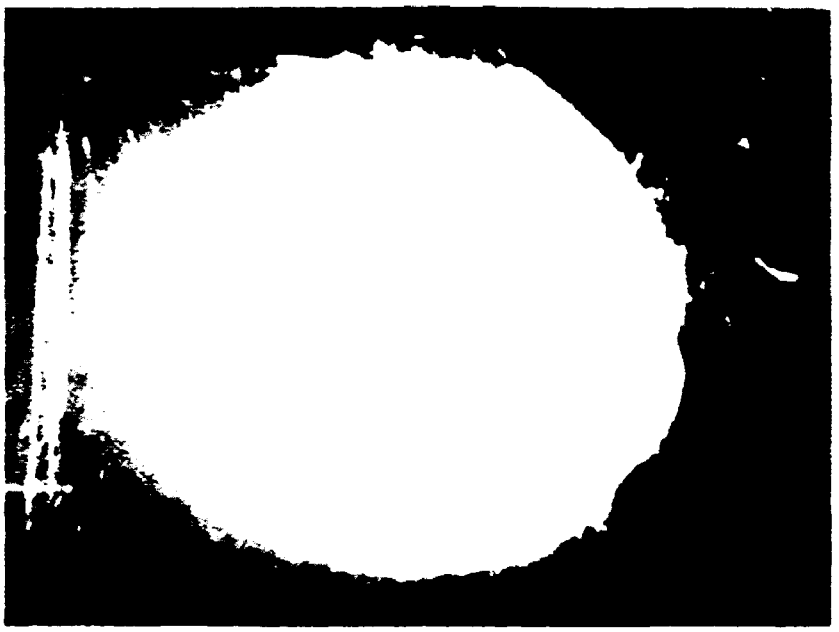

t = 27.1[illegible] ms

R = 1.25 m

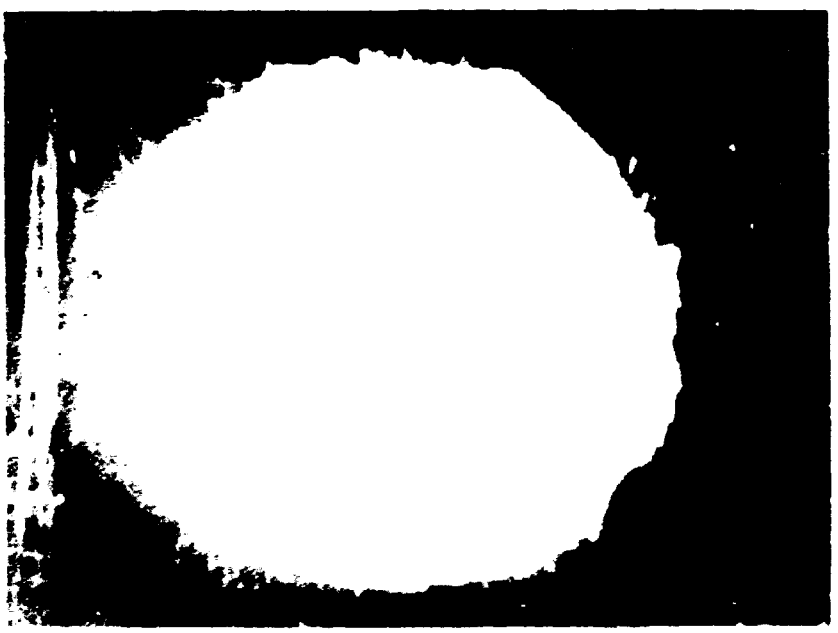

t = 28.4[illegible] ms

R = 1.[illegible] m

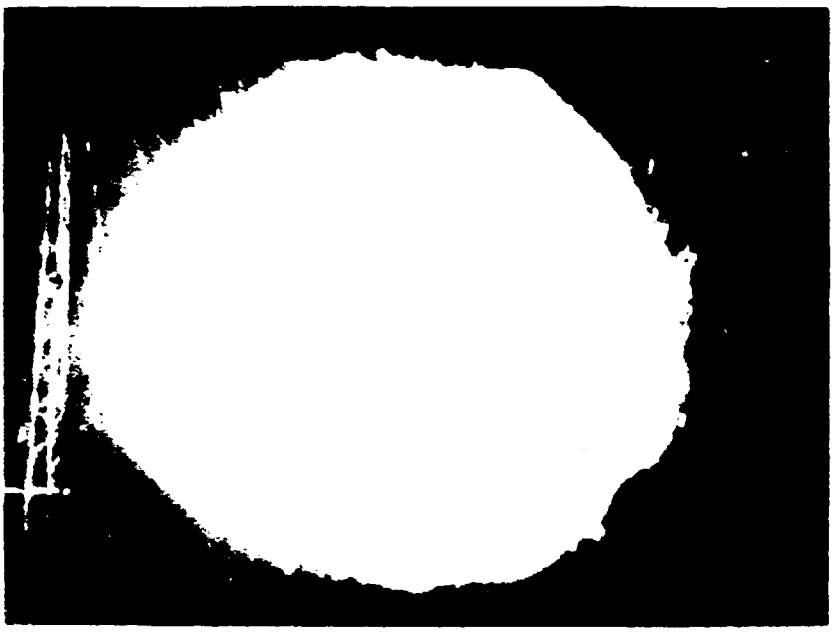

t = 29.63 ms

R = 3.33 m

Title and author(s)

Gas Explosion Characterization, Wave Propagation

G.C. Larsen, J. Roed, S.I. Andersen

Date October 1985

Department or group Engineering Dept.

Groups own registration number(s)

Project/contract no.

Pages 163 Tables 21 Illustrations 121 References 11

ISBN 87-550-1121-7

Abstract (Max. 2000 char.)

A number of experiments have been performed with blast waves arising from the ignition of homogeneous and well defined mixtures of methane, oxygen and nitrogen, contained within spherical balloons with controlled initial dimensions.

The maximum flame speed has been of the order of 100 m/s, resulting in positive peak pressures of 50-100 10^2Pa in 5-10 m distance from the source. The explosion process was found to be reasonable symmetric.

The attenuation of the blast wave due to vegetation and the influence of obstacles as banks, walls and houses on the pressure field have been investigated. The presence of the bank and the house was felt in a zone with a length corresponding to a typical dimension of the obstacles, whereas the overall pressure field is shown to be unaffected by the type of obstacles and vegetation investigated. For the wall and house, reflection factors have been established, and some variation over the surface has been measured.

Descriptors - INIS:

BALLOONS; BLAST EFFECTS; BUILDINGS; EXPERIMENTAL DATA; EXPLOSIONS; FORESTS; HOMOGENEOUS MIXTURES; METEOROLOGY; METHANE; NITROGEN; OXYGEN; PRESSURE MEASUREMENT; SIMULATION; TOPOGRAPHY; WAVE PROPAGATION

Available on request from Risø Library, Risø National Laboratory, (Risø Bibliotek, Forskningscenter Risø), P.O. Box 49, DK-4000 Roskilde, Denmark.
Telephone 02 37 12 12, ext. 2262. Telex: 43116, Telefax: 02 36 06 09

RR 95000107

The scatter of the pressure measurements is estimated for stable, neutral and unstable atmospheric conditions, and an attempt to determine the ground reflection factor has been performed. Finally the accelerations of a house exposed to the blast wave have been examined.

Sales distributors:
G.E.C. Gad Strøget
Vimmelskaftet 32
DK-1161 Copenhagen K, Denmark

Available on exchange from:
Risø Library, Risø National Laboratory,
P.O.Box 49, DK-4000 Roskilde, Denmark

ISBN 87-550-1121-7
ISSN 0106-2840